

Master's thesis for the degree "Alpine Naturgefahren, Wildbach- und Lawinenverbauung"

Snow avalanche activity above Innsbruck, Austria: a dendrogeomorphological approach



Nuria Guerrero Hue

Universität für Bodenkultur Wien

Bundesforschungs- und Ausbildungszentrum für Wald, Naturgefahren und Landschaft (BFW)

June 2021

Master's thesis of the Master Programme "Alpine Naturgefahren, Wildbach- und Lawinenverbauung", Universität für Bodenkultur Wien

Submitted by Nuria Guerrero Hue

Supervisor BOKU Wien: Priv.-Doz. Dipl.-Ing. Dr.nat.techn. Christian Scheidl

Co-supervisor Leopold Franzens- Universität Innsbruck: ao. Univ.-Prof. Mag. Dr. Kurt Nicolussi

Co-supervisor BFW Innsbruck: Dr. Michaela Teich

CERTIFICATION

I hereby declare that I am the sole author of this work. No assistance other than that which is permitted has been used. Ideas and quotes taken directly or indirectly from other sources are identified as such. This written work has not yet been submitted in any part.

A handwritten signature in purple ink, appearing to read 'Nuria G.H.', with a long horizontal stroke extending to the right.

Vienna, June 2021

Nuria Guerrero Hue

AKNOWLEDGEMENTS

Viele haben mir bei dieser Masterarbeit unterstützt, fachlich und persönlich. Ich bedanke mich an euch allen herzlich.

Karl Kleemayr und JT Fischer dafür, dass sie mir die Möglichkeit geben, diese Masterarbeit im BFW durchzuführen und etwas „Neues“ am Institut zu versuchen. Michaela Teich für die Betreuung und Unterstützung mit guten Vorschlägen. Danke für deine Zeit und Motivation, das Vertrauen in mich und den Spielraum zu Entscheiden und zu Gestalten. Christian Scheidl für die guten Tipps und Anregungen. Den MitarbeiterInnen des BFW Innsbruck (1., 2. und 3. Stock) für eure Mitarbeit beim Beprobieren im Wald (auch Andrew und Synnove), Unterstützung mit QGIS oder einfach die netten Gespräche. An zwei super Sekretärinnen Simone Willburger (BFW) und Monika Stanzer (IAN), weil ihr eure Arbeit schnell und mit einem Lächeln erledigt.

Kurt Nicolussi und Thomas Pichler, Danke für euer Interesse, eure Unterstützung und Erklärungen für den „Dendro“ Teil meiner Masterarbeit. Wolfgang Huber, für alle Details über die Lawine des Jänner 2019 und die Begehung im Wald. Poldi Stepanek und Christian Tollinger für den Austausch eurer Informationen und eures Wissens über die alten Arzler Alm Lawinenereignisse.

Meinen Dank an die Österreichische Forschungsförderungsgesellschaft mBH (FFG), dem Förderungsprogramm „FEMtech Praktika für Studentinnen“ des Bundesministeriums für Verkehr, Innovation und Technologie (BMVIT).

Und weil es keine Masterarbeit ohne ein ganzes Masterstudium davor gibt, an alle ProfessorInnen und StudienkollegInnen an der Boku, die sich bemüht haben, keinen starken Dialekt mit mir zu reden. An meine StudienkollegInnen, für das Teilen netter Momente in und außerhalb der Vorlesungen und das Teilen von Lernmaterialien. Insbesondere an die GeographInnen (Mario, Julia, Käsepeter), vor allem an Felix. Und auch an Lucas, Oriol und Lena und die MitbewohnerInnen in Wien. Herzlichen Dank an Rainer („¡gracias por todo chico!“).

An die InnsbruckerInnen, alt und neu, Walter, Stella, Erwin, Maria, Ruth, Anna, Isi, für die Ablenkung und das Zuhören. To all of you who, despite the distance, are still very close (wherever you are: Barcelona, Lleida, Ispra, Luxembourg). And Alexis thanks for your help with R and your motivation to write sometime a paper together!

An meine Familie (Joan, Maria Jose, Fernando, Mirli und die Klammingers) und den kleinen Pau, weil er mich zum Lächeln bringt.

Und zu guter Letzt, an die Stadt Innsbruck und ihre Berge: „Wo immer man sich in Innsbruck befindet, wie städtisch immer die Stadt sein mag: die Berge sind mit dabei – ragend, dräuend, schirmend, mauernd, wie man’s auffassen mag, vor allem aber: überall“ (Hans Weigel, Stadtarchiv).

INDEX

CERTIFICATION.....	3
ACKNOWLEDGEMENTS.....	4
List of abbreviations	8
ABSTRACT	9
KURZFASSUNG.....	11
1. INTRODUCTION	13
2. THEORETICAL BACKGROUND.....	16
2.1 Description of snow avalanches.....	16
2.2 Interaction between snow avalanches and forests	19
2.3 Description of tree rings	22
2.4 Avalanche indicators induced by snow avalanches.....	23
2.5 Position of avalanche indicators in tree rings	27
3 DESCRIPTION OF STUDY AREA	28
3.1 Location	28
3.2 Geology.....	30
3.3 Climate.....	31
3.4 Vegetation	32
3.5 Soil.....	34
3.6 Historical avalanche events	34
3.7 Existing protection measures against snow avalanches.....	36
3.8 Description of the avalanche released in January 2019.....	37
4 MATERIAL AND METHODS.....	41
4.1 Fieldwork.....	41
4.1.1 Selection of trees	42
4.1.2 Description of damage	42
4.1.3 Tree information	43
4.1.4 Coring trees	44
4.2 Dendrochronological procedures.....	45

4.2.1	Sample preparation	45
4.2.2	Tree-ring width	46
4.2.3	Cross-dating.....	47
4.2.4	Estimation of minimum age.....	47
4.2.5	Avalanche indicators in tree rings	47
4.2.6	Abrupt growth changes.....	49
4.3	Detection of avalanche events in tree rings.....	49
4.3.1	Responding trees	49
4.3.2	Weighting of avalanche indicators - reaction classes.....	50
4.3.3	Comparison with historical records.....	51
4.3.4	Spatial distribution of potential avalanche years	51
4.3.5	Ecological and climatical factors.....	51
5	RESULTS.....	52
5.1	Fieldwork and dendrochronology.....	52
5.1.1	Sampled trees and external damages	52
5.1.2	Tree-ring width	54
5.1.3	Eccentricity	55
5.1.4	Cross-dating.....	56
5.1.5	Minimum age.....	57
5.2	Internal signs in tree rings: avalanche indicators	58
5.2.1	Kill date, CW, TRD and CT.....	58
5.2.2	Position of avalanche indicators in the tree ring	61
5.3	Detecting avalanche years.....	61
5.3.1	Avalanche indicators and historical avalanche years.....	61
5.3.2	Avalanche indicators and potential avalanche years.....	62
5.3.3	Temporal distribution of trees with avalanche indicators	64
5.3.4	Spatial distribution of trees with avalanche indicators	67
5.3.5	Eastern arm of the avalanche	71
6	DISCUSSION	73
6.1	Detection of avalanche years	73

6.2	Avalanche indicators (external and internal)	74
6.3	Limitations of this study.....	75
6.3.1	Study site	75
6.3.2	Methodology	75
6.4	Recommendations	80
7	CONCLUSIONS.....	81
	List of figures.....	82
	List of tables	85
	REFERENCES	86
	ANNEX I: Field sheet.....	91
	ANNEX II: Identification key for avalanche indicators	92
	ANNEX III: Calculation of abrupt growth change	98
	ANNEX IV: Tree-ring width diagrams	101

List of abbreviations

Table 1: List of abbreviations

AGC	Abrupt growth change
AAI	Avalanche activity index
AI	Avalanche indicator
BFW	Austrian Research Centre for Forests (in German: <i>Bundesforschungszentrum für Wald</i>)
CT	Callous tissue
CW	Compression wood
D	Dormant season
DBH	Diameter at Breast Height
EE	Early earlywood
EW	Earlywood
Glk	Gleichläufigkeit
LA	Lower area
LW	Latewood
RC	Reaction class
TRD	Traumatic resin ducts
WLV	Austrian Service for Torrent and Avalanche Control (in German: <i>Forsttechnischer Dienst für Wildbach- u Lawinenverbauung</i>)

ABSTRACT

Snow avalanches are natural disturbances that can cause substantial damage to forests and endanger people and material assets. Knowledge of past avalanches is crucial for forest management, planning technical mitigation measures and risk prevention. Dendrogeomorphology can provide information about previous disturbances, for example, tree damages caused by avalanches in forested terrain. By analysing the past growth of trees, both temporal and spatial reconstructions of avalanche activity in forests are possible.

A dendrogeomorphological approach was used to study past avalanche activity in an avalanche path above the city of Innsbruck in Austria. This area is of high importance for recreation (e.g., hiking, biking and skiing) as well as avalanche mitigation. Protection forest and technical protection measures are already in place (braking mounds, catching and deflection dams), which frequently interact with avalanches. It is a well-documented avalanche path, with extensive historical documentation. In January 2019, an avalanche released above the Arzler Alm mountain hut and caused considerable damage to approximately 25 hectares (ha) of forest. This event provided me with the opportunity to conduct the present study. I sampled 104 trees along three altitudinal transects at elevation bands of 1200, 1100 and 1000 m above sea level (a.s.l.) covering the damaged area. Furthermore, I applied a selective sampling scheme below the forest damage along a gully where avalanches that reached the city of Innsbruck had previously been observed. Using an increment borer at least two cores per tree were taken from damaged and undisturbed trees. A mixture of conifers and broadleaved trees (mostly *Picea abies* (L.) Karst, *Fagus sylvatica* L. and *Abies alba* Mill.), as well as old and young trees were selected. In addition, we recorded the exact position of each tree and measured several tree parameters (e.g., diameter at breast height (DBH), tree height) and described the damage. Each core was then prepared following standard dendrochronological procedures. Tree-ring widths from 45 coniferous trees were measured using a binocular microscope and measurement device together with a time-series measurement and analysis program (TSAP-Win). Additionally, a visual detection of specific features, i.e., possible avalanche indicators (traumatic resin ducts, reaction wood, callous tissue) was performed and subsequently reaction classes were assigned (weighting of the indicator). A total of 133 cores were measured and the oldest tree ring was dated to the year 1855, so the period between 1855-2019 was studied. A total of 1471 possible avalanche indicators were observed in 8315 tree rings. Compression wood (CW) and traumatic resin ducts (TRD) were the most common, present in 8% and 9% of tree rings respectively. Avalanche indicators detected were mainly located in the earlywood or latewood positions of tree rings (99.5%), and only 0.5% in the dormant or early earlywood positions.

A tailor-made approach was applied to detect potential avalanche years, i.e., years when an avalanche could have potentially released, considering the characteristics of the area and the avalanche indicators observed in tree rings. A list of potential avalanche years was obtained after applying a set of criteria. The criteria were: exclusion of the first 10 tree rings of juvenile growth, a minimum of 5% of responding trees (avalanche activity index (AAI)), and at least three trees showed an avalanche indicator and at least

one strong reaction (class 4 or 5)). The results, i.e., the spatial distribution of the trees showing strong reactions were then compared with historical records of avalanches and their pathways.

Few strong avalanche reactions were identified, because there were either not enough disturbed trees in specific years or they did not exhibit any spatial pattern clearly attributable to a snow avalanche. Even though it was not possible to reconstruct past avalanche events using dendrogeomorphological methods in the Arzler Alm avalanche path, some tree rings exhibited avalanche indicators for some documented avalanche events (e.g., 1968 and 2019). Also, tree rings have shown that the eastern arm below the "Herzwiese" releases periodically (an eastern arm of the Arzler Alm avalanche path). Additionally, tree rings provided other useful information such as tree minimum age, and we therefore gained additional knowledge about the Arzler Alm avalanche path.

Dendrogeomorphology is a time and resource-consuming methodology, not suitable for every type of forest and therefore not applicable to every avalanche path. This has been exemplified here with the study performed at the Arzler Alm avalanche path (Tyrol, Austria). In this case, it is attributed to a strong anthropogenic influence, especially forest management and recreation activities, which influences the availability of trees by removing affected trees and interferes and alters the avalanche indicators in tree rings. For this reason, I can conclude that being so close to the city of Innsbruck is the great strength (extensive historical documentation about avalanche events) of this study area but at the same time its great weakness (very accessible area for recreational activities and forest management).

KURZFASSUNG

Schneelawinen sind natürliche Störungen, die erhebliche Waldschäden verursachen und Menschen und Sachwerte gefährden können. Das Wissen über vergangene Lawinen ist entscheidend für die Forstbewirtschaftung, die Planung von technischen Schutzmaßnahmen und die Risikoprävention. Die Dendrogeomorphologie kann Informationen über vergangene Störungen liefern, zum Beispiel Baumschäden durch Lawinen in bewaldetem Gelände. Durch die Analyse des vergangenen Wachstums von Bäumen sind sowohl zeitliche als auch räumliche Rekonstruktionen der Lawinenaktivität in Wäldern möglich.

In dieser Arbeit wurde ein dendrogeomorphologischer Ansatz verwendet, um die vergangene Lawinenaktivität in einem Lawinenpfad oberhalb der Stadt Innsbruck in Österreich zu untersuchen. Das Gebiet ist sowohl für Freizeitaktivitäten (z.B. Wandern, Biken und Skifahren) als auch für die Lawinenverbauung von großer Bedeutung. Zum Schutz vor Lawinen wurden bereits Schutzwälder und weitere Maßnahmen wie Bremshöcker, Auffang- und Ablenkdamme errichtet. Es handelt sich um einen gut dokumentierten Lawinenpfad mit einer umfangreichen historischen Dokumentation. Im Januar 2019 löste sich oberhalb der Arzler Alm eine Lawine und verursachte auf ca. 25 Hektar (ha) Wald erhebliche Schäden. Dieses Ereignis bot mir die Gelegenheit, die vorliegende Studie durchzuführen. Ich untersuchte dazu 104 Bäume entlang dreier Transekten auf den Höhenstufen 1200, 1100 und 1000 m über dem Meeresspiegel (ü.d.M.), die das Schadensgebiet abdeckten. Außerdem wendete ich ein selektives Beprobungsschema unterhalb der Waldschäden entlang einer Rinne an, in der zuvor Lawinen beobachtet wurden, die sogar die Stadt Innsbruck erreichten. Mit einem Zuwachsbohrer wurden mindestens zwei Kerne pro Baum von geschädigten und ungestörten Bäumen entnommen. Es wurde eine Mischung aus Nadelbäumen und Laubbäumen (hauptsächlich *Picea abies* (L.) Karst, *Fagus sylvatica* L. und *Abies alba* Mill.), sowie alten und jungen Bäumen ausgewählt. Zusätzlich haben wir die genaue Position jedes Baumes erfasst und verschiedene Baumparameter (z.B. Durchmesser in Brusthöhe (DBH), Baumhöhe) gemessen und die Schäden beschrieben. Jeder Kern wurde dann nach dendrochronologischen Standardverfahren aufbereitet. Die Jahrringbreiten von 45 Nadelbäumen wurden mit einem binokularen Mikroskop und einem Messgerät zusammen mit einem Zeitreihenmess- und Analyseprogramm (TSAP-Win) gemessen. Zusätzlich wurde eine visuelle Erkennung spezifischer Merkmale, d.h. möglicher Lawinenindikatoren (traumatische Harzkanäle, Reaktionsholz, Kallusgewebe) durchgeführt und anschließend Reaktionsklassen zugeordnet (Gewichtung des Indikators). Insgesamt wurden 133 Bohrkern vermessen. Der älteste Jahrring wurde auf das Jahr 1855 datiert, sodass der Zeitraum der Untersuchungen zwischen 1855-2019 angegeben werden kann. Insgesamt wurden 1471 mögliche Lawinenindikatoren in 8315 Jahrringen beobachtet. Druckholz und traumatische Harzkanalreihen zählten zu den Häufigsten und kamen in 8 % bzw. 9 % der Jahrringe vor. Die entdeckten Lawinenindikatoren befanden sich hauptsächlich in den Früh- oder Spätholzpositionen der Jahrringe (99,5%), und nur 0,5% in den Ruheperiode oder frühen Frühholzpositionen.

Es wurde ein maßgeschneiderter Ansatz angewandt, um potenzielle Lawinenjahre zu erkennen. Das sind Jahre, in denen die Lawine unter Berücksichtigung der Eigenschaften des Gebiets und der in den Jahrringen beobachteten Lawinenindikatoren potenziell ausgelöst worden sein könnte. Eine Liste von potenziellen Lawinenjahren wurde anhand von verschiedenen Kriterien erstellt. Dabei mussten mindestens 5% der Bäume einen Indikator zeigen (avalanche activity index (AAI)), dies mussten mindestens drei Bäume sein und einer davon musste eine starke Reaktion zeigen (Klasse entweder 4 oder 5). Die damit ermittelte räumliche Verteilung der Bäume und deren Stärke ihrer Reaktionen auf unterschiedliche Ereignisse wurden anschließend mit historischen Aufzeichnungen von Lawinen und deren Laufwegen verglichen.

Es wurden wenige starke Lawinenreaktionen identifiziert, da es entweder nicht genügend gestörte Bäume in bestimmten Jahren gab oder sie kein räumliches Muster aufwiesen, die eindeutig auf eine Schneelawine zurückzuführen sind. Daher war es nicht möglich, vergangene Lawinenereignisse mit dendrogeomorphologischen Methoden im Lawinengang der Arzler Alm zu rekonstruieren. Allerdings zeigten einige Jahrringe Hinweise darauf, dass sich unterhalb der "Herzwiese" periodisch Lawinen lösten und einen östlichen Arm bildeten, der erhebliche Waldschäden verursachte. Zusätzlich lieferten die Jahrringe weitere nützliche Informationen wie das Mindestalter der Bäume, wodurch wir zusätzliche Erkenntnisse über den Lawinenpfad der Arzler Alm gewinnen konnten.

Die Dendrogeomorphologie ist eine zeit- und ressourcenaufwendige Methode, die nicht für jeden Waldtyp geeignet ist und daher auch nicht auf jeden Lawinenpfad angewendet werden kann. Dies wurde hier am Beispiel der Studie am Lawinenpfad Arzler Alm (Tirol, Österreich) gezeigt. In diesem Fall kann man auf einen starken anthropogenen Einfluss schließen, insbesondere auf die Forstbewirtschaftung und Freizeitaktivitäten. Dies führt dazu, dass Bäume entfernt werden und die Lawinenindikatoren in den Jahrringen gestört und verändert werden. Aus diesem Grund kann ich schlussfolgernd sagen, dass die Nähe zur Stadt Innsbruck die große Stärke (umfangreiche historische Dokumentation über Lawinenereignisse) dieses Untersuchungsgebietes ist, aber gleichzeitig auch seine Schwäche (sehr zugängliches Gebiet für Freizeitaktivitäten und Forstbewirtschaftung).

1. INTRODUCTION

Snow avalanches are natural disturbances that can cause substantial damage to forests and endanger people and material assets. In the last century, due to the increasing use of Alpine area for settlements, outdoor leisure activities and traffic routes, avalanche risk has increased significantly (McClung & Schaerer, 2006; Rudolf-Miklau et al., 2015). Consequently, the need of protection and prevention measures against snow avalanches has also been raised. A better knowledge of past avalanche events therefore provides valuable information to deal with these natural disturbances (Kogelnig-Mayer et al., 2011; Neumann, 2011; Stoffel et al., 2010).

Trees record evidence of past geomorphic activity in their tree rings providing information with annual or sub-annual resolution. That is the reason why trees are called “silent witnesses” and are considered natural archives which remain in the landscape after a geomorphic event (Aulitzky, 1992; Favillier et al., 2018; Stoffel et al., 2010). Therefore, dendrogeomorphology is a useful tool which provides information about previous disturbances caused by avalanches in forested terrain. By analysing the past growth of trees, both temporal and spatial reconstructions of the avalanche activity in forests are possible (Stoffel & Bollschweiler, 2008; Stoffel & Corona, 2014).

Dendrochronology is the science of dating tree rings (Kaennel & Schweingruber, 2021). This research field has evolved from measuring and dating tree rings only to current use of tree rings, wood density and the use of stable isotopes to date and reconstruct environmental processes (Gärtner et al., 2015; Stoffel et al., 2010; Stoffel & Corona, 2014). Interest in gathering information about old avalanches through tree rings started in North America in the late 1960s (e.g. (Burrows & Burrows, 1976)). This was the beginning of dendrogeomorphology, a subfield of dendrochronology which utilizes dated tree rings to study and date geomorphic processes such as rockfall, debris flow or snow avalanches (Kaennel & Schweingruber, 2021; Stoffel & Bollschweiler, 2008). It was J. F. Shroder in the 1970s-80s (Shroder, 1978, 1980), who provided the foundation and methodologies for this discipline still used today (Butler & Stoffel, 2013). Using tree rings to study geomorphic processes has expanded over the last decades to numerous mountainous regions worldwide (Favillier et al., 2018; Stoffel et al., 2013). While this method has already been used frequently in other European countries, mainly in France and Switzerland (Favillier et al., 2018; Stoffel et al., 2013), there is still little experience related to the reconstruction of snow avalanche activity during recent centuries in Austria (Kogelnig-Mayer et al., 2011). In dendrogeomorphological studies tree rings are not only counted and measured, but also external and internal evidence of damage is carefully observed. External damages like breakage of crown or branches, tilting or uprooting and scarring can be observed when examining a tree in the forest. Conversely internal evidence must be visually detected in tree rings with a microscope. These include specific features such as reaction wood, growth eccentricity, callous tissue or abrupt growth changes. More recently, tangential rows of traumatic resin ducts (TRD) occurring in some coniferous species are extensively used (Stoffel et al., 2010; Stoffel & Corona, 2014). Regarding tree species, most studies have been carried out using coniferous tree species, given that annual rings and damage (e.g. reaction wood,

traumatic resin ducts) are generally more clearly defined (Stoffel et al., 2010, 2013). Despite this, over the last years studies with broadleaved tree species are also being performed more regularly (e.g. (Casteller et al., 2018)). The study of natural hazards using dendrogeomorphology in general and snow avalanches in particular is a useful tool to gain knowledge about past events, in which sometimes it may be the only source of information. Tree rings can provide information on minimum frequency, magnitude, and extent of previous events (Favillier et al., 2018; Stoffel et al., 2010; Stoffel & Bollschweiler, 2008). This is considered key not only for future forest management but also for an integral risk management. Understanding past avalanche activity is needed to develop prevention and protection measures against avalanches such as land-use planning, building restrictions, design of technical defense structures, etc. (Favillier et al., 2018; McClung & Schaerer, 2006; Stoffel & Bollschweiler, 2008). Additionally, with the development of snow avalanche simulation models a more recent use of dendrogeomorphological results is the calibration of these models (Casteller et al., 2018; Favillier et al., 2018; Stoffel et al., 2010). Despite the numerous scientific publications, Stoffel et al. (2013) stated that there were no clear guidelines and objective standards to perform field sampling and interpretation of signals in tree rings. Therefore they published some standards to perform fieldwork, analysis, and interpretation (Corona et al., 2012; Stoffel et al., 2013; Stoffel & Corona, 2014).

In Austria, there are around 18,000 damaging avalanche paths and more than 6,000 have a potential impact on settlement areas (Rudolf-Miklau et al., 2015). One of them is the Arzler Alm avalanche path above the city of Innsbruck in Tyrol. This area is of high importance for recreation (e.g. hiking, biking, skiing and hunting) as well as avalanche mitigation. Protection forest and technical protection measures are already in place (braking mounds, catching and deflection dams), which frequently interact with avalanches (Adams et al., 2018; Barbolini et al., 2009; Fischer et al., 2013; Rudolf-Miklau et al., 2015). In January 2019, an avalanche released above the Arzler Alm mountain hut and caused considerable damage to approximately 25 hectares (ha) of forest (Fischer, 2019). The destructive power of this event was greater than expected by experts, highlighting the need to gain knowledge about previous avalanche events to improve current and future protection, as well as risk assessment. This event provided me with the opportunity to conduct the present study.

The Arzler Alm avalanche path has released repeatedly in the past and caused destruction of infrastructure, buildings and forest (Fischer et al., 2013; Rudolf-Miklau & Sauermoser, 2011; Stepanek, 2012). Other types of geomorphological disturbances (i.e., debris flow, rockfall) do not occur in the area. Being located close to the city of Innsbruck makes it a well-documented avalanche path and therefore suitable to conduct a dendrogeomorphological study (Corona et al., 2012; de Bouchard d'Aubeterre et al., 2019; Kogelnig-Mayer et al., 2011; Muntán, 2016 and L. Stepanek, personal communication, 2019).

To carry out this study, I mostly used the methods described in the scientific literature e.g. (Stoffel et al., 2013; Stoffel & Bollschweiler, 2008; Stoffel & Corona, 2014), with regards to study design and field sampling. For the interpretation and classification of internal and external avalanche indicators, criteria presented in (Kogelnig-Mayer et al., 2011) and (Stoffel & Corona, 2014) were considered. Moreover, in

2017 Favillier et al. (2017) proposed a procedure (the so called 4-step approach) to identify avalanche event years using tree-ring data, where the noise induced by climate conditions or exogenous disturbances is minimized (Favillier et al., 2017). It has been already applied in France (de Bouchard d'Aubeterre et al., 2019; Mainieri et al., 2020) and Switzerland (Favillier et al., 2018) and therefore was considered as an appropriate approach to pursue in Austria, in the Arzler Alm avalanche path. In addition, expert advice in dendrochronology from K. Nicolussi from the University of Innsbruck has been strongly considered.

The aim of the present study was to reconstruct temporally and spatially the avalanche activity in the Arzler Alm avalanche path (Tyrol, Austria) using dendrogeomorphological methods and to prove the feasibility of such an approach in a highly managed forest.

To perform this, specific research questions were addressed:

- Is it possible to perform this type of dendrogeomorphological analysis in the Arzler Alm avalanche path, a well-documented area but with strong influence of anthropogenic factors (e.g. forest management, recreation, game browsing)?
- Which external tree damages and which internal avalanche indicators are more suitable and practical to use and show better explanatory power?
- Can the 4-step approach proposed by (Favillier et al., 2017) be applied in the Arzler Alm?
- If past avalanche events can be reconstructed, do they match with the historical information available?
- Is it possible to infer unknown avalanche events?

2. THEORETICAL BACKGROUND

2.1 Description of snow avalanches

Snow avalanches are defined as large masses of snow or ice that move rapidly down a mountainside or over a precipice, which can also contain rocks, earth or entrained tree trunks (woody debris) ((Rudolf-Miklau et al., 2015) (EAWS, 2021; Margreth, 2004). They originate in steep terrain (inclination between 25-60°), can reach velocities up to 300 km/h, have a volume of more than 100 m³ and a path length of more than 50 m (EAWS, 2021; Rudolf-Miklau et al., 2015).



Figure 1: Zones of an avalanche path (adapted from (Fellin, 2013)).

Avalanche formation is the process where accumulated snow starts moving and is a function of terrain topography (slope exposure, steepness, and surface roughness), snow characteristics and forest stand structure (Bebi et al., 2009; Schneebeli & Bebi, 2004). The avalanche path is where avalanches move and it has three zones, which are specific for every avalanche (McClung & Schaerer, 2006; Rudolf-Miklau et al., 2015) (Figure 1):

- Starting zone (or release zone, zone of origin): is the location where the unstable snow fails and begins to move, most commonly on slopes with an inclination between 25-60°. A minimum inclination for snow accumulation and avalanche formation is approximately 25°. At slopes with inclination higher than 60°, sufficient snow accumulation is not likely.
- Avalanche track (or transport, transition zone): is the slope that connects the starting zone with the runout zone. Avalanche speed attains its maximum value in the avalanche track.

- Runout zone (or deposition zone): is an area with an average inclination less than 10°. The avalanche stops and debris is deposited because the inclination is insufficient for further movement.

The term multiple starting zones applies when several starting zones well separated by ridges or forests, connect to a single track.

In 1981 the first detailed avalanche classification was published by the United Nations Educational, Scientific and Cultural Organization (Rudolf-Miklau & Sauer Moser, 2011; UNESCO, 1981). According to the form of movement in the avalanche path, there are three types of avalanches:

- Powder (cloud) avalanche: avalanche fine-grained, dry powder in which most of the flowing snow is suspended in the air by turbulence (powder cloud). Speeds: 100-300 km/h. Associated with strong pressure waves which cause damage in front of the deposition area (EAWS, 2021). They can reach heights of 50 m or more (Margreth, 2004). The average densities are in the range of 2-15 kg/m³ (Rudolf-Miklau et al., 2015).
- (Dense) flow avalanche: avalanche that moves mainly flowing (turbulent) or gliding on the ground (ground or snow surface), laminar or channelized ÖNR 24805 (Österreichisches Normungsinstitut, 2010). There is permanent contact between the individual ice particles. Typical densities are in the range of 100-300 kg/m³.
- Mixed avalanche: mixture of powder and dense flow avalanche. Powder snow avalanches always develop from flow avalanches; therefore, both avalanche types generally occur together as a mixed avalanche. The proportion of each component/part is different in every single avalanche. Depending on which form of movement dominates, it is referred to as a "dense flow avalanche with a powder cloud" or a "powder avalanche with a flowing component" ÖNR 24805 (Österreichisches Normungsinstitut, 2010). Mixed-motion avalanches are very frequent (UNESCO, 1981) and are also the most common type of major disaster avalanches (Rudolf-Miklau et al., 2015).

Inside the snowpack takes place a slow and continuous movement down the slope (on a scale of mm to meters per day). We can distinguish two types of movement (Figure 2) (Margreth, 2007):

- Snow creep is the result of vertical settlement of the snow cover and internal shear deformation parallel to the slope. The cause of these motions is the weight of the snow cover. Typical creep rates are mm to cm per day. At the ground, the snow creep is zero.
- Snow glide is the slip of the entire snowpack over the ground without essential deformation within the snowpack. Typical glide rates are mm to meters per day.

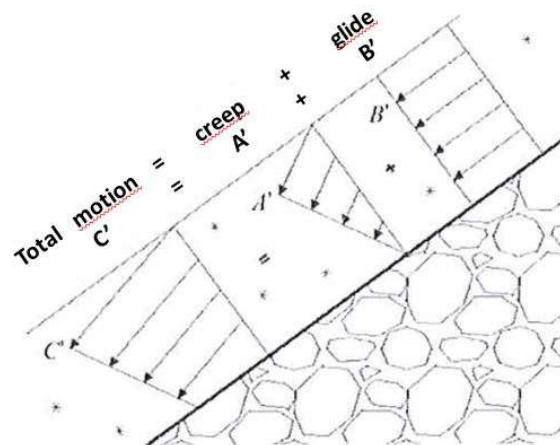


Figure 2: Schematic diagram of the creep and glide movement of the snow cover (adapted from (Österreichisches Normungsinstitut, 2010)).

If snow creep and snow glide are strong, trees cannot grow vertically and therefore are curved or tilted (Figure 3 and Figure 8) (Rudolf-Miklau et al., 2015).



Figure 3: Damaged bench due to snow movement in the study site (Foto: N. Guerrero Hue).

Internally avalanche mass is not homogeneous so mixed avalanches “are believed to consist of a dense core with a fluidised (saltation) layer on top, and possibly in front of it, surrounded by a powder cloud (suspension layer) (Barbolini et al., 2009)” as shown in Figure 4.

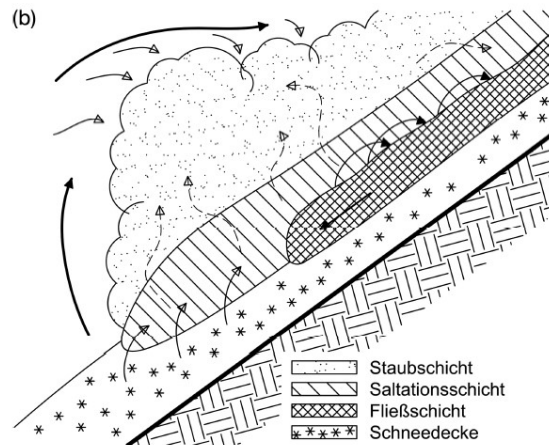


Figure 4: A schematic figure of a mixed avalanche showing the powder component (Staubschicht), re-suspension layer (Saltationsschicht), flow component (Fließschicht) and snow surface (Schneedecke) (Rudolf-Miklau et al., 2015) after (Österreichisches Normungsinstitut, 2010).

These layers are described by (Barbolini et al., 2009) as follows:

- The dense core is characterized by a frictional contact between the snow particles, where each particle is in persistent contact with other particles. The density is on the order of 300 kg/m^3 , and a typical flow depth is 1–3 m.
- The fluidised or saltation layer consists of particles that interact in pairwise collisions, where the dynamics of the interstitial air may be assumed to play a rather limited role and persistent particle–particle contacts do not arise. The density is in the range of $10\text{--}100 \text{ kg/m}^3$, and a typical depth of this layer is 2–5 m. The fluidised layer can precede the dense core of the avalanche by many tens of meters. Occasionally this layer, also called transition layer, is seen as the lowest layer of the powder component (Rudolf-Miklau et al., 2015).
- The powder cloud is a turbulent suspension of snow particles in air, where particle collisions are comparatively unimportant and the dynamics are dominated by turbulent entrainment, settlement of snow particles and air flow. The density is on the order of 3 kg/m^3 , and the flow depth can range from a few tens of meters to 100 m or more.

2.2 Interaction between snow avalanches and forests

The interaction between forests and snow avalanches in subalpine forest ecosystems is multifaceted. As rapid mass flow, avalanches entail a substantial hazard to forests, settlements, and infrastructures. However, avalanches also determine the characteristics and dynamics of mountain ecosystems, shaping landscapes and contributing to biodiversity and thus determining forest structure and function (Bebi et

al., 2009; Brang, 2001). Moreover, forests can contribute to stabilizing the snow cover (Schneebeli & Bebi, 2004) and therefore can affect the likelihood of avalanche release, having a protective function (Bebi et al., 2009). Generally, forests can reduce the danger of avalanches, however this strongly depends on stand structure, avalanche size and the position of the forest in the avalanche path (Bebi et al., 2009; Feistl et al., 2014; Teich et al., 2012). Nevertheless, it is a very complex interaction, still being investigated (Rudolf-Miklau et al., 2015; Teich et al., 2012).

Depending on the position of the forest related to the avalanche path, their interaction varies. In situations where avalanches release above the treeline, forests cannot hinder their formation and, if avalanches exceed a certain size, they usually destroy the forest below. The forest's braking effect on avalanches that release high above the tree line is generally very limited (Bebi et al., 2009; Margreth, 2004; Rudolf-Miklau et al., 2015; Teich et al., 2012).

Forests in the release area influence the conditions of the snowpack and therefore the formation, size and even the reach of avalanches (Schneebeli & Bebi, 2004; Teich et al., 2012). Trees modify snow mechanical properties by intercepting falling snow, modifying the radiation and thus the temperature at the snow surface and decreasing near-surface wind speeds (Figure 5) (McClung & Schaerer, 2006; Schneebeli & Bebi, 2004). Trees are also an additional roughness element compared to open, non-forested terrain. As a result of these factors and processes, there are less weak layers in the snowpack in forests, so forested terrain is less prone to trigger avalanches (Schneebeli & Bebi, 2004). Forests can prevent avalanches on slopes, however when large avalanches are already moving, the protective effects of the forest can be overwhelmed and may not reduce any harm caused by the avalanche. Large avalanches often break trees and develop into a mixed flow of snow and trees, creating greater mass and increased damage potential (McClung & Schaerer, 2006).

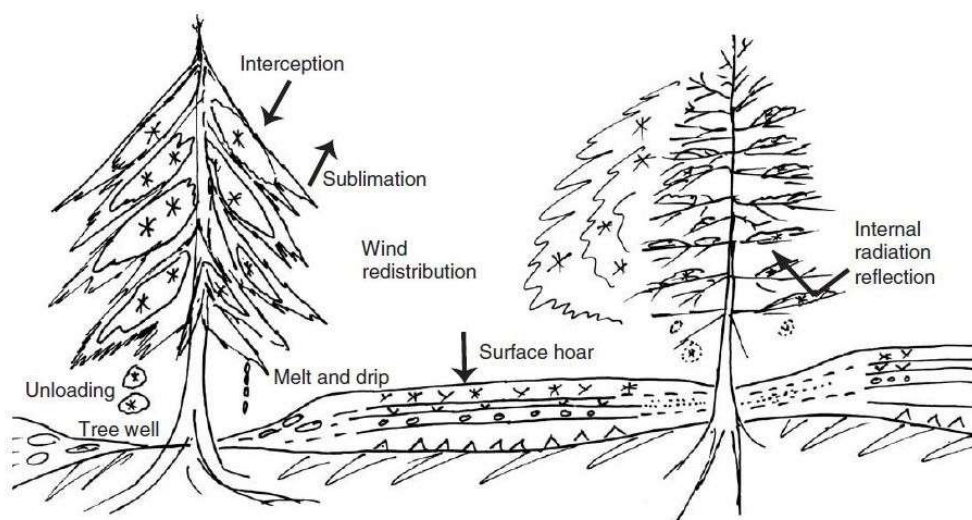


Figure 5: Effects of forest on the snowpack (adapted from (Schneebeli & Bebi, 2004)).

Forests in an avalanche track can also reduce lateral spread and contribute to slowing down avalanches in the depositional area, because an avalanche loses energy when trees break (Margreth, 2004). For flowing avalanches, it is assumed that, in order to break a trunk, snow pressure between 10 and 50 kN/m² is required; for powder snow avalanches, the values are approximately 3 to 5 kN/m² lower (Rudolf-Miklau et al., 2015). Small avalanches can flow between trees without damaging them (McClung & Schaerer, 2006).

In the runout zone, the velocity is often low, so that the forest may have a better retarding effect and may reduce the reach of avalanches, depending on the tree spacing, tree height and elasticity, and type of avalanche. However, forest cover cannot be relied on to stop all avalanches because avalanches may either move through the trees or break them (McClung & Schaerer, 2006; Rudolf-Miklau et al., 2015).

In general, the possibility of avalanche release in forests, and so their frequency, intensity and magnitude, depends on snow characteristics but also on the forest stand structure and topography (Bebi et al., 2009 and references therein). Large, destructive avalanches can destroy forests without significantly reducing their velocity given that tree fracture consumes relatively little of the avalanche's energy (Bebi et al., 2009). In case of small and medium avalanches, forests are indeed able to reduce avalanche speeds and limit their runout (Feistl et al., 2014; Teich et al., 2012). Consequently, speed reduction of avalanches by forests not only depends on where they release but also on the size of the avalanche.

Regarding tree species, the presence of needles in winter is decisive. Falling snow can be intercepted by needles (in case of evergreen conifers) or by twigs (deciduous trees), the latter are less effective in case of low temperatures during snowfall because the snowflakes stick less to twigs without needles (Schneebeli & Bebi, 2004). The intercepted snow provides a larger air resistance compared to winter-bare tree species, so these trees are more likely to be broken or uprooted (Rudolf-Miklau et al., 2015). It is worth to point out, that if stand densities are comparable, larch trees (deciduous conifer) are almost equally effective preventing avalanche formation as spruce or fir trees (evergreen conifers) (Schneebeli & Bebi, 2004; Teich et al., 2019).

To what extent trees and forests are damaged by avalanches depends on the energy of the avalanche but also on the characteristics of the forest (DBH, density, age, presence of gaps, tree species) and location in terrain. Many trees will be destroyed and / or uprooted, others will survive with broken branches or broken crowns, others will have scars due to abrasion. Some trees can show all these damages together or nothing and survive intact (Stoffel & Bollschweiler, 2008; Stoffel & Corona, 2014). However, not all avalanches damage vegetation. Sometimes the snowpack covers small shrubs and trees, preventing damage. Avalanche paths at high latitudes or altitudes may not have vegetation (McClung & Schaerer, 2006).

The influence of avalanches on individual trees is that they develop morphological responses, which are found in their tree rings and are studied in dendrogeomorphology. Some indicators can be used to reconstruct avalanche events based on characteristics in tree rings (further detailed in chapter 2.4) (Bebi et al., 2009).

2.3 Description of tree rings

Trees grow in vertical and radial directions. Vertical growth is the increase in height and radial growth is the increase in diameter. The radial growth of plants happens through the vascular cambium, a thin layer of plant tissue capable of dividing, which is found in the trunk, branches and lignified roots. It creates new cells of xylem on the inside (wood) and phloem on the outside (bark) (Kaennel & Schweingruber, 2021; Neumann, 2011). Cell division, i.e., tree growth is limited to the vegetation period. In latitudes of the temperate zone, it starts in spring and ends in autumn. Outside the vegetation period, cell formation ceases and “dormancy” sets in (Stoffel & Bollschweiler, 2008).

Quantity and quality of wood cells formed varies throughout the growing period. In conifers it can be distinguished between earlywood and latewood (Figure 6). In early stages of the growing season, cambium cells form large, thin-walled earlywood (EW) cells with rather light colour, which are called tracheids and primarily serve the transport of water. Later in the vegetation period latewood (LW) is produced, which is characterised by smaller and denser tracheids. Due to their thicker cell walls, these layers are darker in appearance and serve to increase the stability of the tree. The transition from earlywood to latewood can occur gradually or abruptly (Stoffel & Bollschweiler, 2008) (ANNEX II: Identification key for avalanche indicators).

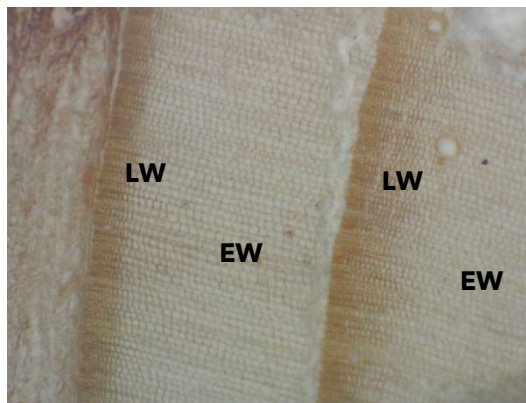


Figure 6: Two tree rings of *Picea abies* with earlywood (EW) and latewood (LW) (Foto: N. Guerrero Hue).

Consequently, one distinct tree ring is formed every year and it can be defined as the layers of cells produced in one growing season. Latewood-earlywood boundaries of successive tree rings are distinct and mostly extend around the entire circumference of the stem (Kaennel & Schweingruber, 2021; Stoffel & Bollschweiler, 2008).

2.4 Avalanche indicators induced by snow avalanches

Snow avalanches can cause different mechanical damages to trees, depending on the impact force and frequency of the avalanche, and the flexibility of the tree (dependent on its diameter and height), as well as the position of the tree in the avalanche path (Rudolf-Miklau et al., 2015). These damages can be used for the dating of past geomorphic events. Some damages are external and can be observed in the field, but others are internal and must be identified with a microscope in a laboratory.

- Decapitation of trees and elimination of branches

Snow avalanches may completely or partially break tree crowns and / or its branches. If a tree is decapitated, one or several lateral branches will try to take the lead and thus replace the broken crown. This results in a tree-shape called "candelabra" (Stoffel & Bollschweiler, 2008) (Figure 7).



Figure 7: Trees with candelabra form due to breakage of the main stem (Foto: N. Guerrero Hue).

- Tilted and curved stems

Trees can lose their vertical position due to a geomorphological process (Figure 8). Either the sudden pressure induced by an event and deposition of material (e.g., avalanche snow, debris-flow material) or the slow but ongoing movement of snow cover (creep and glide, Section 2.1) can lead to either the inclination or curvature of the stem (Stoffel & Bollschweiler, 2008). In a cross-section, eccentric growth (where the pith is not centered) and reaction wood can be observed. As trees will always try to recover their verticality, the stem will be curved at the lower part but will be straight higher up.



Figure 8: Curved *Fagus sylvatica* in the study area (Foto: N. Guerrero Hue).

- Wounding of trees (scars and chaotic callous tissue, CT)

Injuries can be observed on a tree's stem, in its branches or roots due to an avalanche impact. Bark is removed and the wound can reach the cambium. Scars appear due to impact, abrasion of snow or from other material entrained and transported (uprooted trees, rocks, etc.) (Figure 9a). The tree reacts to the local destruction of the cambium by producing chaotic callous tissue (CT) (Figure 9b) at the edges of the injury almost immediately to try to close the wound (Stoffel & Bollschweiler, 2008).



Figure 9 a, b: On the left a scar on a *Fagus sylvatica* tree in the study site and on the right inside the yellow circle, an example of chaotic callous tissue in a tree ring (frost ring) (Fotos: N. Guerrero Hue).

- Tangential rows of traumatic resin ducts (TRD)

A few weeks after a damaging event, some conifer species, e.g. *Larix*, *Picea* or *Abies* produce tangential rows of traumatic resin ducts near the scar (TRD) (Figure 10). These rows of resin ducts appear tangentially aligned and are more numerous the closer to the injury, while normal resin ducts are scattered (Neumann, 2011; Stoffel & Bollschweiler, 2008). However, TRDs do not occur in *Pinus*, as this genus produces copious amounts of resin without necessarily suffering from mechanical wounding (see Stoffel & Bollschweiler, 2008).



Figure 10: A row of traumatic resin ducts in earlywood (Foto: N. Guerrero Hue).

- Reaction wood and eccentricity

If the equilibrium of a tree is disturbed, e.g., on steep slopes or by strong wind, the tree reacts with the formation of reaction wood. This tissue consists of rather round-shaped cells of higher density. In conifers it appears on the downslope of the trunk and is called compression wood (CW). In contrast, in broadleaved trees it is produced on the upslope side and is called tension wood (Kaennel & Schweingruber, 2021; Neumann, 2011). Compression wood cells have thickened cell walls and appear darker in cross-section (Figure 11). Tree rings of reaction wood will be considerably larger, this mostly leads to eccentric growth because the pith is not centered (Kaennel & Schweingruber, 2021; Neumann, 2011; Stoffel & Bollschweiler, 2008).



Figure 11: Compression wood covering more than the half of a tree ring of *Picea abies* (Foto: N. Guerrero Hue).

- Abrupt growth change

Tree rings can show two different classes of growth change as a consequence of avalanches: suppressions (negative change) and releases (positive change) (Altman et al., 2014; Stoffel et al., 2013; Stoffel & Bollschweiler, 2008). This feature used to infer past events must be calculated using the ring-width data (ANNEX III: Calculation of abrupt growth change).

Growth suppressions can appear in trees directly affected by an avalanche. They might have lost their crown or branches, have some injuries, or be tilted. Due to the damage, their radial growth is slowed down for several years. Therefore, tree rings formed after the event are suddenly narrower than they previously were.

Growth releases in contrast, can appear in trees that were not damaged by the avalanche, but whose growth was influenced by surrounding trees (Altman et al., 2014). With the elimination of neighbouring trees, survivor trees benefit from better resources (improved light conditions, nutrients, water, less competition) after the avalanche. This is reflected in their tree rings, showing an abrupt and sustained increase in their radial growth (Altman et al., 2014; Stoffel, 2005).

2.5 Position of avalanche indicators in tree rings

Reactions as defined above can be used for the dating of past avalanche events together with other information provided by tree rings: their position within the annual ring.

Tree ring formation occurs during the vegetation period, from spring to autumn in temperate climate zones, while CT and TRD appear immediately after mechanical impact (Kogelnig-Mayer et al., 2011; Stoffel, 2005). Taking this into account, a tree ring is a kind of intra-annual calendar and can be used to distinguish which type of geomorphic process caused the damage (Figure 12). Kogelnig-Mayer et al. (2011) used the position of TRD and CT within the tree ring to differentiate between snow avalanche and debris flow events occurring in the same study site. In the present study we applied this procedure and therefore considered the internal signals recorded immediately after the dormant season (D) or in the earliest section of the earlywood (EE) to be consequence of snow avalanches.

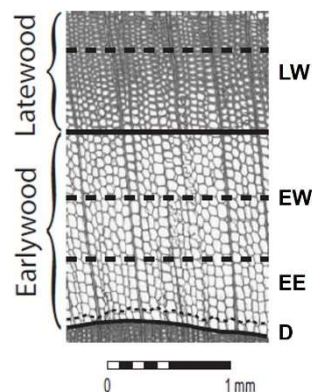


Figure 12: Tree rings are subdivided into latewood (LW), earlywood (EW), early earlywood (EE) and dormant season (D) (adapted from (Stoffel, 2005)).

3 DESCRIPTION OF STUDY AREA

3.1 Location

The Arzler Alm avalanche path area is located north of the city of Innsbruck (47° 15' 45.58" N, 11° 23' 40.34" E), in the region of Tyrol, Austria (Figure 13). The area lies on the south slope of the Nordkette mountain ridge and is located between 596 - 2315 m a.s.l.. The avalanche path is mostly forested and has a surface of 230 ha.

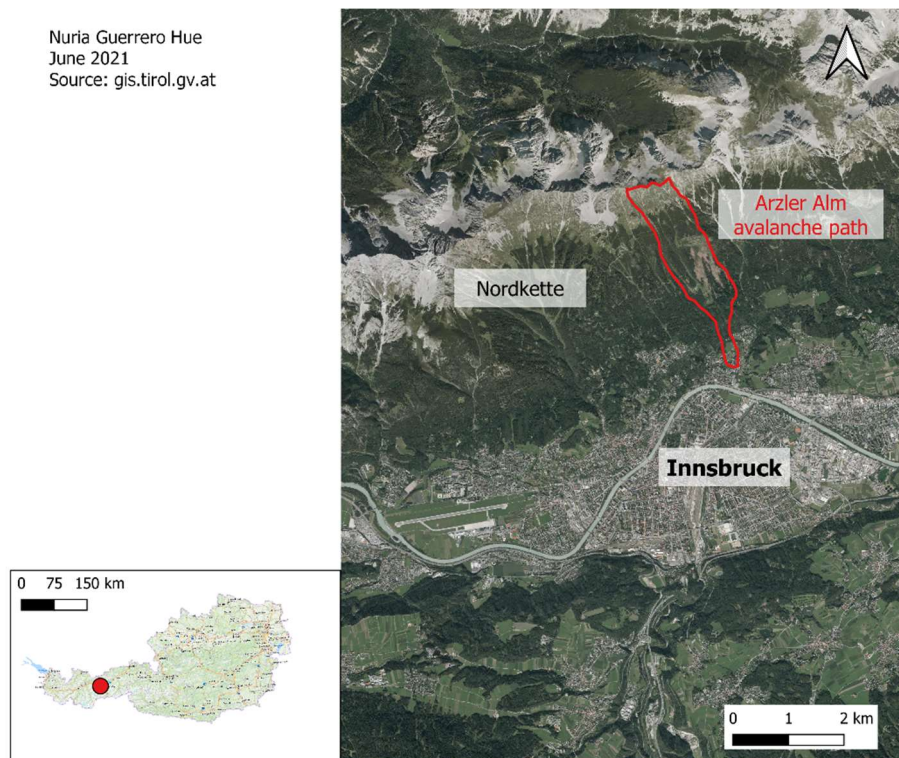


Figure 13: Location of the Arzler Alm avalanche path (in red), situated on the Nordkette ridge, north of the city of Innsbruck (Austria).

Innsbruck is in the Inn valley, a southwest-northeast typical U-shaped valley in western Austria. The city is divided by the river Inn, which gives it its name. The study area lies north of this river, on the south slope of the Nordkette ridge. In the lower part of the study area is a small torrent called Duftbachl, which flows into the river Inn (Stepanek, 2012). Further morphometric details of the avalanche path are provided in Figure 14.

Nuria Guerrero Hue
April 2021
Source: basemap.at

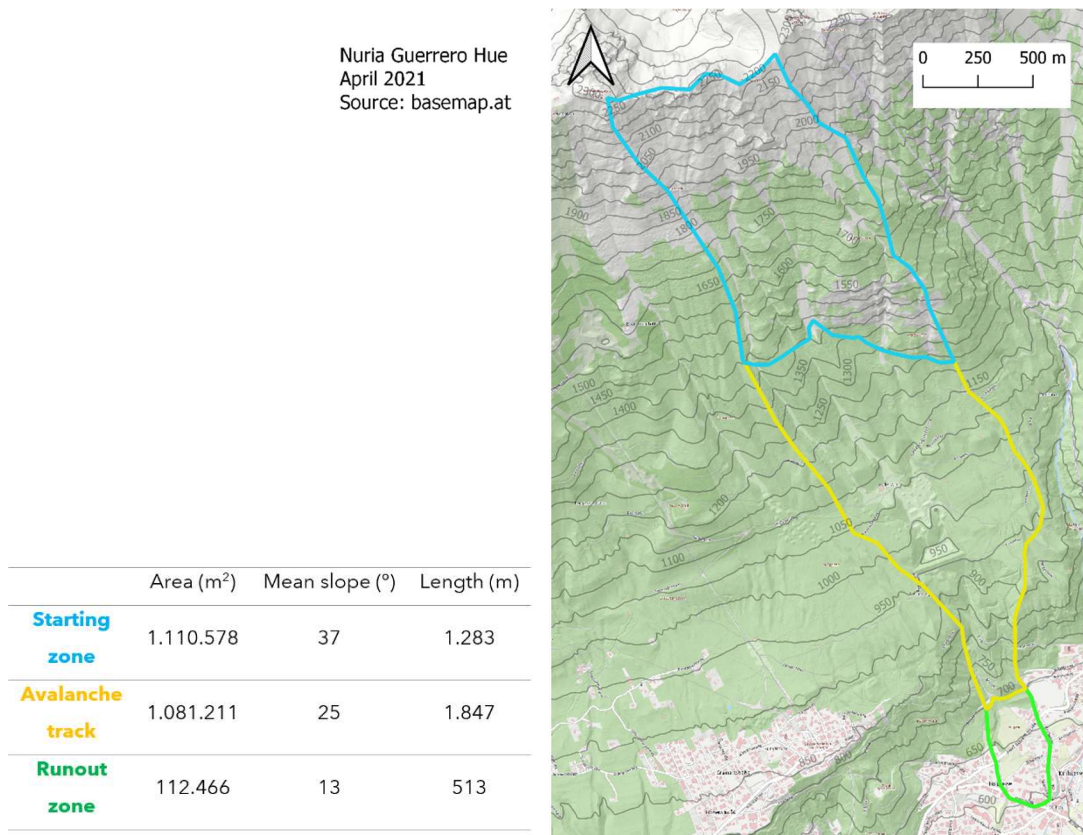


Figure 14: Parts of Arzler Alm avalanche path and morphometric parameters of each part.

Tyrol, the Nordkette ridge and specifically the Arzler Alm area have a strong recreational use by the citizens of Innsbruck: either for walking, alpine hiking, mountain biking or skiing in winter, and is also a hunting domain. There are also some meadows and pastures in the area with agricultural use (Figure 15). The well frequented mountain hut called "Arzler Alm" at 1607 m a.s.l. gives the name to the avalanche path (Stepanek, 2012). The land in the Nordkette is primarily privately owned and divided into small parcels, the smallest being less than 50 m². This fragmented private property is jointly managed by the city of Innsbruck for more than 100 years. Forest management including harvesting, provides some income to the owners as well as maintains the protective function of the forest (W. Huber, personal communication, 2019). All these socioeconomic activities on the slopes of the Nordkette have a strong influence on the vegetation including on each tree.



Figure 15: Multifunctional use of the area (hikers, a bike, livestock, and avalanche protection measures) (Foto: N. Guerrero Hue).

3.2 Geology

The Inn Valley belongs to a large sinistral fault separating (ENE-WSW) the Northern Calcareous Alps from other geologic units to the south (Innsbruck Quartz Phyllite Complex, Ötztal-Stubai Metamorphic Complex). The Northern Calcareous Alps extend from Liechtenstein to Baden bei Wien (approximately 500 km) and are a main geologic unit of the Eastern Alps. They are mainly composed of carbonate sedimentary rocks, subordinately of siliciclastic rocks and cherty sediments (radiolarite); volcanic rocks are very rare (Krainer & Meyer, 2016).

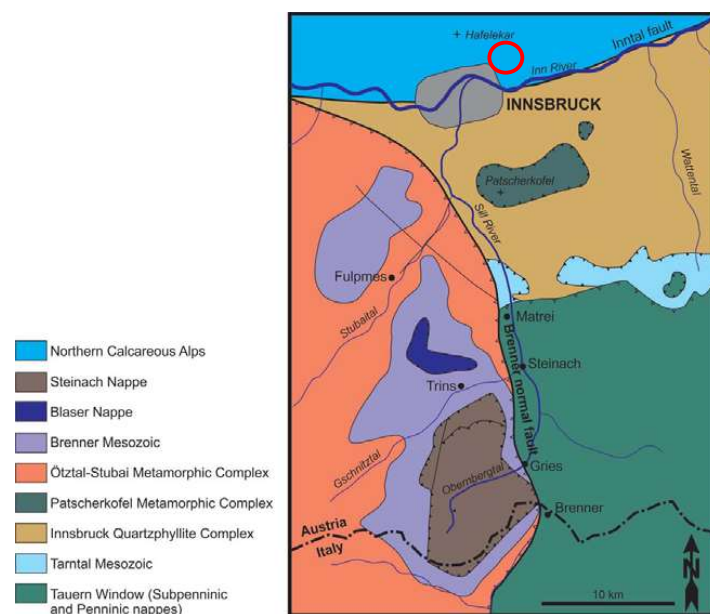


Figure 16: Simplified geologic map around Innsbruck (Krainer & Meyer, 2016).

The city of Innsbruck is situated on the alluvial fan formed by the river Sill at the confluence with the Inn river. The mountain range north of the city is called Karwendel and is part of the Northern Calcareous Alps. The study area (marked with a red circle in Figure 16) is on the south slope of the Nordkette ridge, which belongs to the Karwendel mountains.

3.3 Climate

Innsbruck and part of the Inn valley have a transitional climate from the subcontinental dry inner Alps to the cool, humid peripheral Alps (Kilian et al., 1994). According to the Köppen-Geiger classification, the city of Innsbruck has a warm humid continental climate (Figure 17) (climate-data.org, 2021).



Figure 17: Monthly mean temperature (red) and precipitation (blue) in Innsbruck (climate-data.org, 2021).

There are two meteorological stations in the city of Innsbruck belonging to the Central Institution for Meteorology and Geodynamics (in German: Zentralanstalt für Meteorologie und Geodynamik, ZAMG). One is situated at the University of Innsbruck and the other at the Innsbruck airport, and both are at 578 m a.s.l.. For the period 1981-2010 the mean annual temperature was 9.1°C and mean annual total precipitation was 899 mm (ZAMG, 2021). The dry south wind (Foehn) influences the climate of the area.

Snow

Due to its geographical location in the middle of the Alps and its altitude 574 m a.s.l., Innsbruck has a climatic predisposition for precipitation to occur in the form of snow during the winter months. Meteorological data related to snow measured in the city of Innsbruck for the period 1981-2010 (ZAMG, 2021) is shown in Table 2. Snow data from the weather stations at the Seegrube (1905 m a.s.l.) cannot be presented, due to lack of quality control (C. Tollinger, personal communication, 2020).

Table 2: Meteorological data related to snow in Innsbruck, measured at two meteorological stations at 578 m a.s.l. (1981-2010) (ZAMG, 2021).

mean annual amount of fresh snow	99 cm
absolute annual maximum value of snow depth	67 cm
annual number of days with a snow depth of at least 1 cm	63 days
annual number of days with a snow depth of at least 20 cm	12 days

The location of the study area in the Nordkette ridge, with an east-west orientation, can lead to quite large accumulations of snow (Stepanek, 2012). This is shown by the data of the weather station at the Seegrube (1905 m a.s.l.), located north-west of the study area. The mean annual total precipitation there is 1614 mm (1981-2010) (Hydrographischer Dienst, 2021) and the maximum amount of 3-day new snow is 323 cm (Tollinger, 2011). Furthermore, as explained later in this chapter (Section 3.8), in winter 2018/2019 a total of 8.2 m of fresh snow was measured at this station during a precipitation period of 17 days (Siegele et al., 2019). In higher parts of the Arzler Alm avalanche path some small wet snow avalanches can release until late spring (May, June) and their runout can reach the meadows around the mountain hut. These are small avalanche events, which happen indeed quite often, but do not endanger important settlements or infrastructure (M. Teich, personal communication, 2021).

3.4 Vegetation

According to the Forest Ecoregions of Austria by Kilian et al. 1994, Innsbruck is in the Northern intermediate Alps ecoregion ("Wuchsgebiet 2.1: Nördliche Zwischenalpen - Westteil"), that is the "zwischenalpine Fichten-Tannenwald-Gebiet". This interalpine spruce-fir forest ecoregion is a transition zone between the continental spruce forest ecoregion of the Inner Alps and the humid mixed deciduous forest ecoregions of the peripheral Alps, which are characterized by frequent precipitation. The spruce-fir forest is the main forest community in the submontane and montane belt; however, spruce has been often promoted by forest management and covers a larger proportion of the land area. Other natural forest communities are spruce-fir-beech forest ("Fichten-Tannen-Buchenwald") and scots pine forests ("Rotföhrenwälder"). At subalpine levels the spruce forest ("Fichtenwald") is well developed.

The study area lies on the montane altitudinal belt and the main tree species present are Norway spruce (*Picea abies* (L.) Karst.) and European beech (*Fagus sylvatica* L.), with a considerable presence of other conifers such as European silver fir (*Abies alba* Mill.), Scots pine (*Pinus sylvestris* L.) and European larch (*Larix decidua* Mill.) (Figure 18). At the highest elevation, under subalpine conditions, some mountain pines (*Pinus mugo* Turra) grow surrounded by alpine meadows and rocky steep slopes. Below 700 m a.s.l. there is no forest because this area is primarily comprised of urban and agricultural use.

Nuria Guerrero Hue
April 2021
Source: maps.tirol.gv.at & basemap.at

Vegetation

- Beech-fir forest
- Spruce-pine forest
- Spruce-fir forest
- Spruce forest
- Krummholz stand / Mountain pine

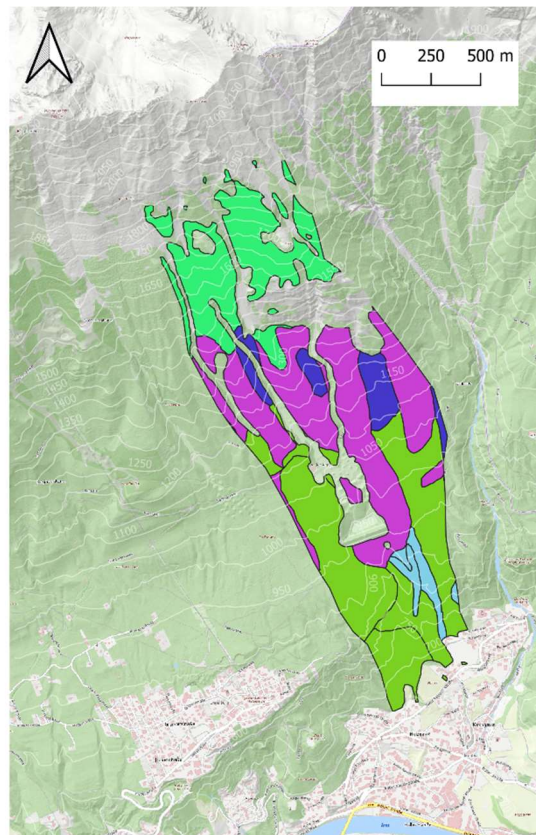


Figure 18: Vegetation of the Arzler Alm avalanche path.

3.5 Soil

In the study area calcareous rocks, loamy materials and undifferentiated alluvial or glacial deposits are present (Figure 19) (Umweltbundesamt, 2021). These soil types are classified by the Food and Agriculture Organization of the United Nations as calcaric lithosol, orthic rendzina, orthic luvisol and calcaric fluvisol (FAO, 2015).

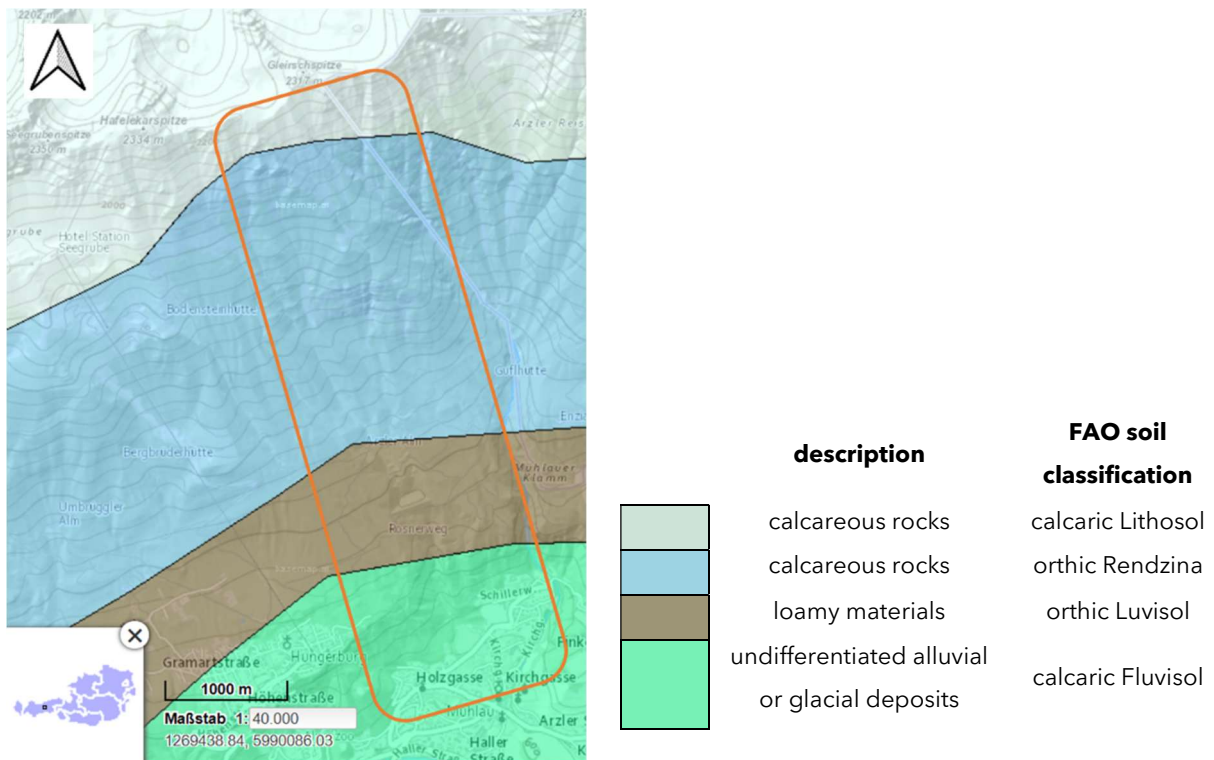


Figure 19: Soil types of the study area (in orange) according to FAO classification (Umweltbundesamt, 2021).

3.6 Historical avalanche events

The study area belongs to the municipality of Innsbruck and the avalanche deposition area lies in the district of Mühlau, a small village located north of the city centre. It can be considered as an avalanche in urban context and this fact makes it a well-documented avalanche path, with extensive historical records. The oldest documented avalanche event occurred in 1859 and since then, several catastrophic events have been recorded by means of a variety of historical archives (e.g., aerial photographs, newspaper articles, old avalanche documentation) and "silent witnesses". Snow avalanche events reached houses in Mühlau in 1859, 1875, January 1923, February 1935 and January 1968 (Fischer et al., 2013; Stepanek, 2012) (Figure 20). The documented extents of some big and small avalanches were provided by the Austrian Service for Torrent and Avalanche Control (WLV for its acronym in German) (Figure 21).

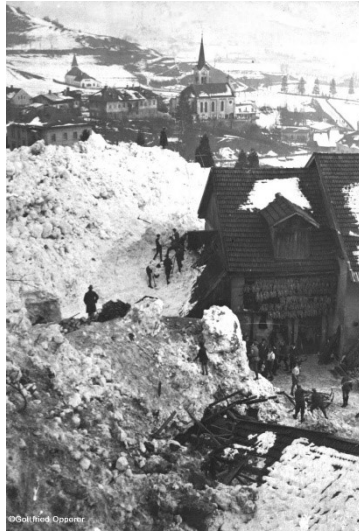


Figure 20: Avalanche debris reached the district of Mühlau (Innsbruck, Austria) on the 5th February 1935 (provided by L. Stepanek).

Nuria Guerrero Hue
April 2021
Source: WLV & basemap.at

Documented avalanches

- 1935
- 1967
- 1968
- 1970
- 1974

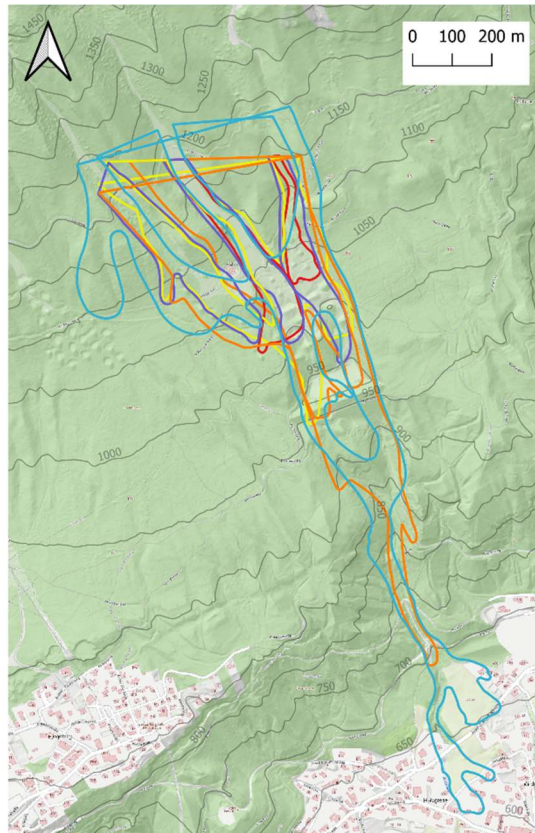


Figure 21: Documented extents of avalanche events in the Arzler Alm avalanche path before 2019.

Before January 2019, the previous event recorded in the catchment happened one year before. In January 2018, a total of 70,000 m³ of snow and debris were deposited around a series of deflection and catching dams. Despite the large deposited volume, no remarkable forest damages were reported, as it mainly flowed through some meadows (Adams et al., 2018).

3.7 Existing protection measures against snow avalanches

Due to this frequency of catastrophic events some protection measures were gradually developed (Adams et al., 2018; Kofler et al., 2018; Stepanek, 2012). After the catastrophic winter of 1951 a master plan for integral mitigation measures started in 1953, including not only technical defense structures but also forestry measures (Stepanek, 2012). This protection scheme against avalanches has been constantly developed, extended and updated, and measures are still ongoing, because of the constant threat to the population (Tollinger, 2011). Between 1935 and 1942 braking mounds (concrete wedges and earth cones) (Figure 22) as well as catching and deflection dams were erected in the avalanche path, east of the mountain hut. After the powder snow avalanche of 1968 a 20 m high catching earth dam was built (1974-1977) (Kofler et al., 2018; Stepanek, 2012). Additionally, sustainable forest management is carried out especially focusing on maintaining the protective function of the forest against avalanches (W. Huber, personal communication, 2019).

Nuria Guerrero Hue
April 2021
Source: gis.tirol.gv.at

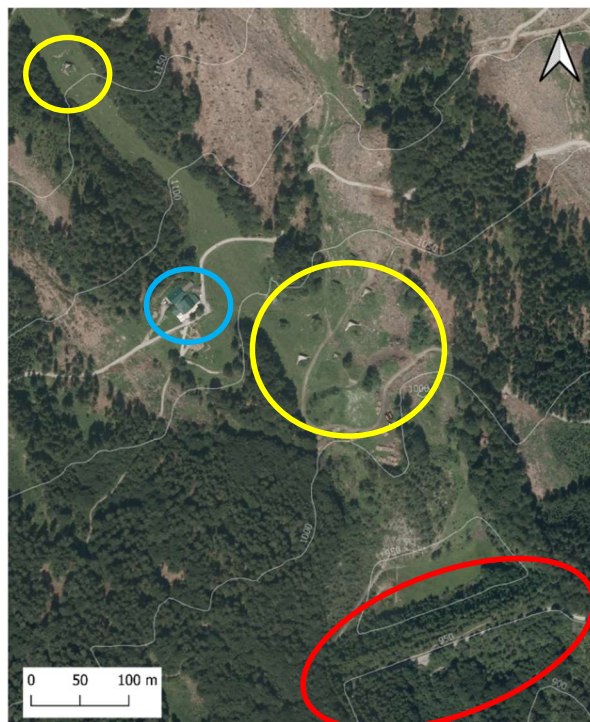


Figure 22: Some protection measures (the braking mounds (in yellow), and the catching earth dam (in red)) built close to the Arzler Alm mountain hut (in blue) (Orthophoto 2019).

Another important non-technical protection measure in the Arzler Alm avalanche path is the snow avalanche hazard zone plan (Amt der Tiroler Landesregierung, 2021; Forstgesetz, 1975) conducted by the Austrian Service for Torrent and Avalanche Control (Figure 23). This institution is constantly updating those plans with new results provided by the latest state-of-the-art of avalanche simulation models and improved input data (Tollinger, 2011).

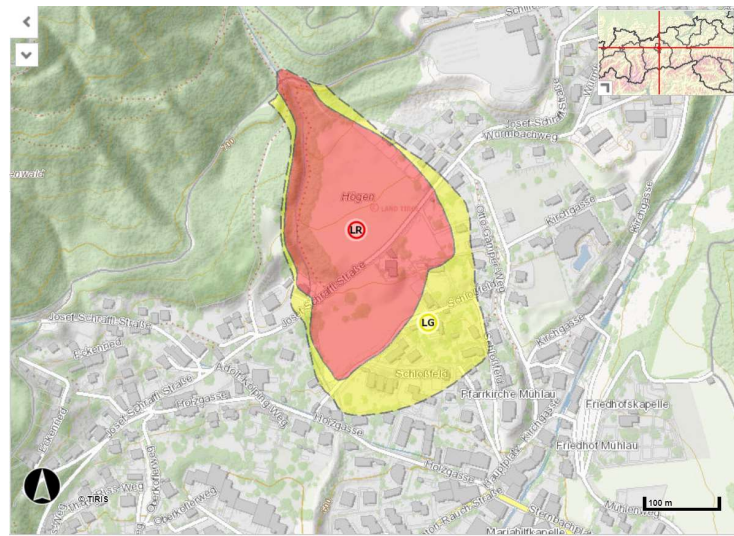


Figure 23: Snow avalanche hazard zone plan. The runout zone of the Arzler Alm avalanche path reaches the district of Mühldorf (Innsbruck). The red zone (avalanche pressure $> 10 \text{ kN/m}^2$) and yellow zone (avalanche pressure $1 - 10 \text{ kN/m}^2$) are calculated considering a design event with return period of 150 years (Amt der Tiroler Landesregierung, 2021; Forstgesetz, 1975).

3.8 Description of the avalanche released in January 2019

In the winter of 2018/2019 an unusual high amount of snow fell which consequently led to a high avalanche activity in the Eastern Alps (Siegele et al., 2019). On 14th of January 2019, a large avalanche was released above the Arzler Alm mountain hut, which caused extensive forest damage. A total of 8.2 m of fresh snow was measured on the Seegrube above Innsbruck (1905 m) over the entire precipitation period of 17 days (from 30.12.2018 to 15.01.2019) (Siegele et al., 2019). The Avalanche Warning Service Tyrol had reported a very high avalanche danger level (5/5) for that day because of fresh snow and strong wind. Precautionary closures of transportation routes were required (Office of the Tyrolean Provincial Government, 2021).



Figure 24: The Nordkette mountain ridge with the Arzler Alm avalanche, January 2019. In yellow, the earth dam at 945 m a.s.l. (Foto: LWD Tirol in (Siegele et al., 2019).

Due to the event documentation carried out by the Austrian Research Centre for Forests (BFW, for its acronym in German) (Fischer, 2019), it can be stated that the dominant process was a powder cloud avalanche with only a small dense flow portion. A slab avalanche released spontaneously below the Gleirschjöchl, fell across the Herzwiese meadow (1400-1550 m a.s.l.) and then split into various avalanche arms. The release volume was estimated to 29,000 m³ and because of entrainment (0.5 - 1 m) along the avalanche track its volume increased up to 80,000 - 160,000 m³. The avalanche deposition area was estimated with approximately 2.5 ha and deposit heights of up to approximately 3 m. The estimated deposited volume of debris is around 100,000 m³, which included a lot of foreign material: 5,000 m³ of damaged and broken trees were removed according to the forestry office of Innsbruck (W. Huber, personal communication, 2020). The maximum avalanche runout reached the edge of the catching earth dam located at about 945 m a.s.l. (Figure 24). Fortunately, there were neither human victims nor infrastructure damaged; however, a bare spot without trees is still clearly visible from the city of Innsbruck today. This event was categorized as having a destructive size of 3 - 4 and an „extreme - XL“ intensity (scale in (McClung & Schaerer, 2006). A summary of avalanche's characteristics can be found in Table 3.

Table 3: Characteristics of the avalanche event at the Arzler Alm on the 14th of January 2019. Some data could only be estimated (Fischer, 2019; Siegele et al., 2019).

Type of avalanche	powder cloud avalanche with only a small dense flow portion
Starting zone	slab avalanche
Release volume	29.000 m ³
Entrainment	0,5 - 1 m
Avalanche volume estimated	80.000 – 160.000 m ³
Deposition area	2,5 ha
Deposition height	3,0 m
Deposition volume estimated	100.000 m ³
Intensity WLIV	XL - extreme
Destructive size	3 - 4
Triggering factor	spontaneous avalanche directly related to the precipitation period

From April to December 2019 forestry workers were organized to clean the area of broken and downed trees and to eliminate the danger of debris being transported downslope. Additionally, the braking mounds close to the Arzler Alm hut were restored after woody debris was removed (Figure 25 a and b). This event together with the considerable archival material of old avalanches (Section 3.6) provided the opportunity to conduct the present study. It will be from now on referred as the “avalanche of January 2019” or simply “avalanche 2019”.

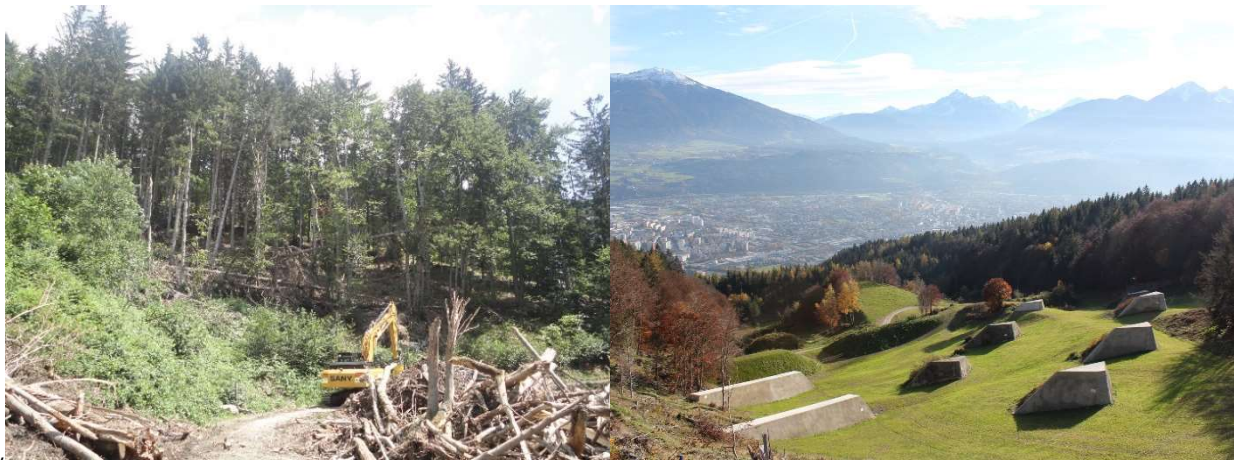


Figure 25 a, b: On the left, forestry workers remove all woody debris after avalanche 2019 (Foto - July 2019) and on the right, renovated protection measures close to the Arzler Alm mountain hut (Foto - November 2020) (Fotos: N. Guerrero Hue).

As an example of the tremendous impact and pulling forces that occurred inside the avalanche, it is noteworthy to mention that an emblematic 180-year-old fir (*Abies alba*) was transported 200 m downhill from its original position (Figure 26). Forest workers found it quite intact, with its approx. 40 m long stem and approx. 140 cm diameter. It means that around 20 tons were pulled out of the ground and moved by the avalanche 200 m downhill.



Figure 26: Stump of a 180 year old *Abies alba* tree killed and transported 200 m downhill by the avalanche in January 2019 (Foto: N. Guerrero Hue).

4 MATERIAL AND METHODS

4.1 Fieldwork

Sampling strategy was designed following the recommendations from various scientific papers (Stoffel et al., 2013; Stoffel & Bollschweiler, 2008; Stoffel & Corona, 2014) and input from K. Nicolussi and M. Teich. The study area was divided in two parts (Figure 27), according to topography, forest area damaged in January 2019 and the location of a protection earth dam (located at approx. 945 m a.s.l.). Uphill of the earth dam sampling was performed along three altitudinal transects at elevations of 1200, 1100 and 1000 m a.s.l. covering the damaged area. Additionally, some trees at 1050 m a.s.l. were also sampled, to cover some arms of the avalanche affected in 2019. Below the earth dam a selective sampling scheme was carried out along the gully, where avalanches had previously been observed until 1968, named "lower area" (LA).

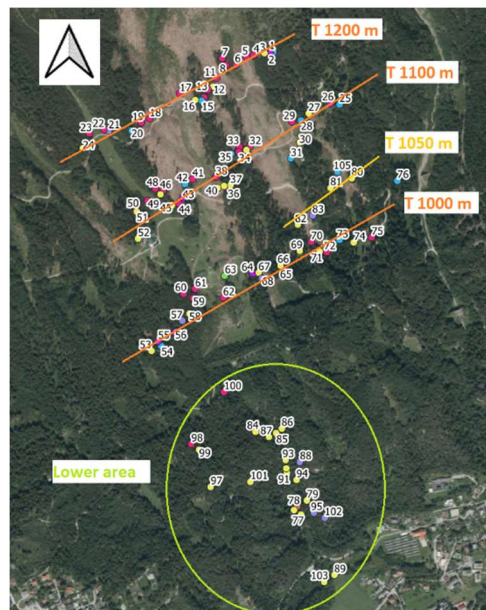


Figure 27: Sampling strategy: altitudinal transects (T1200, T1100, T1050, T1000) and a selective sampling in the lower area (LA; circled) (orthophoto 2019).

As Stoffel et al. 2013 suggest sampling at least 100 trees in an avalanche path, I pursued this goal and cored approximately 25 trees per transect.

4.1.1 Selection of trees

Sampling of a tree was carried out after a careful visual inspection of it and its surroundings. To perform a proper sampling, the following criteria were followed (Stoffel et al., 2013; Stoffel & Bollschweiler, 2008; Stoffel & Corona, 2014):

- Mixture of trees damaged and undisturbed trees were selected. This means either trees clearly damaged by the avalanche (Section 2.4) or undisturbed trees without any type of external damage.
- Trees with external signs of damages not caused by avalanches were avoided. Other possible causes that could have damaged tree's cambium such as rockfall, game, wood harvesting, road construction, biotic agents (insects, fungus, woodpeckers, etc), abiotic (lighting, frost, etc.), anthropogenic, were to be excluded.
- Mixture of tree species, including not only conifers but also broadleaved trees.
- Balance of old and young trees or rather small and large diameter classes.
- Trees located in their original position (even broken, leaning, fallen or stumps). Trees that could have been removed and transported by the avalanche 2019 were avoided.
- Distance between trees: no rule could be applied. Depending on field and forest conditions.

Some broken, leaning, fallen or tilted trees and stumps were also chosen, which represented possible evidence of avalanche impact. In case of leaning or fallen trees the direction (azimuth) of the stem was measured. By fallen trees also its length was measured. If trees were broken, with or without a stump, or uprooted it was noted on the field sheet.

4.1.2 Description of damage

In case of damaged trees, type, position, and degree of damage was described and recorded. Options from the field sheet are (ANNEX I: Field sheet):

- Types of damages due to snow avalanche:
 - dead
 - scar
 - bordering callous tissue (overgrowing)
 - eccentricity (stem not round)
 - broken branches or crown (flag)
 - tilting (inclined, leaned)
 - broken top (decapitation)
 - new vertical stem ("candelabra" from)
 - uprooted

- If other types of damages present, it was described (e.g., insect holes, woodpecker, harvesting, anthropogenic)
- Age: recent (with resin) or old (overgrowing tissue)
- Position: stem, branches and / or roots
- Degree: low, medium, high (considering the probability that the tree recovers from the damage and survives)

4.1.3 Tree information

In addition to tree species, several tree and terrain parameters were measured (DBH, tree height, crown height, slope, social status) and position of each tree was recorded with a GPS device (Emlid Reach RS +, device with typical measurement precision: vertical 14mm; horizontal 7mm) (Figure 28 a and b).



Figure 28 a, b: Some fieldwork devices, on the left the GPS device and on the right the forest calliper used to measure tree diameter (Fotos: N. Guerrero Hue).

Also, information about surroundings of the tree was noted (if there were other trees around, meadow, forest road, hiking path) and the position related to the avalanche 2019 (in the middle of the path, in the margin or outside). Some pictures of every tree, damages and surroundings were taken, and the tree was marked with flagging.

4.1.4 Coring trees

At least two cores per tree were taken using an increment borer (Haglöfs, 0.5 cm diameter) (Grissino-Mayer, 2003) (Figure 29). One core was taken in the contour line direction (from the side, lateral) to avoid reaction wood. A second core was taken to catch possible reaction wood. This means from downhill of the tree for conifers and from uphill for broadleaves. In case the tree had external damages as scars or callous tissue, a core was taken in the direction of the damage (in the middle of the scar or right next to it) and another core was taken at the opposite side of it, to see if the tree had reacted to the damage. Coring height was usually 1.30 m. If this was not possible, a comfortable height for coring was chosen. Height was measured from uphill and written down for each core.



Figure 29: Coring a tree with the increment borer (Foto: N. Guerrero Hue).

Coding of trees and cores:

Each core was coded including this information: tree location, tree number and core letter.

- Location: abbreviation for each transect (T1200, T1100, T1050, T1000) or for the lower area (LA).
- Tree number: each sampled tree had a number, starting from one and following consecutive numbering for whole sampling (so that each number was used only once).
- Core letter: depending on the coring direction through the stem (Figure 30):
 - o A: core in direction of contour line (lateral)
 - o B: core in direction of possible reaction wood
 - o C: direction of scar / damage or next to it
 - o D: opposite to C
 - o O: opposite to reaction wood (exceptional cases)

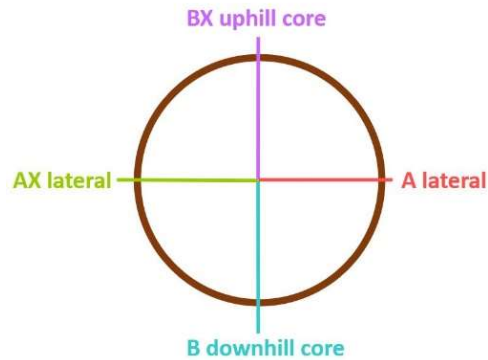


Figure 30: Coding of cores depending on the coring direction through the stem, in this case for a conifer (core B taken from downhill of the tree to catch possible reaction wood).

One example is core T1100-074B (example of field sheet in ANNEX I: Field sheet). The tree was located in the transect at 1100 m a.s.l., it was the 74th tree sampled and this core was taken to capture possible reaction wood (B).

4.2 Dendrochronological procedures

4.2.1 Sample preparation

Each core was prepared following standard dendrochronological procedures (Stoffel, 2005; Stoffel & Bollschweiler, 2008). First, samples were gradually extracted from their storage envelopes and put on a metallic reusable support. Special attention was given to the orientation of wood-fibres: where they must be vertically oriented for later analysis (Stoffel, 2005). Next, cores were prepared by cutting their upper surface with a razor blade and then white chalk powder was spread on the core to better distinguish the tree rings (Gärtner et al., 2015; Stoffel, 2005) (Figure 31a). The support allowed turning the core and cutting different surfaces in case the core was twisted.

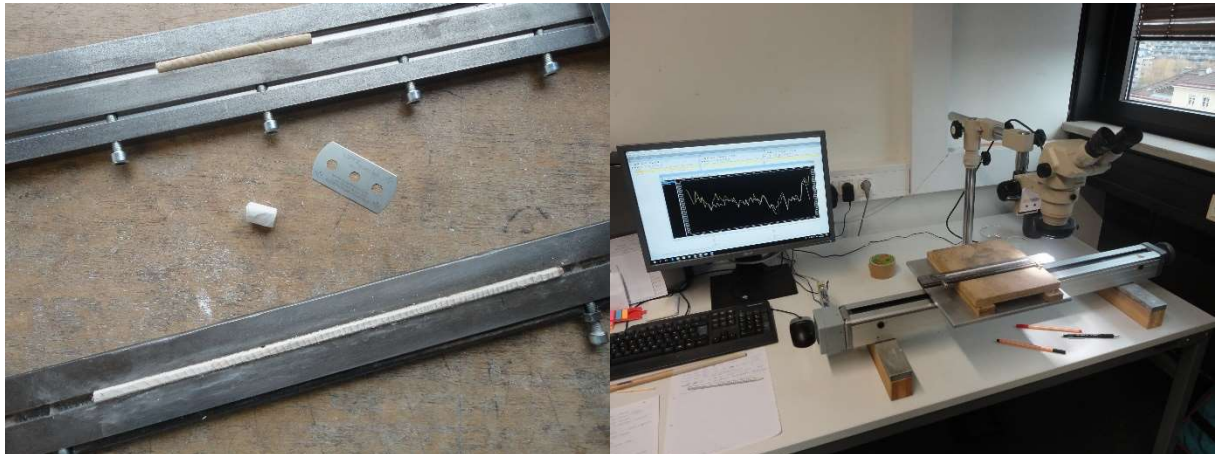


Figure 31 a, b: On the left, preparation of cores using a razor blade and chalk. On the right, digital positioning table connected to a binocular microscope and time-series analysis software to measure tree rings (Fotos: N. Guerrero Hue).

4.2.2 Tree-ring width

Tree rings were measured using a digital positioning table (LINTAB) connected to a binocular microscope and the time-series analysis software TSAP-Win (Version 4.64, Rinntech 2011) (Figure 31b). Tree rings were measured to the nearest 0.01mm at approximately 40x magnification.

Tree-ring width must be measured perpendicular to latewood, which generally corresponds to the radial growth direction. Measurements started from the outermost tree ring (corresponding to year 2019 for most of the trees) and continued until the pith or end of the core was reached. Next, if the core did not contain the pith, the number of missing rings until the pith was estimated using a transparent foil sheet which contained concentric circles to represent different ring sizes. Additionally, it was observed if the last tree ring, called waney edge (“Waldkante” in German), was completely formed or not. Finally, some tree rings were marked with dots as follows: starting from the bark (2019) a dot was drawn every ten years (2009, 1999, 1989, etc.), two dots every fifty years (1969, 1869) and three dots every 100 years (1919). This procedure was helpful to find a specific tree ring in later steps (Neumann, 2011; Stoffel, 2005).

In case cores reached beyond the pith, each side from the pith was measured separately and considered as a different core. To designate those pieces exceeding the pith, an X was added to the core name. That is, if core T1100-036a was longer than the pith, this piece was designated as a new core as T1100-036ax (Figure 30).

4.2.3 Cross-dating

When all cores were measured, series were cross-dated to each other in order to detect possible mistakes such as false rings or missing rings. This consisted in comparing visually and statistically (Glk) all series of the same tree with TSAP-Win. Detected problems were amended.

The parameter *Gleichläufigkeit* (Glk) is used by cross-dating, to express the quality of accordance between time series (i.e., measured cores). Glk measures the year-to-year agreement between the interval trends of two chronologies and is expressed in % (Kaennel & Schweingruber, 2021; Rinn, 2011). With values of Glk > 60% can be considered that there is a reasonably good match between the two ring width series or a ring width series and a chronology (K. Nicolussi, personal communication, 2020).

Ring-width series were also cross-dated with two regional reference chronologies. The closest chronologies available to the study area, both for spruce, were: one for low elevation forest stands in Bavaria (south Germany) (Wilson et al., 2004) and the other one for high elevation forest stands in the Zillertal (a valley in Tyrol, Austria) (Vospertnik et al., 2014). First, local chronologies were established after standardization of the individual tree-ring series. This was done separately for each site (i.e., T1200, T1100, T1000, LA). Second, each local site chronology was cross-dated with both regional chronologies.

4.2.4 Estimation of minimum age

A coarse estimation to obtain the minimum age of sampled trees was performed in three steps. First, the number of tree rings of the longest core of each tree was used. Second, the number of missing rings until pith was estimated (see Section 3.5.2) and third, the number of missing rings until coring height was calculated. Considering the mean annual height growth of the different tree species available, 15, 20 or 10 tree rings were added for *Picea* and *Pinus*, for *Abies* and for *Larix* respectively (considering coring height 1.30 m, otherwise it was calculated proportionally).

4.2.5 Avalanche indicators in tree rings

After measuring ring width, a careful visual observation of all tree rings was carried out using the microscope to search for internal avalanche indicators. As explained in Section 2.4, features such as traumatic resin ducts (TRD), compression wood (CW), callous tissue (CT) or abrupt growth changes (AGC) can be seen within annual rings and are called growth disturbances, growth anomalies or avalanche indicators in the literature. We decided to use the term "avalanche indicators" (AI).

TRD, CW or CT were observed and type, position and / or intensity was noted (Figure 32). For this purpose, an identification key was prepared to facilitate classification (ANNEX II: Identification key for). Separately, AGC were to be calculated using tree-ring width (Section 4.2.6).



Figure 32: A tangential row of traumatic resin ducts in the middle of earlywood cells. Avalanche indicator with intensity 3 (moderate) following Table 4 (Foto: N. Guerrero Hue).

Criteria to define each avalanche indicators and their intensities are based on their appearance and / or persistence in the tree-ring series, adapted from Stoffel & Corona (2014), as shown in Table 4. Three reaction intensities were considered: weak, moderate and strong. In case of compression wood, it was only noted which tree rings showed compression wood cells in at least half of the tree-ring width as a sign of a strong reaction. In later analysis only avalanche indicators in dormant (D) or early earlywood (EE) positions were considered (Chiroiu et al., 2015; Kogelnig-Mayer et al., 2011; Stoffel, 2005). Finally, the AI observed in the first decade of juvenile growth were excluded, as seedlings tend to produce more CW or TRD (Stoffel & Bollschweiler, 2008).

Table 4: Definition of intensities of avalanche indicators (AI) based on their intensity (appearance and/or persistence) in the tree-ring series (adapted from (Stoffel & Corona, 2014)). Not applicable (N/A).

Avalanche indicator	Parameter	weak AI	moderate AI	strong AI
Injuries, callous tissue		N/A	N/A	presence of callous tissue or injury
	intensity			4
Traumatic Resin Ducts		tangentially aligned, with clearly observable gaps between TRDs (< 50% ring width)	compact, but not completely continuous rows (50-90% ring width)	extremely compact and continuous rows (>90% ring width)
	intensity	2	3	4
Compression wood	duration	2 - 3 yrs	4 - 8 yrs	≥ 8 yrs
	intensity	2	3	4

4.2.6 Abrupt growth changes

AGC are calculated using the ring width data. R statistical software (R Development Core Team, 2013) was used in this step and the input data were the ring width files obtained with TSAP-Win. Both suppressions and releases are commonly identified by a decreased or an increased radial growth exceeding a predefined threshold (Altman et al., 2014). In scientific papers there are many different methods to detect AGC based on tree-ring data (Altman et al., 2014; Stoffel & Corona, 2014; van der Maaten-Theunissen et al., 2015; Zrost et al., 2008). For example, Altman et al. (2014) used 24 different methods to calculate AGC, i.e. only releases.

My intention was to calculate AGC as in Stoffel & Corona (2014), but how exactly to perform this calculation is not described in their publication. After an extended literature search and applying different methods and tests to my data, but without obtaining satisfactory results, I had to discard to use AGC as indicator of avalanches in this study (further details in ANNEX III: Calculation of abrupt growth change). Therefore, growth changes were not considered as an avalanche indicator in following steps.

4.3 Detection of avalanche events in tree rings

The common steps for the detection of avalanche events are: identifying the number of trees showing AI, weighting of the signal (AI), comparing with historical records and observing spatial distribution (Favillier et al., 2017; Muntán, 2016; Neumann, 2011; Stoffel, 2005; Stoffel & Bollschweiler, 2008).

4.3.1 Responding trees

In the first step a minimum number or percentage of responding trees must be set. It is not accepted to infer an avalanche event based on a reaction of a single tree (Butler & Sawyer, 2008). Since my main references used different thresholds, I combined them in a tailor-made approach, as I was getting and observing my results.

The Avalanche Activity Index (AAI) is the percentage of trees showing responses in their tree rings in relation to the number of sampled trees being alive in a year. It is also called Shroder Index, Index value or I_t .

For my analysis I used a threshold of at least $AAI \geq 5\%$ of trees showing a reaction for a specific year as was done in Favillier et al. (2017). Regarding the number of trees showing an AI in a year, a minimum of three disturbed trees in one year was set according to Corona et al. (2012) and Meseşan et al. (2019). Some authors set a minimum number of trees alive per year (de Bouchard d'Aubeterre et al., 2019;

Mainieri et al., 2020). In my case with the two previous parameters fixed, a minimum of 10 trees alive per year (sample depth) was defined.

4.3.2 Weighting of avalanche indicators - reaction classes

Subsequently a weighting of the AI was performed, that is, a reaction class (RC) was assigned to each type of AI as shown in Table 5. I decided to continue working with the same reference (Stoffel & Corona, 2014), however different rating criteria are available, and some authors even decide not to carry out this weighting step (Martin & Germain, 2016; Muntán, 2016). The idea behind this step is that some of the specific features in tree rings, which can be used as avalanche indicators, are more likely caused by snow avalanches than others, which might have been caused by other factors (ecological, climatical, anthropogenic). According to Stoffel & Corona (2014) RC 4 and 5 can be considered as the consequence of a snow avalanche with high certainty. That is why scars and strong TRDs are assigned RC 5 (the highest) and weak TRDs are assigned RC 1 (the lowest).

Table 5: Reaction classes assigned to each type of avalanche indicators (AI) based on the weighting criteria of (Stoffel & Corona, 2014).

Reaction class	Type and intensity of avalanche indicator
5	Strong TRD, strong scar
4	Kill date, moderate TRDs, callus tissue, strong reaction wood
3	Moderate reaction wood
2	Weak reaction wood
1	Weak TRDs

Moreover, Meseşan et al. (2019) determined at least one tree with an AI with RC 4 or 5 was needed to infer an avalanche event. Therefore, only those years which had a RC 4 or 5 AI were further considered. As a result of these steps, a list of potential avalanche years was obtained.

To sum up, AI were identified (ANNEX II: Identification key for avalanche indicators), classified according to their intensity (Table 4) and then assigned a RC (Table 5). The AI in the first decade of juvenile growth were excluded. After applying some thresholds ($AAI \geq 5\%$, at least 3 trees with AI and at least one RC 4 or 5) a list of potential avalanche years was obtained for two datasets. The dataset named "all positions" included all AI present in all positions in a tree ring (i.e., D, EE, EW, LW). In the other dataset, named "filtered positions", AI were filtered according to their position in a tree ring, so only those located in the D or EE positions were considered.

4.3.3 Comparison with historical records

Next, I checked if any known avalanche year (documented with historical records) appeared on those lists. This step is performed as a validation of the procedure and can help to adjust the thresholds fixed in previous steps by considering the historical events in the study area (see references at the beginning of Section 4.3).

4.3.4 Spatial distribution of potential avalanche years

Since the exact location of each tree sampled was recorded with a GPS device, the spatial distribution of trees with avalanche indicators with strong RC was observed by means of a geographic information system software (QGIS). Here I looked at the distribution of damaged trees: if they were grouped, arranged in a strip, or distributed evenly throughout the area, where they were placed in the terrain considering the geomorphology, and, in case of documented avalanche years, if the pattern of damaged and undisturbed trees was similar to the available documented extent. This step helped to decide in a visual way if a potential avalanche would be comprehensible, according to the spatial distribution of damaged trees. Ideally, there should be various trees with strong reactions in the same year (see references at the beginning of Section 4.3).

4.3.5 Ecological and climatical factors

Ecological and climatical factors can induce similar reactions as geomorphological disturbances in tree rings and radial growth (Favillier et al., 2017; Neumann, 2011; Stoffel & Bollschweiler, 2008). For this reason, insect outbreak episodes or extremely cold and/or dry years must be considered if coinciding with any potential avalanche year detected (Favillier et al., 2017).

In the Nordkette mountain ridge there are no records of any insect outbreak episodes affecting the tree species present (in our case, mainly *Picea abies* and *Fagus sylvatica*) (W. Huber, personal communication, 2020). According to K. Nicolussi (personal communication, 2020) the following climate extremes could have influenced the growth of trees in the south-exposed study area: 1947 warm summer, 1976 dry year, 2003 dry year, 2018 warm summer.

5 RESULTS

5.1 Fieldwork and dendrochronology

5.1.1 Sampled trees and external damages

For this study we sampled 104 trees distributed across the avalanche track and deposition area. Tree species sampled were mainly *Picea abies* and *Fagus sylvatica* (41 and 37 trees respectively). In addition, *Abies alba* (11), *Pinus sylvestris* (7), *Larix decidua* (6), *Betula pendula* (1) and *Ostrya carpinifolia* (1) were sampled, as shown in Figure 33.

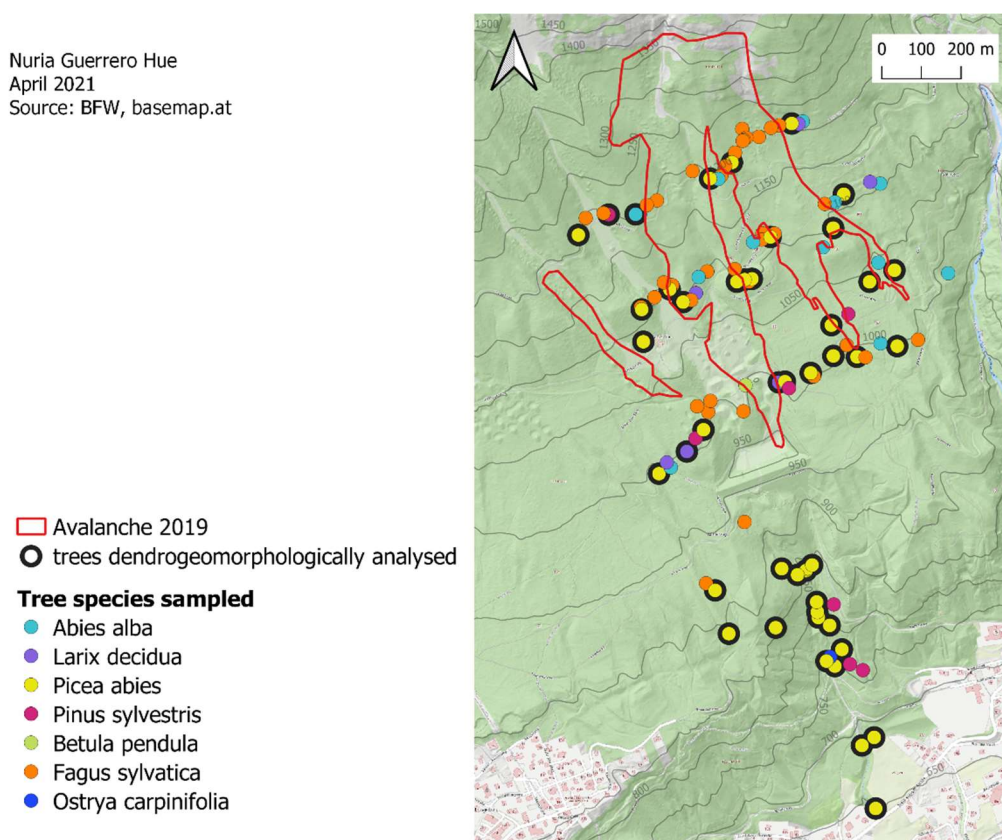


Figure 33: Distribution of tree species sampled in the study area and outlined in black those trees dendrogeomorphologically analysed. In red the extent of avalanche 2019.

From 104 sampled trees, 42 were externally undisturbed (Figure 34). Among the 62 disturbed trees, a variety of external damages were observed: broken branches or broken crowns in trees at higher transects affected by the avalanche 2019, trees showing a candelabra shape through the whole sampling area and insect holes in trees of the lower area. It was considered that 27 trees were damaged by the avalanche 2019, the other damages were assumed to be older.

Of course, type of damage and number of trees damaged were influenced by the sampling strategy. Moreover, it must be noted that some types of damages initially planned to consider, were however mostly avoided in the field (i.e., stumps, tilted or leaning trees), as discussed in Section 6.3.2.

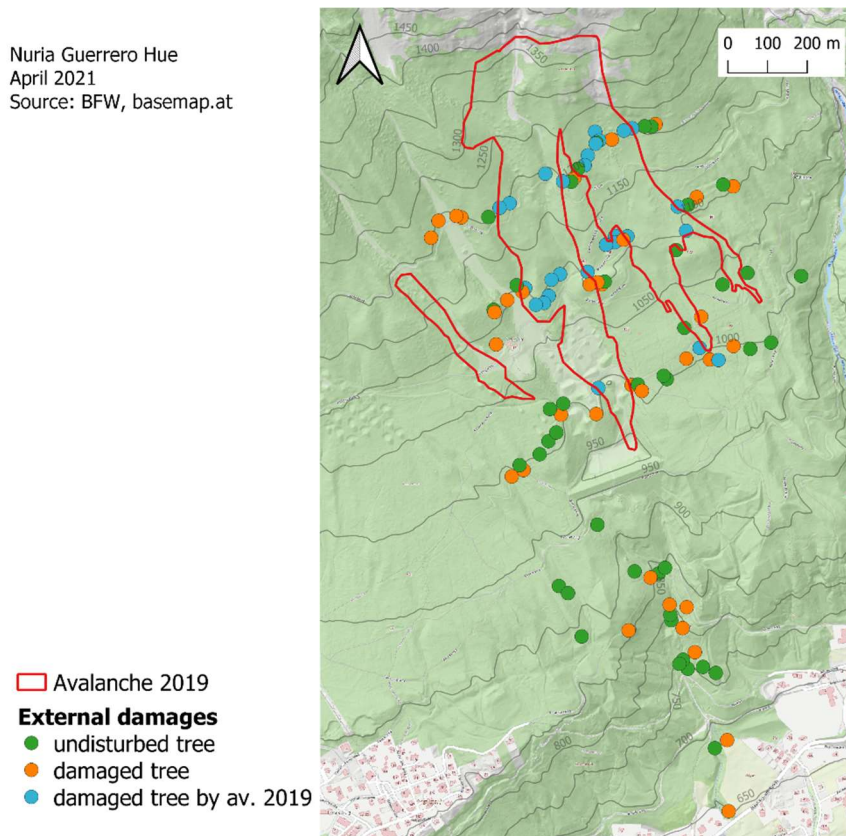


Figure 34: Spatial distribution of trees with and without external damage: damaged trees in orange and undisturbed trees in green. In blue, trees with damages attributed to the avalanche 2019, in red its extent.

Trees with damages attributed to the avalanche 2019 did not fit exactly with the extent of the avalanche (Figure 34). This is because the area mapped corresponds to the extension of deposited snow, but damaged trees were found further away, due to the powder snow cloud. Therefore, the forest area affected by the avalanche was different than the deposited snow (i.e., trees with broken branches in the middle of the crown).

5.1.2 Tree-ring width

For the dendrogeomorphological analysis only 45 trees were used, due to time-constraints (see trees outlined in black in Figure 33). For that purpose, only conifers distributed throughout the entire sampled area were chosen, considering that not all AI are to be observed in broad-leaved trees and that almost all referenced studies used conifers. This means that for those 45 trees, tree-ring width was measured, AI present in tree rings were observed and their intensity and position in tree ring were noted.

From the analysed trees, 21 were externally undisturbed and 24 were damaged. It was considered that 4 trees were damaged by the avalanche 2019 and that the other 20 trees were previously damaged. There were 133 cores from these 45 trees, and in total 8315 tree rings were carefully measured and observed. Figure 35 shows the sample depth in number of trees and number of cores available for each calendar year.

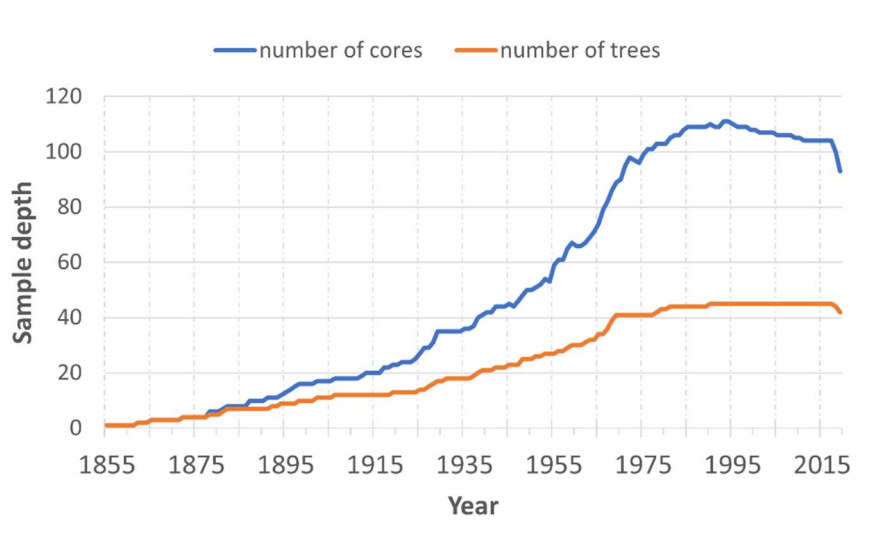


Figure 35: Number of trees and number of cores available for each year (sample depth) (1855-2019).

The oldest tree ring was dated to the year 1855 and therefore the period between 1855-2019 could be studied. In total 165 years could be examined. The shortest core was only 27 tree rings long. Mean ring width is $2.829 \text{ mm} \pm 1.032$. The widest tree ring measured 12.664 mm and the narrowest 0.01 mm. All ring width diagrams for the 45 trees are shown in ANNEX IV: Tree-ring width diagrams.

5.1.3 Eccentricity

Two trees showed clear eccentricity between two of their ring width series: tree no. 24 showed eccentricity starting from year 1999 and tree no. 51 from 1984 (Figure 36 and Figure 37).

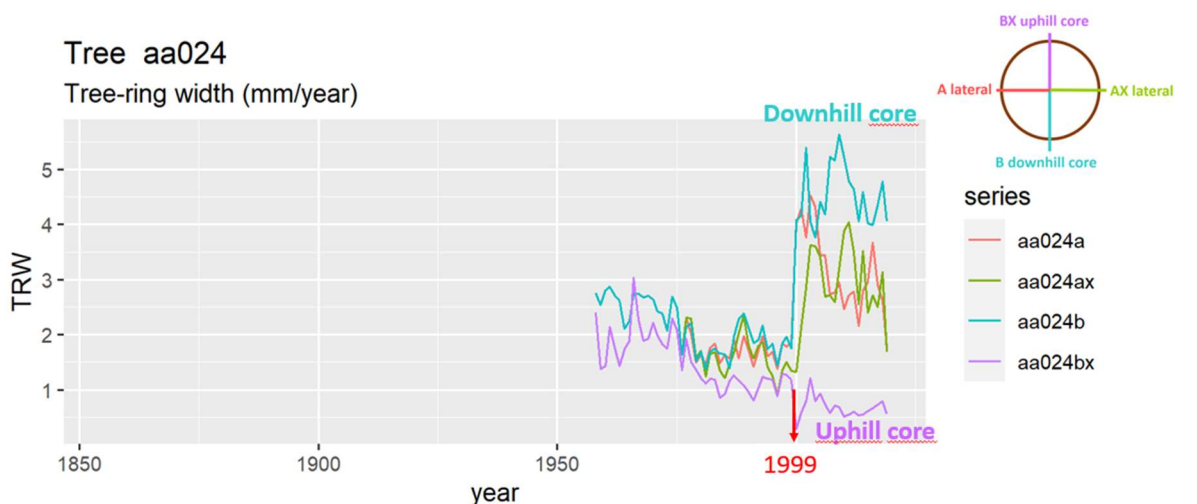


Figure 36: Tree-ring width diagram of tree no. 24 showing eccentricity from year 1999.

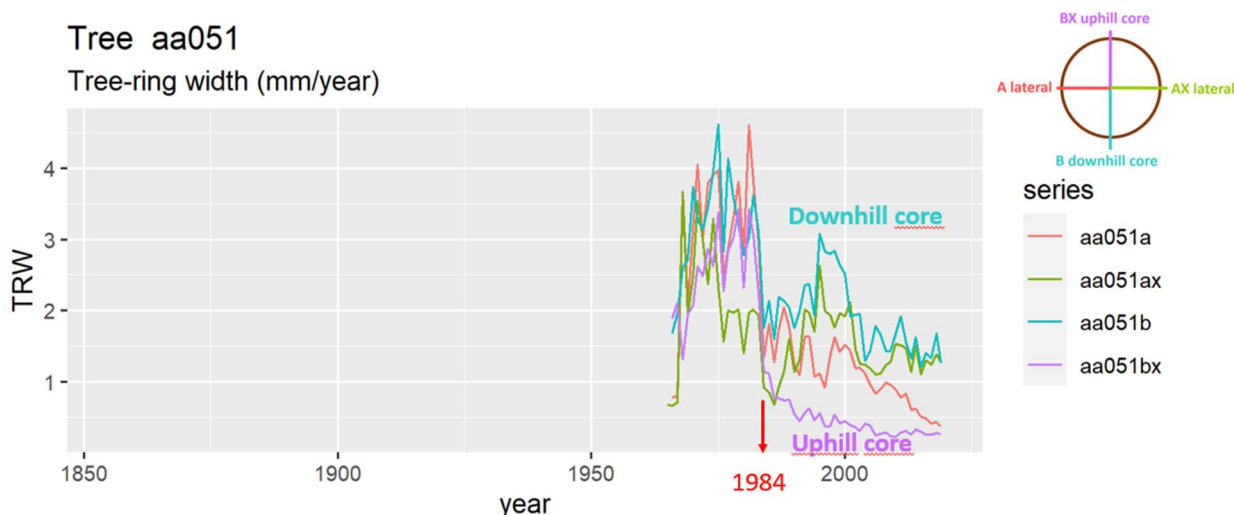


Figure 37: Tree-ring width diagram of tree no. 51 showing eccentricity from year 1984.

In case of tree no. 24, its tree rings exhibited in following years CW and TRD. However, tree rings of tree no. 51 presented no additional AI in the following years. Neither year 1984 nor 1999 appeared in the lists of potential avalanche years (Table 8, Table 9). Therefore, eccentricity could not be used to confirm the potential avalanche years detected with the applied criteria (Section 4.3.).

5.1.4 Cross-dating

All ring width series of each tree were cross-dated to each other and so, the kill date of trees sampled dead could be established (Section 5.2.1). Additionally, missing rings could be identified, and all series could be correctly dated. In a following step, averaged ring width series of the different sites (T1200, T1100, T1050, T1000, LA) were cross-dated with two regional reference chronologies (Figure 38 and Figure 39). Most series did not show a significant fit with those chronologies ($G_{lk} < 60\%$). However, some trees located in the LA site presented a reasonably good match with the low elevation chronology from Bavaria (G_{lk} between 57-74%) as it can be seen in the lowest graph of Figure 38.

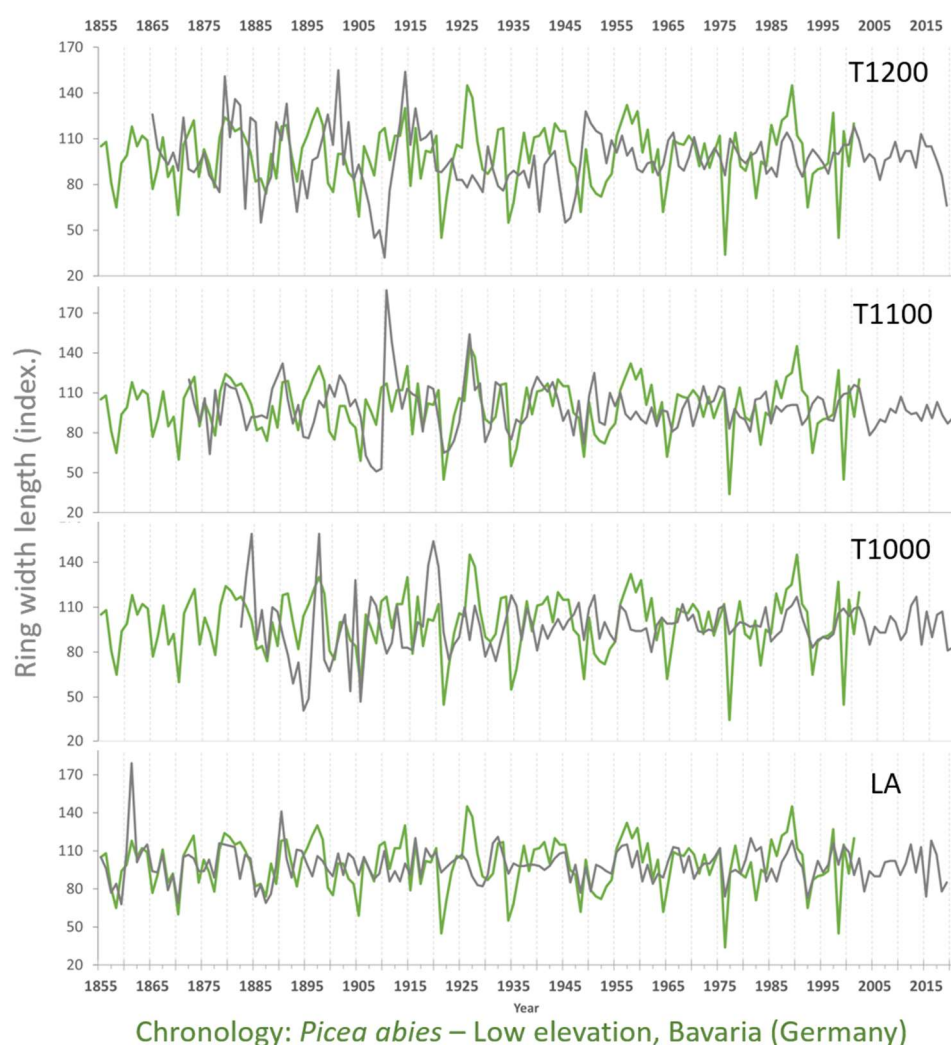


Figure 38: Local site chronologies (T1200, T1100, T1000, LA; in grey) in comparison with a regional spruce chronology (low elevation, Bavaria, Germany; in green).

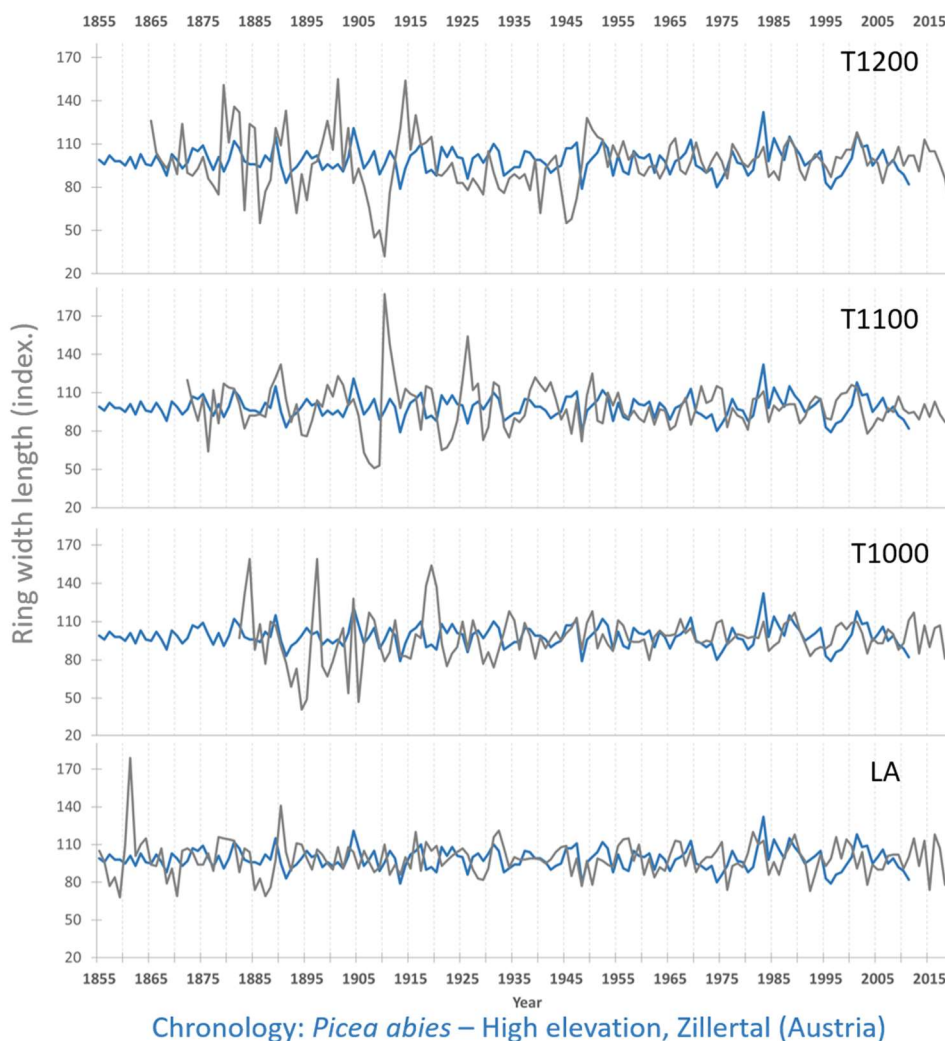


Figure 39: Local site chronologies (T1200, T1100, T1000, LA; in grey) in comparison with a regional spruce chronology (high elevation, Zillertal, Austria; in blue).

5.1.5 Minimum age

The minimum age of trees considering the length of the tree-ring series, pith-offset estimates and correction for sampling height range from 51 (*Picea abies*) to 189 years old (*Abies alba*), with a mean tree age of 102 years (Figure 40). In general, the oldest trees were located in the LA site, which is less influenced by recent avalanche events and was reached by an avalanche for the last time in 1968. Between 1200 m a.s.l. and 1000 m a.s.l. a weak pattern could be perceived: the oldest trees were located on elevated ground and the younger in gullies or next to meadows.

Nuria Guerrero Hue
 April 2021
 Source: gis.tirol.gv.at

Estimated minimum tree age

- 50 - 70
- 70 - 90
- 90 - 110
- 110 - 130
- > 130

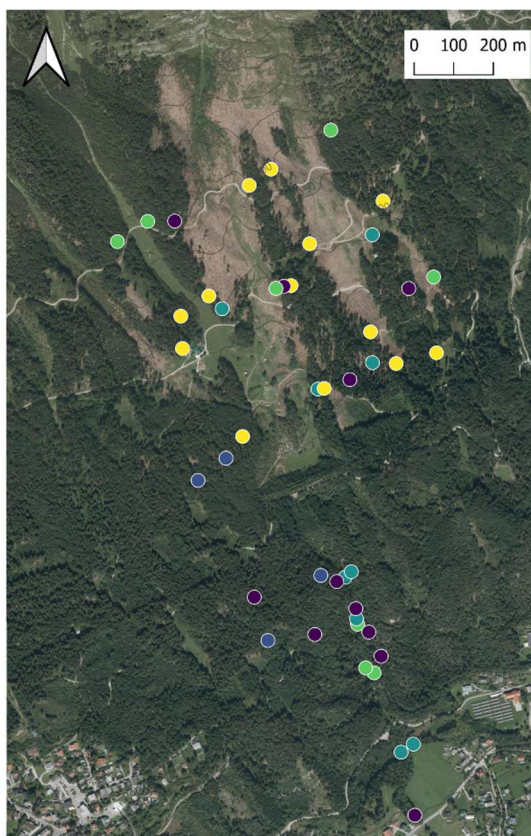


Figure 40: Estimated minimum tree age of analysed trees shown by age classes (considering the length of the tree-ring series, pith-offset estimates and correction for sampling height).

5.2 Internal signs in tree rings: avalanche indicators

5.2.1 Kill date, CW, TRD and CT

After the methodology described in Sections 4.2 and 4.3, the following AI were used: kill date, CW, TRD, and CT. Details about eccentricity and AGC in Section 5.1.3 and ANNEX III: Calculation of abrupt growth change, respectively.

Four trees in the study area were considered to be dead in Autumn 2019. In the forest it was difficult to identify if they were dead if they died because of the avalanche or if they were previously dead. With cross-dating, I could date when they died: two trees during Autumn/Winter 2018/2019, one tree during Autumn/Winter 2017/2018 and the fourth tree was dying in Autumn 2019. One of those trees was excluded from further analyses as it was a stump and was clearly felled. Therefore, its kill date was not considered for the detection of avalanche events.

It is worth to mention here that one tree (no. 16) with a broken stem due to avalanche 2019 and located at the edge of an undisturbed forest stand, was sampled as a dead tree (Figure 41). But surprisingly after cross-dating its ring width series to each other, we found that the cambium was partly still alive as it formed radial growth in one out of four cores in vegetation period of 2019. In other words, it was cored twice through the whole stem and four cores were available. Three of these cores ended in 2018 and only one core had a tree ring corresponding to vegetation period of 2019. We informally called it a “zombie tree ring”. In later steps this tree has been considered as killed by the avalanche 2019, because with a partly surviving cambium would most likely not survive for long.

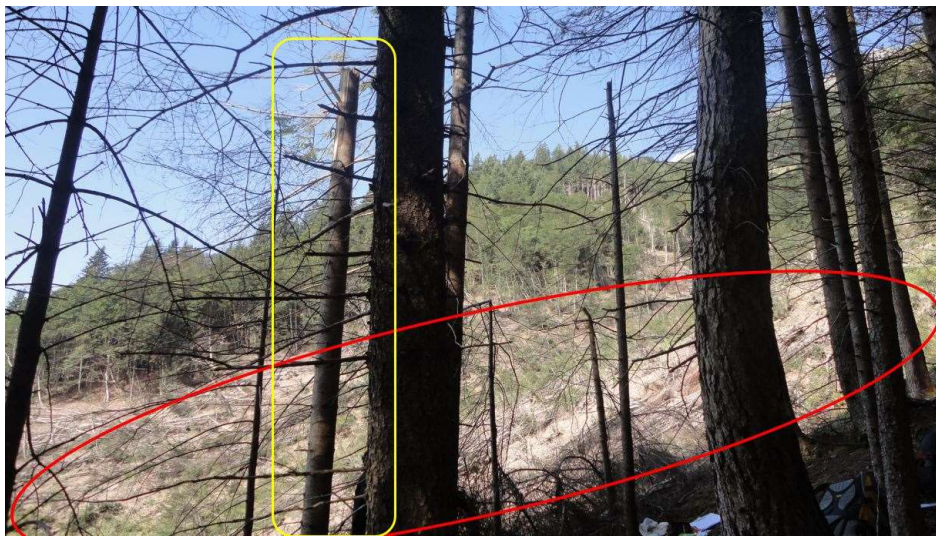


Figure 41: Tree no.16 (in yellow) with broken stem but partly still active cambium, i.e., growing in one out of four sampled stem sides next to the damaged area by the avalanche in January 2019 (in red) (Foto: N. Guerrero Hue).

Considering CW, TRD, CT and kill date as the AI hereafter, a total of 1472 AI were observed in 8315 tree rings. Every tree had several AI, varying from tree nr. 99 with only eight AI to tree nr. 93 with seventy four AI. Additionally, from the 165 years analysed only 13 years had no AI considering the 45 trees. Therefore, almost all years showed some type of AI in some tree. CW and TRD were the AI most common, present in 8% and 9% of tree rings, respectively. Table 6 includes all AI observed, with any intensity and any position in a tree ring.

Table 6: Number, percentage and type of avalanche indicators observed in tree rings.

	Compression wood	Traumatic resin ducts	Callous tissue, injury	Dead	Total analysed
Nr. years with	141	131	17	3	165
% years	85	79	10	1.8	
Nr. trees with	42	44	14	3	45
% trees	93	98	31	6.6	
Nr. Tree rings with	683	766	20	3	8315
% tree rings	8.2	9.2	0.2	0.04	

In some samples, tree rings had more than one AI in the same ring. In 34 cases, the same type of AI was present more than once in the same tree ring (i.e., two rows of TRD in the same tree ring, Figure 42) and in 39 cases, a tree showed more than one type of AI in one year (i.e., one tree ring with CW and a row of TRD). There was even one tree ring showing four rows of TRD (core 56a, year 1945).

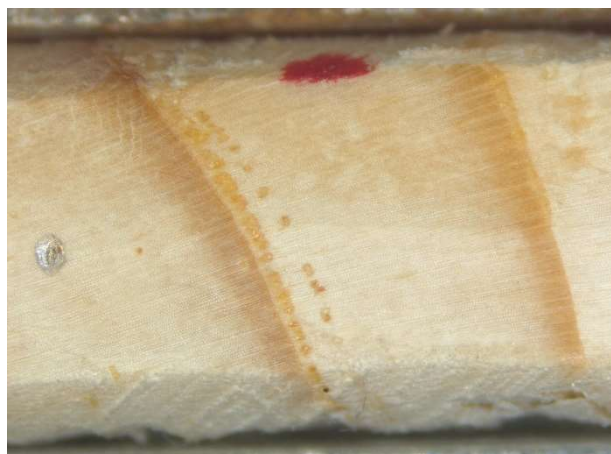


Figure 42: Example of a tree ring with two rows of traumatic resin ducts (TRD). First row of TRD has intensity 3 (moderate AI) and second row of TRD has intensity 2 (weak AI) following Table 4 (Foto: N. Guerrero Hue).

5.2.2 Position of avalanche indicators in the tree ring

Some authors using dendrogeomorphology for the detection of avalanche events consider only avalanche indicators situated in the “dormant” or early earlywood positions in tree ring (Favillier et al., 2017; Kogelnig-Mayer et al., 2011). In my observations almost all the TRD and CT detected in tree rings were in either EW or LW (99.5%), even for documented avalanche years. Considering that small avalanches might release until May or June, I decided to continue analysing the data with two datasets (“all positions” and “filtered positions”, see end of Section 4.3.2).

5.3 Detecting avalanche years

5.3.1 Avalanche indicators and historical avalanche years

Table 7 shows which type and how many AI were observed in tree rings for years with historical avalanches, considering the “filtered dataset”. There is almost no AI in those years and the highest RC achieved is 4 and the AAI varies from 0-10%.

Table 7: Number of avalanche indicators (AI) and their reaction class present in tree rings for historical avalanche years, considering only dormant and early earlywood positions in tree rings. Compression wood (CW), callous tissue (CT) and traumatic resin ducts (TRD).

year	sample depth	Nr Trees w CW	Nr Trees w CT	Nr Trees w TRD	dead	Nr trees w AI	AAI (%)	Reaction class (max)
1859	1	0	0	0	0	0	0	0
1875	4	0	0	0	0	0	0	0
1923	13	1	0	0	0	1	8	3
1935	18	0	0	0	0	0	0	0
1968	39	4	0	1	0	4	10	3
2019	42	0	0	0	1	1	2	4

Avalanche years 2019 and 1968 are the most recent avalanche events, had the highest sample depth and the most reliable documentation. Year 1968 had the highest values related to responding trees (in number and in AAI). However, year 2019 showed very low AAI and only 1 tree with AI. The rest of historical avalanche years had almost no trees with AI and very low RC. Therefore, the values related to the responding trees in those years could not be used to define tailor-made thresholds to detect potential avalanche years. Neither the numbers (Table 7) nor the maps (Figure 45) highlighted historical event years compared to the rest of years. In addition, considering Table 7, Table 8 and Table 9, some potential years showed more AI than historical years.

5.3.2 Avalanche indicators and potential avalanche years

For the “filtered positions” dataset a total of 7 potential avalanche years were obtained, containing only one of RC 5 (Table 8). The AAI ranged from 7-17% and the number of trees with AI ranged between 3-4, out of the 45 trees analysed. However, no historical avalanche year appeared in this “filtered” list.

The list of years obtained for the dataset “all positions” (Table 9) revealed 32 potential years with only three of RC 5, including the 7 years obtained with the “filtered positions” dataset. In this case, the AAI ranged from 10 to 43% and number of trees with AI ranged between 3 and 19. From the documented avalanche years, only year 2019 appears in this second list. Comparing both tables, it could be seen that years 1992 and 1946 are in the list of “all positions” but not the list of “filtered positions”. This means that the AI with RC 5 were in EW or LW positions in the tree ring. No eccentricity started to occur in any of those years.

Table 8: List of potential avalanche years for dataset “filtered positions” (Avalanche indicators (AI) only in dormant and early earlywood position in tree ring), including number and type of AI. Compression wood (CW), callous tissue (CT), traumatic resin ducts (TRD) and Avalanche activity index (AAI). Highlighted years with reaction class 5.

year	sample depth	Nr Trees w CW	Nr Trees w CT	Nr Trees w TRD	dead	Nr trees w AI	AAI (%)	Reaction class (max)
2005	45	3	0	0	0	3	7	4
2000	45	4	0	0	0	4	9	4
1974	41	3	0	0	0	3	7	4
1969	41	1	0	2	0	3	7	4
1951	26	3	0	1	0	3	12	5
1938	20	3	0	0	0	3	15	4
1934	18	3	0	0	0	3	17	4

Table 9: List of potential avalanche years for dataset “all positions” (Avalanche indicators (AI) in any position in tree ring), including number and type of AI. Compression wood (CW), callous tissue (CT), traumatic resin ducts (TRD) and Avalanche activity index (AAI). Highlighted years with reaction class 5.

year	sample depth	Nr Trees w CW	Nr Trees w CT	Nr Trees w TRD	dead	Nr. trees w AI	AAI (%)	Reaction class
1992	45	2	0	13		15	33	5
1951	26	3	0	3		4	15	5
1946	23	1	0	8		8	35	5
2019	42	0	0	7	1	8	19	4
2018	44	1	0	17	1	19	43	4
2016	45	1	0	9		10	22	4
2013	45	1	0	11		12	27	4
2011	45	2	1	5		7	16	4
2008	45	2	0	5		7	16	4
2005	45	3	0	11		13	29	4
2000	45	4	0	15		17	38	4
1996	45	0	0	12		12	27	4
1991	45	2	0	6		8	18	4
1983	44	1	0	7		8	18	4
1982	44	1	0	15		16	36	4
1979	43	1	0	12		13	30	4
1978	42	1	0	4		5	12	4
1977	41	2	0	4		6	15	4
1974	41	3	0	1		4	10	4
1972	41	0	1	8		8	20	4
1971	41	1	1	11		12	29	4
1969	41	1	0	8		8	20	4
1960	30	2	0	6		7	23	4
1957	28	0	1	4		4	14	4
1947	23	1	0	9		10	43	4
1938	20	3	0	0		3	15	4
1937	19	0	0	8		8	42	4
1934	18	3	0	4		6	33	4
1927	15	1	1	4		5	33	4
1924	13	2	0	2		4	31	4
1915	12	0	0	4		4	33	4
1913	12	1	0	2		3	25	4

Here it should be emphasized that only avalanche year 2019 is included in the “all positions” list, any other avalanche year appears in none of both tables due to the applied criteria. In year 1969 there is one tree with AI with RC 4, which might be attributed to the avalanche in January 1968, as AI can appear with some delay.

5.3.3 Temporal distribution of trees with avalanche indicators

In Figure 43 and Figure 44 the temporal distributions of AI for both datasets are shown, including type of AI, number of trees with the respective AI in a certain year, and the sample depth for each year. Documented avalanche years are marked with a red dot and the orange dots correspond to the potential avalanche years obtained in previous steps. The first thing noticed was the considerably reduced number of trees with AI in the "filtered positions" dataset. The second thing was that neither potential nor the historically documented avalanche years had a higher number of trees with AI as expected. Third, in marked years there was any tree with CT and only one was dead. When all positions in tree rings were considered, the most numerous AI was TRD. However, when filtering according to their position, CW prevailed. This shows that most of TRD are located in the EW or LW, as described.

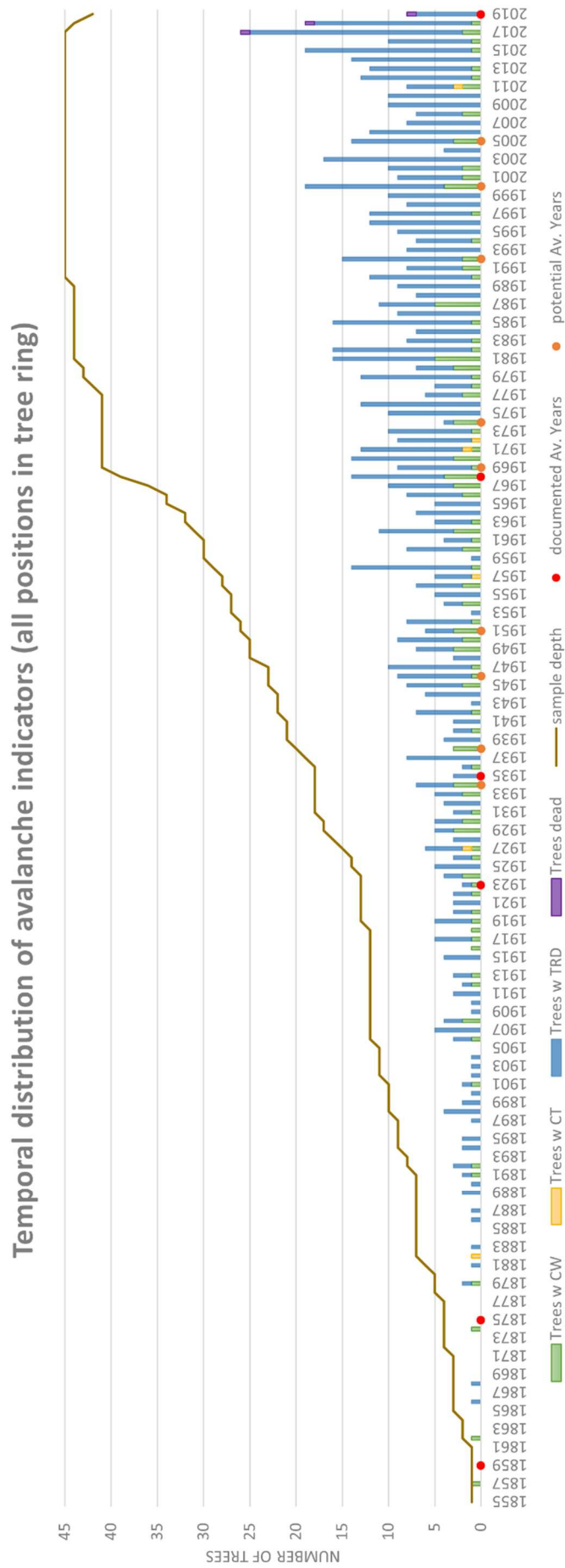


Figure 43: Temporal distribution of number and type of avalanche indicators (considering all positions in tree ring, i.e. dormant, early earlywood, earlywood, latewood). Compression wood (CW), callous tissue (CT) and traumatic resin ducts (TRD).

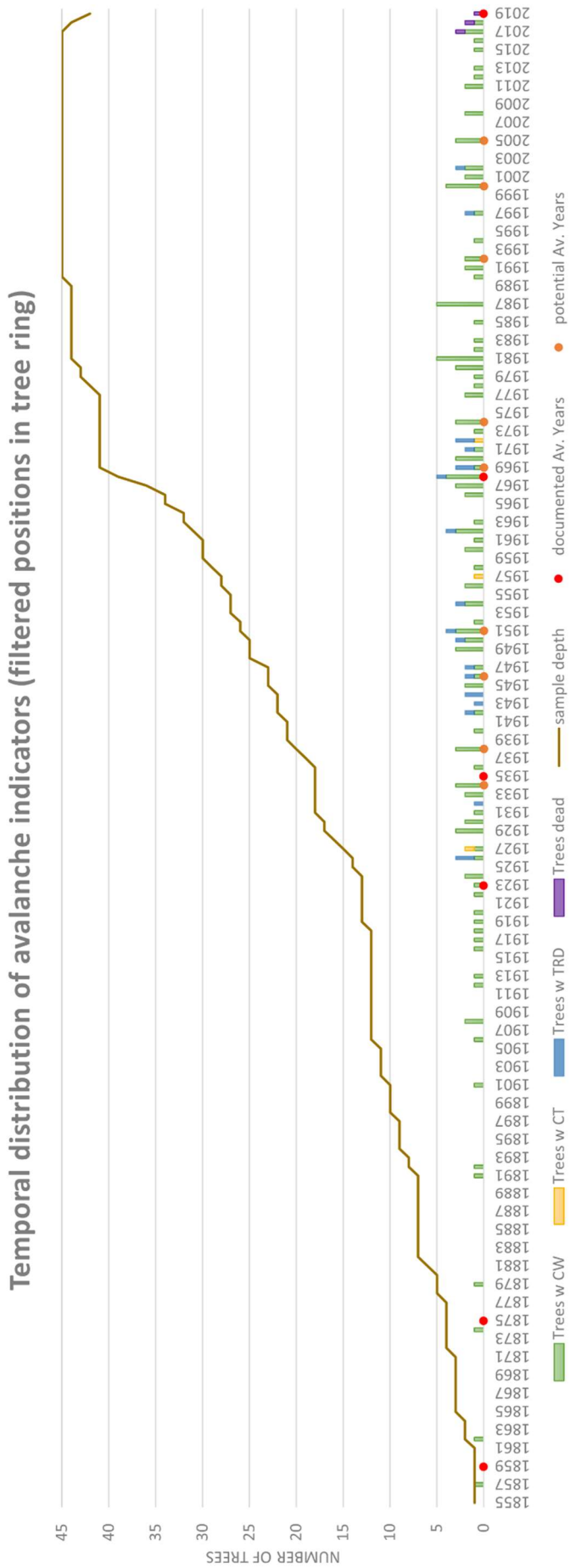


Figure 44: Temporal distribution of number and type of avalanche indicators (considering only dormant and early earlywood positions in tree ring).
 Compression wood (CW), callous tissue (CT) and traumatic resin ducts (TRD).

5.3.4 Spatial distribution of trees with avalanche indicators

Next, AI (type, intensity, and RC) were mapped to carefully observe their spatial distribution through the avalanche area. This was done for years with documented big avalanches (2019, 1968, 1935, 1923) and years of small avalanches with the runout extension available (1974, 1970, 1967) (provided by the WLV) (Figure 45). Documented avalanches which took place in 1859 and 1875 were not mapped because of lack of trees alive at that time (too small sample depth) and no runout available. In addition, all potential years with RC 5 or 4 were mapped (years from Table 8 and Table 9) (Figure 46). Two groups of maps showing the spatial distribution of trees with AI (shown corresponding RC) and undisturbed trees were produced. These maps only show the “filtered positions” dataset. In Figure 45 the spatial distribution of trees with AI is shown for those years with historical events for which we had the runout mapped, either big or small events. Figure 46 shows the most relevant potential avalanche years obtained after the “detection steps” (see Section 4.6.1) from the “filtered positions” dataset.

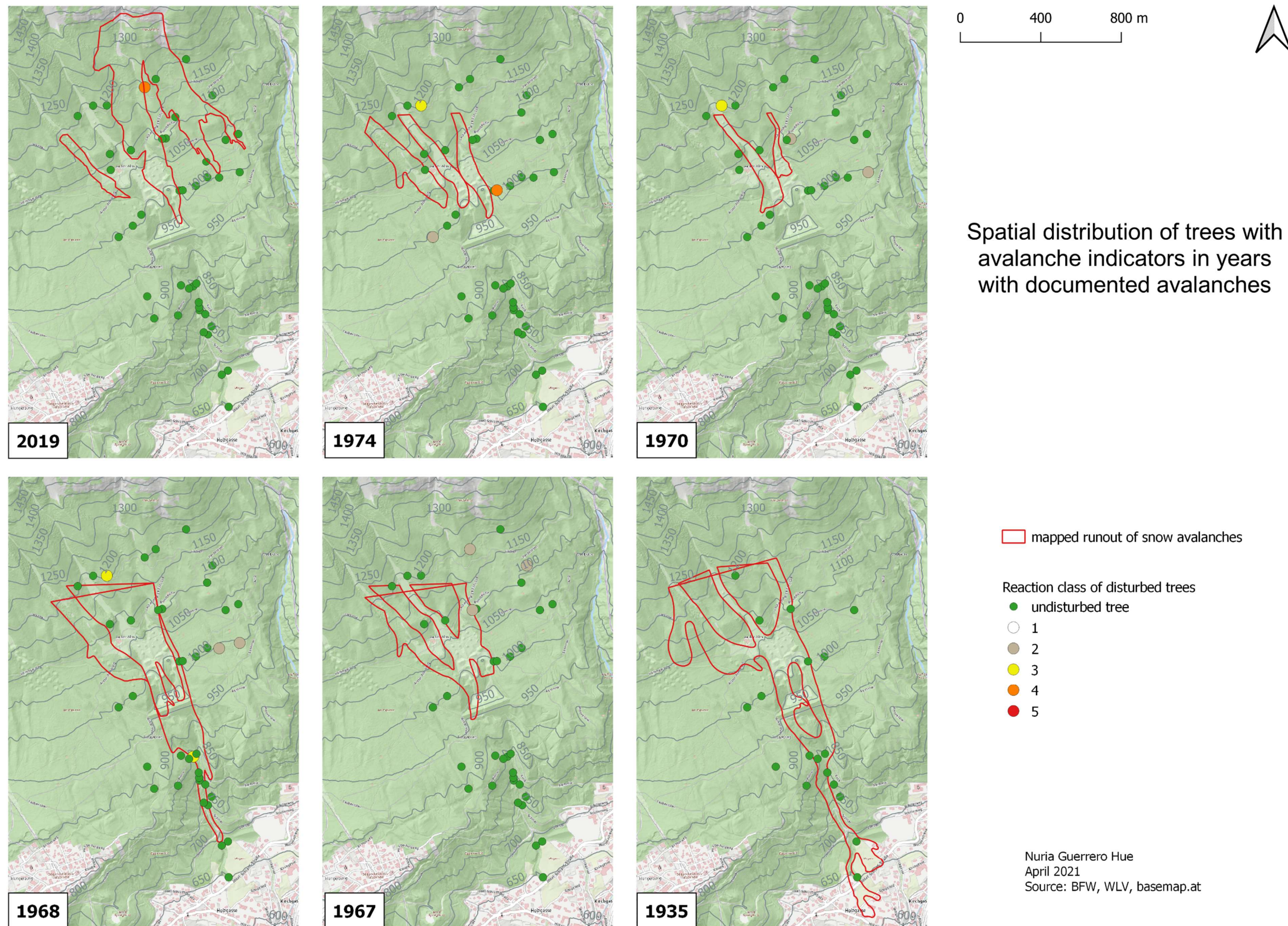


Figure 45: Spatial distribution of trees with avalanche indicators in years with documented avalanches.

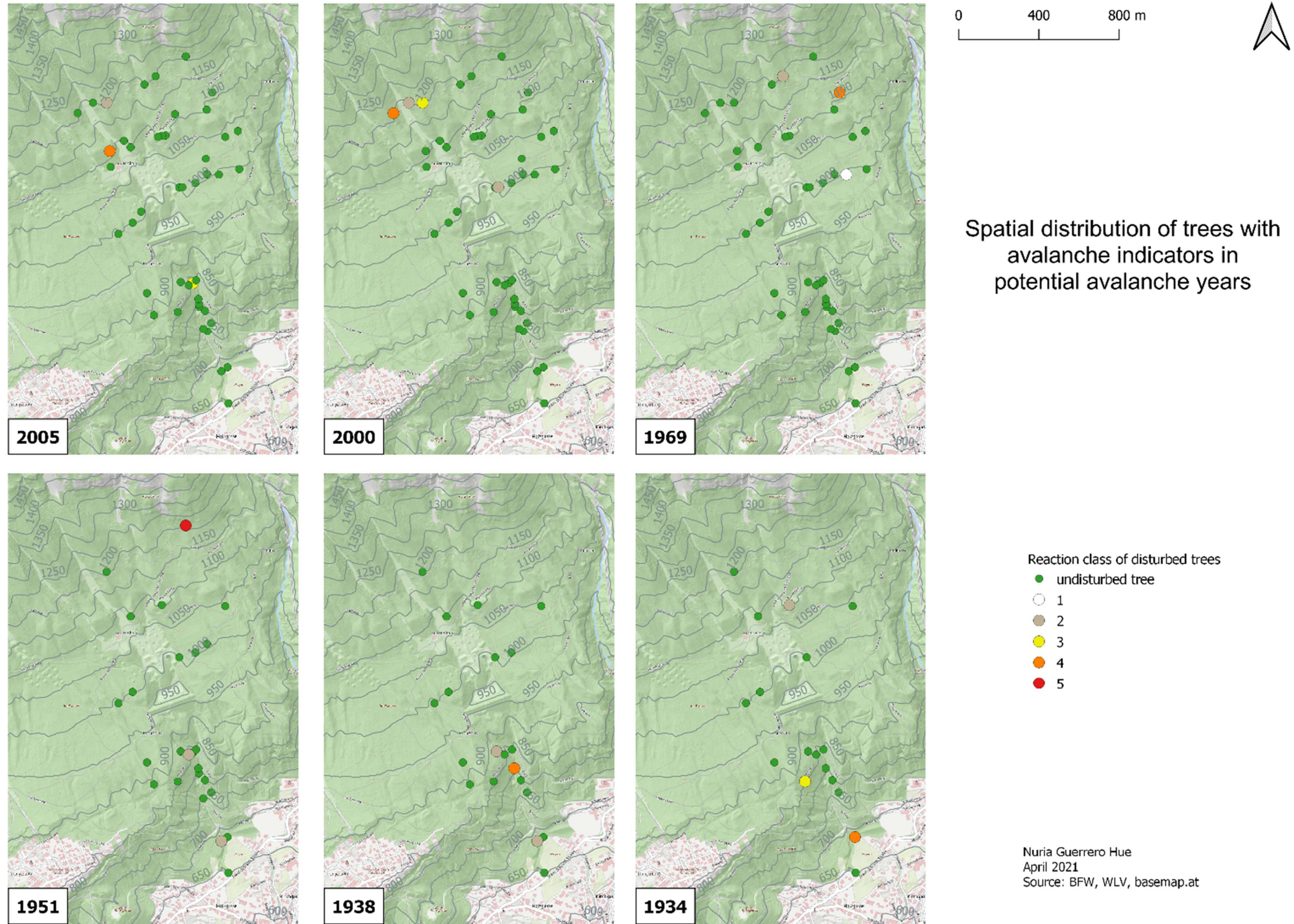


Figure 46: Spatial distribution of trees with avalanche indicators in potential avalanche years obtained after the detection steps.

In both groups of maps, it can be observed that only few trees showed AI in the selected years and that most of the analysed trees grew undisturbed. Another point is that, when several trees had AI in the same year, those trees were scattered throughout the whole study area, not exhibiting any spatial pattern in the terrain clearly attributable to a snow avalanche.

Figure 45 shows that some damaged trees were inside or at the border of the affected area, but most disturbed trees were outside for all years. Some damaged trees were very close to (few tens of metres) or surrounded by undisturbed trees. In such cases, it would be expected, that an avalanche would affect also neighbouring trees to a greater or lesser degree. Year 1968 (i.e., growing season after the avalanche in February 1968) exemplifies this: there were many undisturbed trees inside the mapped runout and only one disturbed tree inside the runout had only a RC 3 (no strong reaction). Another tree with RC 3 on the north was most probably affected by the avalanche, but it is located outside the documented area. Also, in year 1968 there were two trees with RC 2 outside of the mapped runout, i.e., east of the main avalanche path. Considering that the AI in these four disturbed trees were consequence of the avalanche, they would be not enough to spatially reconstruct the extent of the avalanche, if it would not be documented.

The maps of Figure 46 show for years 1951, 1938 and 1934 several trees damaged located in the LA site close to Mühlau district. However, there were no historical records of any avalanches for those years. Three trees damaged in 2000, were very close to each other in the north-west corner of the studied area. They were close to the meadows uphill of the mountain hut. These damages (i.e., CW) could be indeed attributed to late spring avalanches, which often take place in this area.

Winter 1950/1951 was a large avalanche winter in the Alps (Nicolussi et al., 2007; Rudolf-Miklau & Sauer Moser, 2011). There are historical records that the Arzler Alm avalanche released three times in January 1951, reaching the protection measures around the mountain hut (Nessizius, 1966) (Figure 47). Also, the Mühlauer Klamm avalanche released (catchment East of Arzler Alm) (WLV, personal communication, 2020). After the detection steps, one single tree showed AI with RC 5 in year 1951. It stands at 1200 m. a.s.l. in the north-east corner of the sampled area, almost at the border between the Arzler Alm and the Mühlauer Klamm avalanche paths. The tree had CW and TRD in EE. In the same year, there were additionally two other trees with AI, both with CW but only RC 2. They are located in the LA site, which was not affected by those avalanches.

5.3.5 Eastern arm of the avalanche

After carefully analysing the results obtained from the detection steps, I focused the analysis on the north-eastern part of the study area, below the "Herzwiese" meadow. Considering both groups of maps (Figure 45 and Figure 46), there were several trees damaged in years 1951, 1967, 1968, 1969 and 1970 at the edge of the Mühlauer Klamm avalanche path. This part was strongly impacted in January 2019 (Figure 40). Additionally, it exists a very exhaustive avalanche documentation for the decades 1940s-1960s, which revealed that in January 1951 various avalanches released in the Arzler Alm avalanche path. They stopped at the surroundings of the braking mounds close to the mountain hut, as observed in some sketches (Figure 47) (Nessizius, 1966).

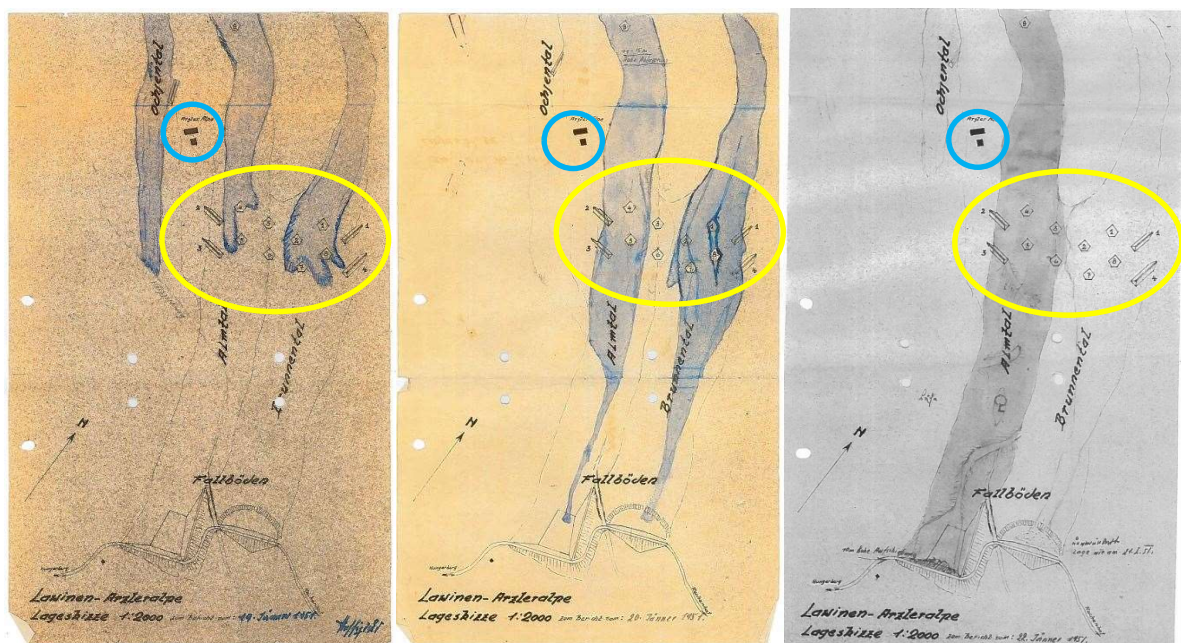


Figure 47a, b, c: Mapped runout of some avalanches released on the 19th, 20th and 22nd January 1951 respectively in the Arzler Alm avalanche path. The mountain hut (in blue) and the technical protection measures (in yellow) (Nessizius, 1966).

However, these sketches focused on the runout area around the technical protection measures and did not include the area higher up. Precisely in this area I could see some trees with AI with strong RC (Figure 45 and Figure 46) for 1951, 1968 and 1969. Likewise, in the year 1969 a tree showed a strong reaction (RC 4) and in 1968 and 1970 there were few trees damaged in this area but only with RC 2. These observations made me check the orthophotos available for this period, knowing that on the 30th of January 1968 the last big avalanche released which ran to the Mühlau district. In an orthophoto from 1970 (Figure 48), an unforested area in the East part can be seen. It is possible that this area also belongs to the avalanche event 1968, but that the later documentation focused on the main path and did not include that eastern part because no major infrastructures were affected.

Nuria Guerrero Hue
 April 2021
 Source: WLV & basemap.at

Reaction class of disturbed trees 1969

- undisturbed tree
- 1
- 2
- 4

Mapped runout of snow avalanches

- ▭ 1968

Orthofoto 1970

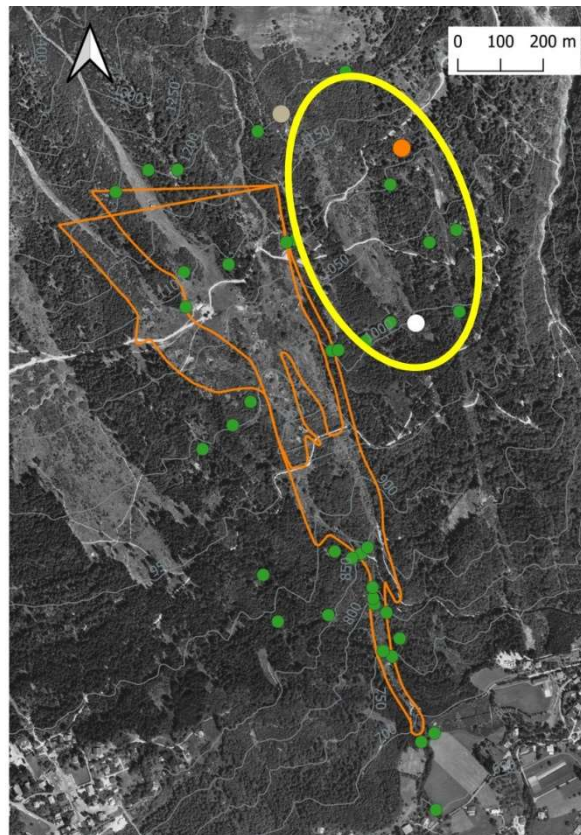


Figure 48: Combination of an orthophoto of year 1970, undisturbed trees in green, disturbed trees with their reaction classes for year 1969 and the mapped runout of avalanche 1968. In yellow the "eastern arm" of the avalanche path.

6 DISCUSSION

The aim of this study was the temporal and spatial reconstruction of the avalanche activity in the Arzler Alm avalanche path using dendrogeomorphological methods. The first point was to check if it is possible to perform this at the chosen study site, as it is a well-documented area but is strongly influenced by anthropogenic factors. In a following step, I wanted to compare avalanche event years identified by the dendrogeomorphological analysis, with the existing extensive archival data and orthophotos. This was expected to confirm known events.

A tailor-made approach to detect potential avalanche years was applied, i.e., years when the avalanche could have potentially released, considering the characteristics of the area and the avalanche indicators observed in tree rings. I followed as much as possible the 4-step approach developed by Favillier et al. (2017), adapting it to our study case and considering aspects from other studies (Kogelnig-Mayer et al., 2011; Meseşan et al., 2019; Stoffel & Corona, 2014) and assistance from K. Nicolussi.

6.1 Detection of avalanche years

The detection of past avalanche events pursued two goals: first, the AI were used to confirm historical avalanche events and second, it was checked if an unknown avalanche event could be inferred from the spatial distribution of trees with AI. Regarding the first step, documented avalanches could not be confirmed, even though few trees did show some strong reactions in tree rings in avalanche years (i.e., 1951, 1968). These signals can be indeed assigned to the documented snow avalanche events, considering the extent of the runout and the position of disturbed trees in the avalanche terrain. The second step did not reveal any unknown avalanche year, because there were only few trees with strong RC and these did not show a spatial pattern attributable to an avalanche. Even though past avalanche events could not be reconstructed, tree rings provided other useful information such as minimum age (length of tree-ring series) and so we still gained some knowledge about the Arzler Alm avalanche path.

A remarkable feature of the avalanche released in January 2019 was its extent, damaging a considerable forested area east of the main path. Strong reactions observed in some trees for years 1951, 1968 and 1969 indicated that this area has been more often affected by avalanches as it is documented (Figure 45, Figure 46 and Figure 48). This can be explained by the fact that, historical avalanche documentation was mainly focused on the runout area or on the interaction with the protection measures. The avalanches released in this eastern part below the "Herzwiese" meadow have never affected the settlement area or important infrastructure (Stepanek, 2012). However, they still initiate considerable damage to the forest on a regular basis as displayed by the AI in tree rings and old orthophotos. Taking this into account, the tree rings have shown that the eastern arm below the "Herzwiese" releases periodically.

6.2 Avalanche indicators (external and internal)

A combination of various AI was needed, as each one provides different information. The challenge was which criteria and thresholds to choose. As pursued here, tailor-made thresholds are a good option, especially if at least few historical records are available to calibrate from. Regarding AI, during fieldwork I decided not to sample tilted, leaning, and curved trees, attributing them to creeping snow throughout the winter season rather than due to avalanches. A deep knowledge of the area and characteristics of avalanches is essential to perform this type of study. Each type of AI provides us with different information, and they are therefore complementary. Key for the reconstruction of events is the repetition, i.e., the more AI observed in different trees in the same year, the better. For this reason, it is worth to include all possible AI (CW, TRD, CT, kill date) and also those excluded in this study (AGC, ideally both releases and suppressions).

The way each AI is detected varies: AGC and eccentricity are calculated or observed by using tree-ring series, otherwise TRD, CW and CT are directly observed in the tree rings with the binocular microscope. The observation of the latter three AI required more time and is somewhat subjective when estimating intensity. To cope with this subjectivity, I elaborated an identification key (available in ANNEX II: Identification key for avalanche indicators).

Some authors do not filter the AI according to their position within the tree ring, as it can make difficult to detect disturbances co-occurring during the dormant season (Martin & Germain, 2016; Muntán, 2016). Kogelnig-Mayer et al. (2011) used the position of AI within the tree ring to distinguish snow avalanches from debris flow happening in the same catchment area. I decided to apply this step (as Favillier et al., 2017; Kogelnig-Mayer et al., 2011) and to take advantage of the intra-annual dating capacity of tree rings, in my case to filter possible disturbances (i.e., forest management, recreational activities). Nevertheless, an overview of the data including EW and LW positions was performed, to detect anything unusual.

Therefore, detailed knowledge of the study area was again necessary, to be aware if other disturbances take place and if late spring avalanches might happen. As described, small wet snow avalanches can release and occur in the upper parts of the Arzler Alm avalanche catchment until late spring and thus AI might be present in the EW of tree rings. Nevertheless, the overall objective must be considered: whether to reconstruct every single small avalanche which releases or to reconstruct big events which endanger settlements, infrastructure, etc. Small spring avalanches are not relevant as input for hazard zone planning.

Unfortunately, the present study could not properly benefit from the information which could have been inferred from the ring width of tree-ring series, that is AGC and eccentricity. Despite this, tree rings provided other useful information as minimum age (length of tree-ring series) and the AI observed in the wood.

6.3 Limitations of this study

From my point of view, the main reasons that might have affected my results are the strong anthropogenic influence in the study area and some intrinsic limitations of the methodology.

6.3.1 Study site

A major factor affecting the results of this study, is that the Arzler Alm avalanche path has a strong anthropogenic influence which interferes and alters the signals in tree rings. As already described in the introduction, forest management and recreation activities take place regularly in the study area, and all these activities can affect tree growth. In case of avalanches or other disturbances, damaged trees are often removed and the evidence in trees disappears. Moreover, the biggest and often oldest trees, are usually removed at the end of the felling cycle. We were aware that it was not the ideal forest to perform a dendrogeomorphological study, however there was a considerable amount of information about old avalanche events. The fact of having those historical records providing details on events has been very useful to better understand the characteristics of the avalanche path and to compare this information with my findings retrieved from the vegetation. This comparison is crucial in dendrogeomorphological studies, to check and calibrate the methodology and results (Corona et al., 2012; de Bouchard d'Aubeterre et al., 2019; Kogelnig-Mayer et al., 2011; Muntán, 2016). Taking this into account we decided to still perform this work because the area is very important for the city and the citizens of Innsbruck. However, I can now conclude that being so close to the city of Innsbruck is the great strength (extensive historical documentation about avalanche events) of this study area but at the same time its great weakness (very accessible area for recreational activities and forest management).

6.3.2 Methodology

Avalanche indicators are not unidirectional

After performing this study, it is important to note that either external (scar, broken top, candelabra form) or internal (eccentricity, reaction wood, TRD, CT) indicators of avalanche are not unidirectional: every single type of damage might have causes other than an avalanche. Climatic, ecological and anthropogenic disturbances can cause a response in tree growth similar to snow avalanches: TRD can be formed after severe meteorological conditions (droughts, water stress) in certain conifers, ungulate fraying and browsing can cause superficial scars (i.e., CT) (Stoffel, 2008), a tree with a candelabra form may be the result of a windthrow or rockfall (Martin & Germain, 2016; Stoffel & Bollschweiler, 2008), and anthropogenic activities influence tree growth and structure of forest stands. For this reason, a considerable sample depth is needed to detect responding trees in the same year and comparison with historical records is important.

In my case these considerations were especially decisive during fieldwork when observing trees with external damages. A sampling strategy was prepared including a long list of possible avalanche indicators according to the literature (Stoffel et al., 2013; Stoffel & Bollschweiler, 2008). However, in the field some types of damages were mostly avoided (i.e., stumps, tilted or leaning trees). Knowing the characteristics of the area, it was considered that tilted or leaning trees were most probably due to snow pressure and snow gliding rather than snow avalanches. Likewise, uprooted trees were avoided if they were not in their original position. In the case of big old trees in the lower area, many of them had small insect holes, which can also affect tree growth. However, some of those trees were sampled but only when their damages were not threatening their survival. It was prioritized to get the oldest samples possible, even if they were coming from slightly damaged trees (due to other reasons rather than avalanches). Similar thoughts are not mentioned in other dendrogeomorphological studies; however, I consider them relevant to mention. I think it is important to differentiate between theory (the sampling protocol) and practice (choosing trees in the field). Trying to assign a list of possible damages due to snow avalanches is not a straightforward endeavour, as described in the literature. Choosing each tree was a subjective process, knowing that “the tree fitting perfectly the book description does not exist”.

Forest management

Another point to mention is that most of our sampling was carried out after sanitation harvesting was performed to clear up the area following the 2019 avalanche. Therefore, recent scars, broken branches or stumps could be a result of the clean-up activity rather than from the avalanche. In those situations, an affected tree and its surroundings were carefully analysed before sampling. Of course, the sampling campaign could have taken place before the sanitation work, but this would have taken more time to complete the sampling and would have been more dangerous to move inside the destroyed forest.

Disturbed und undisturbed trees by an avalanche

As commented, in historical avalanche years only some still living trees showed AI, often surrounded by undisturbed trees. This fact agrees with field observations. During fieldwork I observed in various locations how some trees stand intact in the middle of a destroyed forest. Possible reasons are that some trees were impacted by the dense flow component of the avalanche but others further away were only hit by the powder cloud. This is often attributed to tree species, as evergreen trees offer more air resistance to the powder cloud (Rudolf-Miklau et al., 2015). It can also be because orographic irregularities in the avalanche path enhance an acceleration of the avalanche, due to narrowing or inclination of the terrain (Margreth, 2004). It is difficult to understand, and it is being investigated, what exactly happens inside an avalanche (Rudolf-Miklau et al., 2015). In the end, tree rings corroborated the

observation in the field: trees strongly damaged by an avalanche (i.e., having AI with strong RC) are very close (tens of meters) to undisturbed trees.

All these influences and interactions of avalanches with trees and the terrain must be kept in mind when using dendrogeomorphology to map avalanche events. We tend to draw a line that should separate the damaged area from the undisturbed forest, but this does not correspond to the reality. Indeed, I also had to draw lines in this study, but always having in mind that those borders are relative and undisturbed and damaged trees can be found at both sides of the line.

Sample size

In respect of sample size, in general prevails the rule “the more, the better”, repetition is needed but there must be a limit. As highlighted before, this results in more time and resources. Other studies tend to establish a minimum number of trees to be sampled, mostly related to “an avalanche path” (i.e. the guide followed here (Stoffel et al., 2013)). Surprisingly, I found no publication where the needed sample size was referred to the area of the avalanche path. Favillier et al. (2017) and Stoffel et al. (2013) provide an overview of dendrogeomorphological studies using tree rings to reconstruct past snow avalanches, they specify the number of paths and sample size but not the area of the avalanche path. In the present study, 45 trees were analysed and the total area of the avalanche path is 230 ha, which means approx. 5 trees / ha analysed. Compared to other studies (Table 10), the sampling density is at the upper limit, therefore the sample size cannot be considered insufficient.

Table 10: Comparison of the sampling density of some dendrogeomorphological studies using tree rings to reconstruct past snow avalanches. Details about the area of the avalanche path (ha) and the number of trees sampled.

Study (authors and year)	Area (ha)	Number of trees	Sampling density (trees / ha)
(Favillier et al., 2017)	155 ha of 5 paths (approx. 31 ha / path)	564 (approx. 122 trees / path)	3,9
(Chiroiu et al., 2015)	17 ha	105	6,2
(Oller et al., 2020)	starting zone 37 ha	37	1,0
(Kogelnig-Mayer et al., 2011) (snow avalanches + debris flow)	catchment 70 ha	372	5,3
(de Bouchard d’Aubeterre et al., 2019)	147 ha of 4 paths (approx. 37 ha / path)	306 (approx. 76 trees / path)	2,1
(Corona et al., 2012)	starting zone 50 ha + runout zone 15 ha min. 65 ha	209	3,2
Arzler Alm avalanche path	230 ha	45	5,1

Responding trees

Regarding the number or percentage (AAI) of trees responding to an event, thresholds must be set to separate a signal from noise. But a very wide range of thresholds was found in the literature: the AAI ranges between 5% (Favillier et al., 2017) and 40% (Butler & Sawyer, 2008; Oller et al., 2020), and the minimum number of AI in one year from 3 (Meseşan et al., 2019) to 9 (Favillier et al., 2017). In recent studies those values are often dependent on sample size, as standardised by Corona et al. (2012).

Due to this broad range and after I gained a first overview of my data, I set very low thresholds (AAI \geq 5% and min. 3 AI) and checked what I was obtaining for the historical avalanche events. The idea afterwards was to apply the values of historical avalanche years as thresholds to identify potential avalanche years. However, the historical years showed low values for these parameters (Table 7) and could not be used as thresholds. For this reason, I kept the low thresholds to try to maximise the possibility of detecting some potential years. If thresholds would have been higher (i.e., AAI \geq 40%, as in (Butler & Sawyer, 2008; Oller et al., 2020)), no potential avalanche year would have been obtained with the dataset "filtered positions" (Table 8) and only three years with the dataset "all positions" (Table 9).

Weighting of AI

Not all dendrogeomorphological studies perform a weighting of AI (Muntán, 2016; Oller et al., 2020) and if they do, the rating criteria vary. Due to lack of agreement in this point, between 2012 and 2014 the standards used in this study were published (Chiroiu et al., 2015; Corona et al., 2012; Stoffel et al., 2013; Stoffel & Corona, 2014).

Nevertheless, there are still current studies not rating the AI (Oller et al., 2020). I considered to classify the reactions, given that some external and internal damages are more probable to occur because of an avalanche rather than others. The weighting criteria of Stoffel & Corona (2014) was used and named "reaction classes (RC)" in this study, based on different empirical rating systems (see references therein).

To sum up, dendrogeomorphology is a time and resource-consuming method, not only when sampling (de Bouchard d'Aubeterre et al., 2019) but also including the work in the laboratory (McClung & Schaerer, 2006; Stoffel et al., 2013). In fact, this situation led us to the decision of setting aside a considerable number of cores. Most of these trees were *Fagus sp.* and broadleaved trees are less used in dendrogeomorphological studies (Favillier et al., 2017; Stoffel et al., 2013). Due to this limited information available for broadleaved trees, especially related to the identification and classification of avalanche indicators, I concentrated my work on coniferous trees.

There are considerable references available and the basic steps for the reconstruction of events are usually the same. However, I missed further details or agreement in the different steps to perform such a study, from the design of the fieldwork to the rating criteria of AI. Especially points like sample size, number of trees showing AI and weighting of signals are an open discussion among the scientific community (Chiroiu et al., 2015; Martin & Germain, 2016). For that reason, I applied a tailor-made approach adapted to this study case.

My impression is that studies based on visual methodologies and decisions should be accompanied with more graphic material. For this reason, I made efforts to present pictures and graphs, to illustrate all steps performed (i.e., damages on trees, identification key, ring width graphs, eccentricity, chronologies, etc.). Examples of references with visual documentation are (Kaennel & Schweingruber, 2021; Schweingruber et al., 2007).

6.4 Recommendations

In general, the approach followed in this work is thought appropriate and in line with state of the art of dendrogeomorphological studies. Based on my findings and experience, some recommendations can be given:

- As demonstrated by the present study, this methodology is not suitable for all types of forests. Therefore, a study area with heavily influenced forests should be avoided. After my study, it is especially recommended to avoid forests with anthropogenic influence (e.g., forest management, recreational activities).
- Regarding the avalanche indicators, the classification of their intensities is done visually, which can entail a certain subjectivity and introduce bias. Even with the classification criteria described in the literature, in rare cases reference pictures are provided. Searching references with visual documentation is very helpful.
- With respect to the standard recommendations for sampling, I would avoid tilted and curved trees. These types of damages are usually included as probably caused by snow avalanches. However, after my observations during fieldwork, snow gliding and creeping can cause the same reaction in trees.
- Another point about sampling, which I found confusing, was the suggestion to pursue a mixture of species (Stoffel et al., 2013), which I assumed were conifer and broadleaved trees. Nevertheless, in further steps, I found that there are only few publications using broadleaved trees in dendrogeomorphology and non in the Alps (Favillier et al., 2017; Stoffel et al., 2013). Therefore, my recommendation would be either to sample different tree species (but only conifers) or to search for references about a particular tree species before coring it.
- Finally, a deep knowledge of the avalanche path is essential: to know which type of disturbances might take place and interfere with the information coming from tree rings, where are the oldest trees of the area to be able to study backwards the longest possible time period, and to gather all sources of historical information (reports, witnesses, aerial photographs).

7 CONCLUSIONS

By means of dendrogeomorphology, temporal and spatial reconstructions of past avalanche events can be performed. Unfortunately, this methodology is not suitable for every type of forest and therefore not applicable to every avalanche path. This has been exemplified here with the study performed at the Arzler Alm avalanche path (Tyrol, Austria). This is attributed to a strong anthropogenic influence, especially forest management and recreation activities, which interferes and alters the signals in tree rings or disguise avalanche events by removing affected trees.

Even though it was not possible to reconstruct past avalanche events using dendrogeomorphological methods in the Arzler Alm avalanche path, some tree rings exhibited avalanche indicators for some documented avalanche events (e.g., 1968 and 2019). Also, tree rings have shown that the eastern arm below the "Herzwiese" releases periodically (an eastern arm of the Arzler Alm avalanche path). Additionally, tree rings provided other useful information such as tree minimum age, and we therefore gained additional knowledge about the Arzler Alm avalanche path.

Performing a dendrogeomorphological study is a laborious and time-consuming process. It can hardly be carried out without the assistance of an expert and the appropriate material (i.e., not only a borer is needed, but also a digital positioning table connected to a binocular microscope and the time-series analysis software are essential). Furthermore, there are many internal variations of the general methodology, and some points are an open discussion among scientists, which entails the use of tailor-made adaptations. Based on my findings and experience, I give recommendations and provide illustrations and examples for all steps conducted (i.e., identification and rating of avalanche indicators), which may contribute to refine existing approaches.

List of figures

- Figure 1: Zones of an avalanche path (adapted from (Fellin, 2013)).....	16
- Figure 2: Schematic diagram of the creep and glide movement of the snow cover (adapted from (Österreichisches Normungsinstitut, 2010)).	18
- Figure 3: Damaged bench due to snow movement in the study site (Foto: N. Guerrero Hue).	18
- Figure 4: A schematic figure of a mixed avalanche showing the powder component (Staubschicht), re-suspension layer (Saltationsschicht), flow component (Fließschicht) and snow surface (Schneedecke) (Rudolf-Miklau et al., 2015) after (Österreichisches Normungsinstitut, 2010).	19
- Figure 5: Effects of forest on the snowpack (adapted from (Schneebeili & Bebi, 2004)).	20
- Figure 6: Two tree rings of <i>Picea abies</i> with earlywood (EW) and latewood (LW) (Foto: N. Guerrero Hue).	22
- Figure 7: Trees with candelabra form due to breakage of the main stem (Foto: N. Guerrero Hue).	23
- Figure 8: Curved <i>Fagus sylvatica</i> in the study area (Foto: N. Guerrero Hue).	24
- Figure 9 a, b: On the left a scar on a <i>Fagus sylvatica</i> tree in the study site and on the right inside the yellow circle, an example of chaotic callous tissue in a tree ring (frost ring) (Fotos: N. Guerrero Hue).	25
- Figure 10: A row of traumatic resin ducts in earlywood (Foto: N. Guerrero Hue).	25
- Figure 11: Compression wood covering more than the half of a tree ring of <i>Picea abies</i> (Foto: N. Guerrero Hue).	26
- Figure 12: Tree rings are subdivided into latewood (LW), earlywood (EW), early earlywood (EE) and dormant season (D) (adapted from (Stoffel, 2005)).	27
- Figure 13: Location of the Arzler Alm avalanche path (in red), situated on the Nordkette ridge, north of the city of Innsbruck (Austria).	28
- Figure 14: Parts of Arzler Alm avalanche path and morphometric parameters of each part.	29
- Figure 15: Multifunctional use of the area (hikers, a bike, livestock, and avalanche protection measures) (Foto: N. Guerrero Hue).....	30
- Figure 16: Simplified geologic map around Innsbruck (Krainer & Meyer, 2016).	30
- Figure 17: Monthly mean temperature (red) and precipitation (blue) in Innsbruck (climate-data.org, 2021).	31
- Figure 18: Vegetation of the Arzler Alm avalanche path.....	33
- Figure 19: Soil types of the study area (in orange) according to FAO classification (Umweltbundesamt, 2021).	34
- Figure 20: Avalanche debris reached the district of Mühlau (Innsbruck, Austria) on the 5 th February 1935 (provided by L. Stepanek).	35
- Figure 21: Documented extents of avalanche events in the Arzler Alm avalanche path before 2019.	35

- Figure 22: Some protection measures (the braking mounds (in yellow), and the catching earth dam (in red)) built close to the Arzler Alm mountain hut (in blue) (Orthophoto 2019)..... 36
- Figure 23: Snow avalanche hazard zone plan. The runout zone of the Arzler Alm avalanche path reaches the district of Mühlau (Innsbruck). The red zone (avalanche pressure > 10 kN/m²) and yellow zone (avalanche pressure 1 - 10 kN/m²) are calculated considering a design event with return period of 150 years (Amt der Tiroler Landesregierung, 2021; Forstgesetz, 1975)..... 37
- Figure 24: The Nordkette mountain ridge with the Arzler Alm avalanche, January 2019. In yellow, the earth dam at 945 m a.s.l. (Foto: LWD Tirol in (Siegele et al., 2019)..... 38
- Figure 25 a, b: On the left, forestry workers remove all woody debris after avalanche 2019 (Foto - July 2019) and on the right, renovated protection measures close to the Arzler Alm mountain hut (Foto - November 2020) (Fotos: N. Guerrero Hue)..... 39
- Figure 26: Stump of a 180 year old *Abies alba* tree killed and transported 200 m downhill by the avalanche in January 2019 (Foto: N. Guerrero Hue)..... 40
- Figure 27: Sampling strategy: altitudinal transects (T1200, T1100, T1050, T1000) and a selective sampling in the lower area (LA; circled) (orthophoto 2019). 41
- Figure 28 a, b: Some fieldwork devices, on the left the GPS device and on the right the forest calliper used to measure tree diameter (Fotos: N. Guerrero Hue). 43
- Figure 29: Coring a tree with the increment borer (Foto: N. Guerrero Hue). 44
- Figure 30: Coding of cores depending on the coring direction through the stem, in this case for a conifer (core B taken from downhill of the tree to catch possible reaction wood). 45
- Figure 31 a, b: On the left, preparation of cores using a razor blade and chalk. On the right, digital positioning table connected to a binocular microscope and time-series analysis software to measure tree rings (Fotos: N. Guerrero Hue). 46
- Figure 32: A tangential row of traumatic resin ducts in the middle of earlywood cells. Avalanche indicator with intensity 3 (moderate) following Table 4 (Foto: N. Guerrero Hue). 48
- Figure 33: Distribution of tree species sampled in the study area and outlined in black those trees dendrogemorphologically analysed. In red the extent of avalanche 2019..... 52
- Figure 34: Spatial distribution of trees with and without external damage: damaged trees in orange and undisturbed trees in green. In blue, trees with damages attributed to the avalanche 2019, in red its extent..... 53
- Figure 35: Number of trees and number of cores available for each year (sample depth) (1855-2019). 54
- Figure 36: Tree-ring width diagram of tree no. 24 showing eccentricity from year 1999. 55
- Figure 37: Tree-ring width diagram of tree no. 51 showing eccentricity from year 1984. 55
- Figure 38: Local site chronologies (T1200, T1100, T1000, LA; in grey) in comparison with a regional spruce chronology (low elevation, Bavaria, Germany; in green)..... 56
- Figure 39: Local site chronologies (T1200, T1100, T1000, LA; in grey) in comparison with a regional spruce chronology (high elevation, Zillertal, Austria; in blue)..... 57

- Figure 40: Estimated minimum tree age of analysed trees shown by age classes (considering the length of the tree-ring series, pith-offset estimates and correction for sampling height)..... 58
- Figure 41: Tree no.16 (in yellow) with broken stem but partly still active cambium, i.e., growing in one out of four sampled stem sides next to the damaged area by the avalanche in January 2019 (in red) (Foto: N. Guerrero Hue). 59
- Figure 42: Example of a tree ring with two rows of traumatic resin ducts (TRD). First row of TRD has intensity 3 (moderate AI) and second row of TRD has intensity 2 (weak AI) following Table 4 (Foto: N. Guerrero Hue). 60
- *Figure 43: Temporal distribution of number and type of avalanche indicators (considering all positions in tree ring, i.e. dormant, early earlywood, earlywood, latewood). Compression wood (CW), callous tissue (CT) and traumatic resin ducts (TRD).* 65
- Figure 44: Temporal distribution of number and type of avalanche indicators (considering only dormant and early earlywood positions in tree ring). Compression wood (CW), callous tissue (CT) and traumatic resin ducts (TRD). 66
- Figure 45: Spatial distribution of trees with avalanche indicators in years with documented avalanches. 68
- Figure 46: Spatial distribution of trees with avalanche indicators in potential avalanche years obtained after the detection steps. 69
- Figure 47a, b, c: Mapped runout of some avalanches released on the 19th, 20th and 22nd January 1951 respectively in the Arzler Alm avalanche path. The mountain hut (in blue) and the technical protection measures (in yellow) (Nessizius, 1966)..... 71
- Figure 48: Combination of an orthophoto of year 1970, undisturbed trees in green, disturbed trees with their reaction classes for year 1969 and the mapped runout of avalanche 1968. In yellow the "eastern arm" of the avalanche path. 72

List of tables

Table 1: List of abbreviations	8
Table 2: Meteorological data related to snow in Innsbruck, measured at two meteorological stations at 578 m a.s.l. (1981-2010) (ZAMG, 2021).	32
Table 3: Characteristics of the avalanche event at the Arzler Alm on the 14th of January 2019. Some data could only be estimated (Fischer, 2019; Siegele et al., 2019).....	39
Table 4: Definition of intensities of avalanche indicators (AI) based on their intensity (appearance and/or persistence) in the tree-ring series (adapted from (Stoffel & Corona, 2014)). Not applicable (N/A).	48
Table 5: Reaction classes assigned to each type of avalanche indicators (AI) based on the weighting criteria of (Stoffel & Corona, 2014).	50
Table 6: Number, percentage and type of avalanche indicators observed in tree rings.	60
Table 7: Number of avalanche indicators (AI) and their reaction class present in tree rings for historical avalanche years, considering only dormant and early earlywood positions in tree rings. Compression wood (CW), callous tissue (CT) and traumatic resin ducts (TRD).	61
Table 8: List of potential avalanche years for dataset "filtered positions" (Avalanche indicators (AI) only in dormant and early earlywood position in tree ring), including number and type of AI. Compression wood (CW), callous tissue (CT), traumatic resin ducts (TRD) and Avalanche activity index (AAI). Highlighted years with reaction class 5.....	62
Table 9: List of potential avalanche years for dataset "all positions" (Avalanche indicators (AI) in any position in tree ring), including number and type of AI. Compression wood (CW), callous tissue (CT), traumatic resin ducts (TRD) and Avalanche activity index (AAI). Highlighted years with reaction class 5.	63
Table 10: Comparison of the sampling density of some dendrogeomorphological studies using tree rings to reconstruct past snow avalanches. Details about the area of the avalanche path (ha) and the number of trees sampled.	77

REFERENCES

- Adams, M., Fischer, J.-T., Kofler, A., Tollinger, C., Graf, A., Hoffmann, J., & Fromm, R. (2018). Investigating Avalanche Interaction With Defence Structures Using Unmanned Aerial System Photogrammetry. *International Snow Science Workshop*, 116-120.
- Altman, J., Fibich, P., Dolezal, J., & Aakala, T. (2014). TRADER: A package for Tree Ring Analysis of Disturbance Events in R. *Dendrochronologia*, 32(2), 107-112. <https://doi.org/10.1016/j.dendro.2014.01.004>
- Amt der Tiroler Landesregierung. (2021). *tirisMaps Land Tirol*. <https://maps.tirol.gv.at/>
- Aulitzky, H. (1992). Die Sprache der "Stummen Zeugen" (The language of „silent witnesses“). *Proceedings of International Symposium Interpraevent, Band 6*, 139-173.
- Barbolini, M., Domaas, U., Faug, T., Gauer, P., Hakonardottir, K. M., Harbitz, C. B., Issler, D., Johannesson, T., Lied, K., Naaïm, M., Naaïm-Bouvet, F., & Rammer, L. (2009). *The design of avalanche protection dams Recent practical and theoretical developments*.
- Bebi, P., Kulakowski, D., & Rixen, C. (2009). Snow avalanche disturbances in forest ecosystems-State of research and implications for management. *Forest Ecology and Management*, 257(9), 1883-1892. <https://doi.org/10.1016/j.foreco.2009.01.050>
- Brang, P. (2001). Resistance and elasticity: promising concepts for the management of protection forests in the European Alps. *Forest Ecology and Management*, 145, 107-119.
- Burrows, C. J., & Burrows, V. L. (1976). Procedures for the study of snow avalanche chronology using growth layers of woody plants. Institute of Arctic and Alpine Research, University of Colorado. *Occasional Paper*, 23.
- Butler, D. R., & Sawyer, C. F. (2008). Natural Hazards and Earth System Sciences Dendrogeomorphology and high-magnitude snow avalanches: a review and case study. *Natural Hazards and Earth System Sciences*, 8, 303-309.
- Butler, D. R., & Stoffel, M. (2013). John F. Shroder, Jr.'s 1978 and 1980 papers on dendrogeomorphology. *Progress in Physical Geography*, 37(5), 717-721. <https://doi.org/10.1177/0309133313501107>
- Casteller, A., Häfelfinger, T., Cortés Donoso, E., Podvin, K., Kulakowski, D., & Bebi, P. (2018). Assessing the interaction between mountain forests and snow avalanches at Nevados de Chillán, Chile and its implications for ecosystem-based disaster risk reduction. *Natural Hazards and Earth System Sciences*, 18(4), 1173-1186. <https://doi.org/10.5194/nhess-18-1173-2018>
- Chiroiu, P., Stoffel, M., Onaca, A., & Urdea, P. (2015). Testing dendrogeomorphic approaches and thresholds to reconstruct snow avalanche activity in the Făgăraș Mountains (Romanian Carpathians). *Quaternary Geochronology*, 27, 1-10. <https://doi.org/10.1016/j.quageo.2014.11.001>
- climate-data.org. (2021). *Klima Innsbruck: Wetter, Klimatabelle & Klimadiagramm für Innsbruck*. <https://de.climate-data.org/europa/oesterreich/tirol/innsbruck-859/>
- Corona, C., Lopez Saez, J., Stoffel, M., Bonnefoy, M., Richard, D., Astrade, L., & Berger, F. (2012). How much of the real avalanche activity can be captured with tree rings? An evaluation of classic dendrogeomorphic approaches and comparison with historical archives. *Cold Regions Science and Technology*, 74-75, 31-42. <https://doi.org/10.1016/j.coldregions.2012.01.003>

- de Bouchard d'Aubeterre, G., Favillier, A., Mainieri, R., Lopez Saez, J., Eckert, N., Saulnier, M., Peiry, J. L., Stoffel, M., & Corona, C. (2019). Tree-ring reconstruction of snow avalanche activity: Does avalanche path selection matter? *Science of the Total Environment*, 684, 496-508. <https://doi.org/10.1016/j.scitotenv.2019.05.194>
- EAWS. (2021). *European Avalanche Warning Services Glossary*. https://www.lawis.at/eaws/en/includes/glossary/glossary_en_all.html
- FAO, I. W. G. W. (2015). World reference base for soil resources 2014. International soil classification system for naming soils and creating legends for soil maps. In *World Soil Resources Reports No. 106*. Food and Agriculture Organization of the United Nations Rome.
- Favillier, A., Guillet, S., Morel, P., Corona, C., Saez, J. L., Eckert, N., Cánovas, J. A. B., Peiry, J.-L. L., Stoffel, M., Lopez Saez, J., Eckert, N., Ballesteros Cánovas, J. A., Peiry, J.-L. L., & Stoffel, M. (2017). Disentangling the impacts of exogenous disturbances on forest stands to assess multi-centennial tree-ring reconstructions of avalanche activity in the upper Goms Valley (Canton of Valais, Switzerland). *Quaternary Geochronology*, 42, 89-104. <https://doi.org/10.1016/j.quageo.2017.09.001>
- Favillier, A., Guillet, S., Trappmann, D., Morel, P., Lopez-Saez, J., Eckert, N., Zenhäusern, G., Peiry, J. L., Stoffel, M., & Corona, C. (2018). Spatio-temporal maps of past avalanche events derived from tree-ring analysis: A case study in the Zermatt valley (Valais, Switzerland). *Cold Regions Science and Technology*, 154, 9-22. <https://doi.org/10.1016/j.coldregions.2018.06.004>
- Feistl, T., Bebi, P., Teich, M., Bühler, Y., Christen, M., Thuro, K., & Bartelt, P. (2014). Observations and modeling of the braking effect of forests on small and medium avalanches. *Journal of Glaciology*, 60(219), 124-138. <https://doi.org/10.3189/2014JoG13J055>
- Fellin, W. (2013). Einführung in Eis-, Schnee- und Lawinenmechanik. In *Springer-Verlag* (Vol. 1, Issue 1). Springer-Verlag.
- Fischer, J.-T. (2019). *Ereignismeldung Lawine, Arzleralm-Lawine. WLK.digital.Ereigniskataster*.
- Fischer, J.-T., Stepanek, L., Huber, A., Fromm, R., Zeidler, A., & Kleemayr, K. (2013). Extreme value analysis of design events. *International Snow Science Workshop, Grenoble Chamonix Mont-Blanc-2013*.
- Forstgesetz. (1975). *Bundesgesetz vom 3. Juli 1975, mit dem das Forstwesen geregelt wird. StF: BGBl. Nr. 440/1975*.
- Gärtner, H., Cherubini, P., Fonti, P., Von Arx, G., Schneider, L., Nievergelt, D., Verstege, A., Bast, A., Schweingruber, F. H., & Büntgen, U. (2015). A Technical Perspective in Modern Tree-ring Research-How to Overcome Dendroecological and Wood Anatomical Challenges. *J. Vis. Exp*, 97, 52337. <https://doi.org/10.3791/52337>
- Grissino-Mayer, H. D. (2003). A Manual and Tutorial for the Proper Use of an Increment Borer. *Tree-Ring Research*, 59(2), 63-79.
- Hydrographischer Dienst. (2021). *eHYD - der Zugang zu hydrologischen Daten Österreichs*. <https://ehyd.gv.at/>
- Kaennel, M., & Schweingruber, F. H. (2021). *WSL Glossary of Dendrochronology*. https://www.wsl.ch/dendro/products/dendro_glossary/index_EN
- Kilian, W., Müller, F., & Starlinger, F. (1994). Die forstlichen Wuchsgebiete Österreichs. *FBVA-Berichte*, 82, 55-57.
- Kofler, A., Tollinger, C., Jenner, A., Granig, M., & Adams, M. (2018). Braking mounds in avalanche simulations-a SamosAT case study. *International Snow Science Workshop, Innsbruck, Austria*, 134-138.

- Kogelnig-Mayer, B., Stoffel, M., Schneuwly-Bollschweiler, M., Hübl, J., & Rudolf-Miklau, F. (2011). Possibilities and limitations of dendrogeomorphic time-series reconstructions on sites influenced by debris flows and frequent snow avalanche activity. *Arctic, Antarctic, and Alpine Research*, 43(4), 649-658. <https://doi.org/10.1657/1938-4246-43.4.649>
- Krainer, K., & Meyer, M. (2016). Field trip 8. Innsbruck's geology in a nutshell: from the Hafelekar to the Hötting Breccia. *Geo.Alp*, 13, 215-228.
- Mainieri, R., Favillier, A., Lopez-Saez, J., Eckert, N., Zgheib, T., Morel, P., Saulnier, M., Peiry, J. L., Stoffel, M., & Corona, C. (2020). Impacts of land-cover changes on snow avalanche activity in the French Alps. *Anthropocene*, 30, 1-13. <https://doi.org/10.1016/j.ancene.2020.100244>
- Margreth, S. (2007). Snow pressure on cableway masts: Analysis of damages and design approach. *Cold Regions Science and Technology*, 47(1-2), 4-15.
- Margreth, S. (2004). Die Wirkung des Waldes bei Lawinen. *Forum Für Wissen: Schutzwald Und Naturgefahren*, 21-26.
- Martin, J.-P., & Germain, D. (2016). Can we discriminate snow avalanches from other disturbances using the spatial patterns of tree-ring response? Case studies from the Presidential Range, White Mountains, New Hampshire, United States. *Dendrochronologia*, 37, 17-32. <https://doi.org/10.1016/j.dendro.2015.12.004>
- McClung, D., & Schaerer, P. A. (2006). *The avalanche handbook* (3rd ed.). The Mountaineers Books.
- Meseşan, F., Man, T. C., Pop, O. T., & Gavrilă, I. G. (2019). Reconstructing snow-avalanche extent using remote sensing and dendrogeomorphology in Parâng Mountains. *Cold Regions Science and Technology*, 157, 97-109. <https://doi.org/10.1016/j.coldregions.2018.10.002>
- Muntán, E. (2016). *Snow avalanches in the Pyrenees: Dendrochronological dating, dendrogeomorphological mapping and detection of past snow-avalanche seasons at a regional scale Allaus de neu al Pirineu : datació dendrocronològica, cartografia dendrogeomorfològica i detecció*. Universitat de Barcelona.
- Nessizius, H. (1966). *Begehungsbericht - Lawinen Arzlalpe. Forsttechnischer Dienst für Wildbach- u Lawinenverbauung, Archiv der Gebietsbauleitung Mittleres Inntal*.
- Neumann, M. (2011). *Räumliche und zeitliche Rekonstruktion der Murgangaktivität für alpine Einzugsgebiete eine dendrogeomorphologische Fallstudie*. Universität für Bodenkultur Wien.
- Nicolussi, K., Pindur, P., Schiessling, P., Kaufmann, M., & Thurner, A. (2007). Waldzerstörende Lawinenereignisse während der letzten 9000 Jahre im Oberen Zemmgrund, Zillertaler Alpen, Tirol. In *mitt. Komm. Quartärforsch. Österr. Akad. Wiss* (Vol. 141).
- Office of the Tyrolean Provincial Government. (2021). *Avalanche Warning Service Tyrol*. https://avalanche.report/albina_files/2019-01-14/2019-01-14_en.pdf
- Oller, P., Fischer, J.-T., & Muntán, E. (2020). The historic avalanche that destroyed the village of Àrreu in 1803, Catalan Pyrenees. *Geosciences (Switzerland)*, 10(5), 1-25. <https://doi.org/10.3390/geosciences10050169>
- Österreichisches Normungsinstitut. (2010). *ÖNR 24805 Permanenter technischer Lawinenschutz*.
- R Development Core Team. (2013). *R: A Language and Environment for Statistical Computing*. <http://www.r-project.org>
- Rinn, F. (2011). *TSAP-Win. Time Series Analysis and Presentation for Dendrochronology and Related Applications*. 110.

- Rudolf-Miklau, F., & Sauermoser, S. (2011). *Handbuch Technischer Lawinenschutz*. Ernst & Sohn.
- Rudolf-Miklau, F., Sauermoser, S., Mears, A., & Boensch, M. (2015). *The technical avalanche protection handbook* (John Wiley & Sons (ed.)). John Wiley & Sons.
- Schneebeli, M., & Bebi, P. (2004). Snow and Avalanche Control. *Elsevier*, 397-402.
- Schweingruber, F. H., Börner, A., & Schulze, E.-D. (2007). *Atlas of woody plant stems: evolution, structure, and environmental modifications*. Springer Science & Business Media.
- Shroder, J. F. (1978). Dendrogeomorphological Analysis of Mass Movement on Table Cliffs Plateau, Utah. *Quaternary Research*, 9(2), 168-185. [https://doi.org/10.1016/0033-5894\(78\)90065-0](https://doi.org/10.1016/0033-5894(78)90065-0)
- Shroder, J. F. (1980). Dendrogeomorphology: Review and new techniques of tree-ring dating. *Progress in Physical Geography*, 4(2), 161-188. <https://doi.org/10.1177/030913338000400202>
- Siegele, P., Tollinger, C., & Granig, M. (2019). *Ereignisdokumentation Lawinen, Jänner-Februar 2019*.
- Stepanek, L. (2012). *Mitigative Measures against Snow Avalanches on the Mountains North of Innsbruck*.
- Stoffel, M. (2005). *Spatio-temporal variations of rockfall activity into forests: results from tree-ring and tree analysis*. Université de Fribourg.
- Stoffel, M. (2008). Dating past geomorphic processes with tangential rows of traumatic resin ducts. *Dendrochronologia*, 26(1), 53-60. <https://doi.org/10.1016/j.dendro.2007.06.002>
- Stoffel, M., & Bollschweiler, M. (2008). Tree-ring analysis in natural hazards research-an overview. *Natural Hazards and Earth System Sciences*, 8, 187-202.
- Stoffel, M., Bollschweiler, M., Butler, D. R., & Luckman, B. H. (2010). *Tree Rings and Natural Hazards: A State-of-Art* (Vol. 41). Springer Science & Business Media.
- Stoffel, M., Butler, D. R., & Corona, C. (2013). Mass movements and tree rings: A guide to dendrogeomorphic field sampling and dating. *Geomorphology*, 200, 106-120. <https://doi.org/10.1016/j.geomorph.2012.12.017>
- Stoffel, M., & Corona, C. (2014). Dendroecological dating of geomorphic disturbance in trees. *Tree-Ring Research*, 70(1), 3-20. <https://doi.org/10.3959/1536-1098-70.1.3>
- Teich, M., Bartelt, P., Gret-Regamey, A., & Bebi, P. (2012). Snow avalanches in forested terrain: Influence of forest parameters, topography, and avalanche characteristics on runout distance. *Arctic, Antarctic, and Alpine Research*, 44(4), 509-519. <https://doi.org/10.1657/1938-4246-44.4.509>
- Teich, M., Giunta, A. D., Hagenmuller, P., Bebi, P., Schneebeli, M., & Jenkins, M. J. (2019). Effects of bark beetle attacks on forest snowpack and avalanche formation - Implications for protection forest management. *Forest Ecology and Management*, 438(February), 186-203. <https://doi.org/10.1016/j.foreco.2019.01.052>
- Tollinger, C. (2011). *Studie Lawinensimulationen Arzler Alm-Lawine Innsbruck / Mühlau*.
- Umweltbundesamt. (2021). *BORIS - Bodeninformationssystem*. <https://www.umweltbundesamt.at/boris>
- UNESCO. (1981). *The Avalanche Atlas*. United Nations.
- van der Maaten-Theunissen, M., van der Maaten, E., & Bouriaud, O. (2015). PointRes: An R package to analyze pointer years and components of resilience. *Dendrochronologia*, 35, 34-38. <https://doi.org/10.1016/j.dendro.2015.05.006>
- Vospernik, S., Nicolussi, K., Groff, J., Pichler, T., & Spiecker, H. (2014). Waldwachstum und Klima bei Fichte und Zirbe an Seehöhengradienten in Tirol. *Tagung Sektion Ertragskunde, Lenzen an Der Elbe, Germany*, 160-165.

- Wilson, R. J. S., Esper, J., & Luckman, B. H. (2004). *Utilising historical tree-ring data for dendroclimatology: A case study from the Bavarian Forest, Germany.*
- ZAMG. (2021). ZAMG Zentralanstalt für Meteorologie und Geodynamik. Wetterstationen. <http://www.zamg.ac.at/cms/de/aktuell>
- Zrost, D., Nicolussi, K., & Thurner, A. (2008). Holozäne Lawinenereignisse im Jahrringbild der subfossilen Hölzer des Schwarzensteinmoores, Zillertaler Alpen. In *Verlag der Österreichischen Akademie der Wissenschaften.*

ANNEX I: Field sheet

GENERAL INFORMATION

Date	1/10/19	Team	Michaela Mucic	Marke	<input checked="" type="checkbox"/>	Fotos	<input checked="" type="checkbox"/>
Location	TR1000	GPS Reach	Azi: 84°	Dist: 7'27 m		Saved	<input checked="" type="checkbox"/>

TREE INFO

Tree code	74	Tree species	Fi
DBH (cm) (or trunk or stump diameter)	28	slope (°)	17 18
Height (m) (broken or stump)	22	Crown height (m)	10

SURROUNDINGS: Land cover 10-15m around a "band" of smaller trees (20, 15m)
 - East (Ost): open area, < 1m, small trees (Kochholz jagd unten), no damage
 - West (W): older bigger trees, no damage

1. Why this tree? Choose one reason

standing alone	damaged	broken	big diameter	variety of SP / ages	<u>undisturbed</u>
----------------	---------	--------	--------------	----------------------	--------------------

2. Status (choose one)

<u>upright</u>	leaning	fallen		stump	
Dir (azi)		broken with/ without stump / uprooted		old	new
		Direction (azi)	Length (m)	broken	felled

3. Damages (of avalanche)

Dead	broken branches or crown (flag)	callus tissue (overgrowing)	Tilting (säbelw)	Bending (flexed)	uprooted
scar	eccentricity	new vertical stem	broken top	Other:	

4. Other damages (try to avoid!): Which? _____

5. Age of damage

6. Position of damage

7. Degree of damage

8. Social status

9. Position related to avalanche'19

recent (resin)	old (overgrowing)		
stem	branches	roots	
low	medium	high	
<u>dominant</u>	codominant	dominated	unknown
<u>outside</u>	middle of the path	margin	

CORES INFO: min 2 cores. Why this cores? C.L., reaction wood, scar, callus...

Code & why?	A contour line	B RW NH	uphill	top
height of coring	1'10 m	0'75 m		
Code & why?	C	D		
height of coring			downhill	roots (fallen / leaning)

ANNEX II: Identification key for avalanche indicators

Sources: (Kaennel & Schweingruber, 2021; Kogelnig-Mayer et al., 2011; Schweingruber et al., 2007) and K. Nicolussi.

See also Table 4 for the classification of their intensity and Table 5 for the Reaction Class assigned.

TRAUMATIC RESIN DUCTS (TRD)

Intensity 4: extremely compact and contiguous rows (>90% ring width) → strong AI



Intensity 3: compact, but not completely continuous rows (50-90% ring width) → moderate AI



Intensity 2: tangentially aligned, with clearly observable gaps between ducts (< 50% ring width) → weak AI



Intensity 1: some RD tangentially aligned (at least 3 RD in a row). Not considered as AI.



Example of „normal“ resin ducts, not traumatic:



COMPRESSION WOOD (CW)

„thick-walled, almost round cells with intercellular space. Macroscopically: dark colour“

Considered as AI only if strong / clear CW cells were observed and they were present in $\geq 50\%$ of ring width. Intensity later assigned according to CW duration in consecutive tree rings (see Table 4).

Examples of tree rings with CW covering $\geq 50\%$ of ring width (considered AI):



Examples of tree rings with CW covering $< 50\%$ of ring width (not considered AI):



Example of a „normal“ transition from EW to LW, without CW:



CALLOUS TISSUE (CT)

FROST RING

Example of a frost ring (to observe an example of callous tissue). Frost rings are not caused by avalanches, therefore not considered as an AI.



INJURY

Intensity 4: strong AI



ANNEX III: Calculation of abrupt growth change

Abrupt growth change is another feature used to infer past events, which is calculated using the ring width length data. The R software (R Development Core Team, 2013) was used in this step and the input data were the ring width length files obtained with TSAP-Win. The purpose was to calculate AGC following the table below (Stoffel & Corona, 2014). Nevertheless, other references were searched and carefully read because it was not detailed enough how to perform the calculation.

Definition of intensities for growth suppression and growth release according to (Stoffel & Corona, 2014)

AI	Parameter	weak AI	moderate AI	strong AI
Growth suppression	change in ring width (%)	< 60%	≥ 100 %	≥ 200 %
	duration	≥ 4 yr	< 8 yr but ≥ 4 yr	≥ 8 yr
Growth release	change in ring width (%)	< 50%	≥ 100 %	≥ 150 %
	duration	≥ 4 yr	< 8 yr but ≥ 4 yr	≥ 8 yr

After reading about different methods and doing some tests with my data, I decided to use the methods included in the R package PointRes developed by (van der Maaten-Theunissen et al., 2015). With the package PointRes both releases and suppressions can be calculated however the duration of the growth change is not considered. Two methods are available for the identification of event years (i) normalization in a moving window, and (ii) relative growth change. Both methods were applied to my data. In a first attempt default threshold values were used. As many event years were obtained, in a second attempt the thresholds were increased to get a shorter list of events (less in number but stronger in intensity). Unexpectedly, each method delivered a quite different list of trees with event years. Then the position of trees showing events in both methods was analysed with QGIS and compared with mapped runout of documented avalanches. It was observed the location and distance of trees related to the different extensions (inside affected area, outside, margin). No significant relation was found between event years from PointRes and runouts mapped. Additionally, the tree-ring width diagrams were observed seeking to visually corroborate the trees and years showing AGC. Again, no significant match was found between event years and ring width diagrams. This may be due to not considering the duration of the growth change: PointRes detects tree rings suddenly very wide or narrow but might be not sustained in time. However visually, and for the purpose of this study, it was important that the growth increase or reduction was maintained for some years.

Attempts done with the Arzler Alm data

1. Negative abrupt growth change (suppression) following (Zrost et al., 2008): "ein Wachstumseinbruch, der durch mindestens drei aufeinander folgende Jahrringe mit Breitenwerten, die über 40 Prozent unter dem Breitenmittel der vier vorhergehenden Jahrringe liegen, gekennzeichnet ist".

Tried to program it with R, too complex, deep knowledge of programming needed.

2. There are some R packages focusing on releases and / or suppressions.
 - 2.1. Package Trader calculates only releases (Altman et al., 2014), therefore was discarded as both suppressions and releases were targeted. *Modifying R code required considerable programming skills.*
 - 2.2. Package PointRes (van der Maaten-Theunissen et al., 2015) calculates both types of growth changes with two different methods: relative growth change (percentage) or normalization (standard deviation). Calculation is performed using the tree-ring width of all radii. Both methods were applied to the data. In a first attempt with higher thresholds (details below *). A list of trees was obtained showing abrupt growth changes (either positive or negative). *Each method delivers a quite different list of trees. No good match between methods from same R package.*
 - Trader: only suppressions but not releases can be calculated. It considers their duration.
 - PointRes: suppressions and releases can be calculated, however with the same percentage of change. It does not consider duration.
3. The position of listed trees related to the mapped runout for documented avalanches was examined with QGIS: distance from tree to avalanche affected area was observed, compared avalanche years with growth change years obtained with PointRes. Could listed trees be affected by a documented avalanche event?
No good match between obtained years and documented avalanches runouts.
4. The tree-ring width diagrams of listed trees were observed. Years obtained with PointRes were also visually corroborated as release or suppression.
No good match. Visually I would select other years as growth changes as the ones delivered by PointRes.
My personal impression is that most years from PointRes are individual especially narrow or wide rings but not sustained in time (for at least 3-5 years). This R package has no possibility to consider how long are those growth changes.
5. Further options: use Trader package and consider only releases or use MS Excel.
It was considered interesting to have both suppressions and releases. Perhaps even suppressions seen as more informative related to possible avalanche events.
MS Excel is considered limited to perform these calculations, as it was searched to be able to try different percentages and durations.
6. Rejection of using AGC as avalanche indicator to identify old avalanche events in this work.

Discussion

AGC was thought to be a useful avalanche indicator to detect old avalanches as cited in various scientific literature. However, after a broad literature research, trying different methods, investing much time but without obtaining satisfactory results, it was discarded to be used as indicator of avalanches here.

A possible explanation of unsatisfactory results could be that our study area has a strong anthropogenic influence (forest management, recreation activities). In (Stoffel et al., 2013) is mentioned that the use of growth releases in managed stands can lead to misleading results. This might be the reason why this method did not deliver comprehensible results, as individual trees might have been felled creating an

extremely heterogenous mosaic pattern inside the forest stand. In any case, AGC and especially releases are not considered the best avalanche indicators to date past events (Stoffel & Bollschweiler, 2008) and (Stoffel, 2005) recommends to assess other signs of disturbance events in order to correlate event data.

* Details of methods and thresholds used with PointRes library in R:

Methods for the identification of event and pointer years in (van der Maaten-Theunissen et al., 2015):

- (i) Normalization in a moving window: by normalizing individual tree-ring series in a moving window with each year placed as central point.
 - o Cropper (NC): Thresholds reflect the number of standard deviations (SD) from the local mean that are used to identify event years.
Release / suppression if $|C| > 0.75$ SD
 - o Variant Neuwirth (NN): distinguishes three intensity classes.
Weak $|C| > 1.0$, strong $|C| > 1.28$, and extreme $|C| > 1.645$.

- (ii) Relative growth change (also abrupt growth change) (RGC): relates tree growth in a particular year to the average growth of a specified number of preceding years

Method	Default values	Used thresholds
RGC	rgc.thresh.pos = 60, rgc.thresh.neg = 40	rgc.thresh.pos = 100, rgc.thresh.neg = 100
Norm. Cropper	C.thresh = 0.75	C.thresh = 1.75
Norm. Neuwirth	N.thresh1 = 1, N.thresh2 = 1.28, N.thresh3 = 1.645	N.thresh1 = 1.28, N.thresh2 = 1.645, N.thresh3 = 2.0

default values but series.thresh = 0.001

```
py.rgc <- pointer.rgc(aa.rwl, nb.yrs = 4, rgc.thresh.pos = 60, rgc.thresh.neg = 40, series.thresh = 0.001)
```

```
py.nc <- pointer.norm(aa.rwl, window = 5, method.thresh = "Cropper", C.thresh = 0.75, series.thresh = 0.001)
```

```
py.nn <- pointer.norm(aa.rwl, window = 5, method.thresh = "Neuwirth", N.thresh1 = 1, N.thresh2 = 1.28, N.thresh3 = 1.645, series.thresh = 0.001)
```

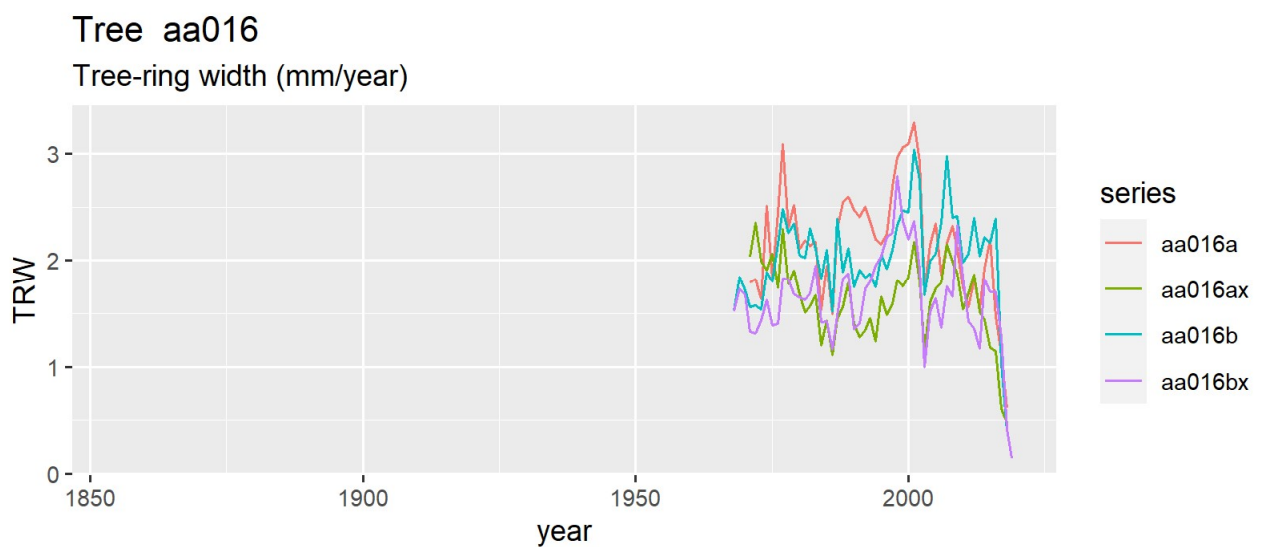
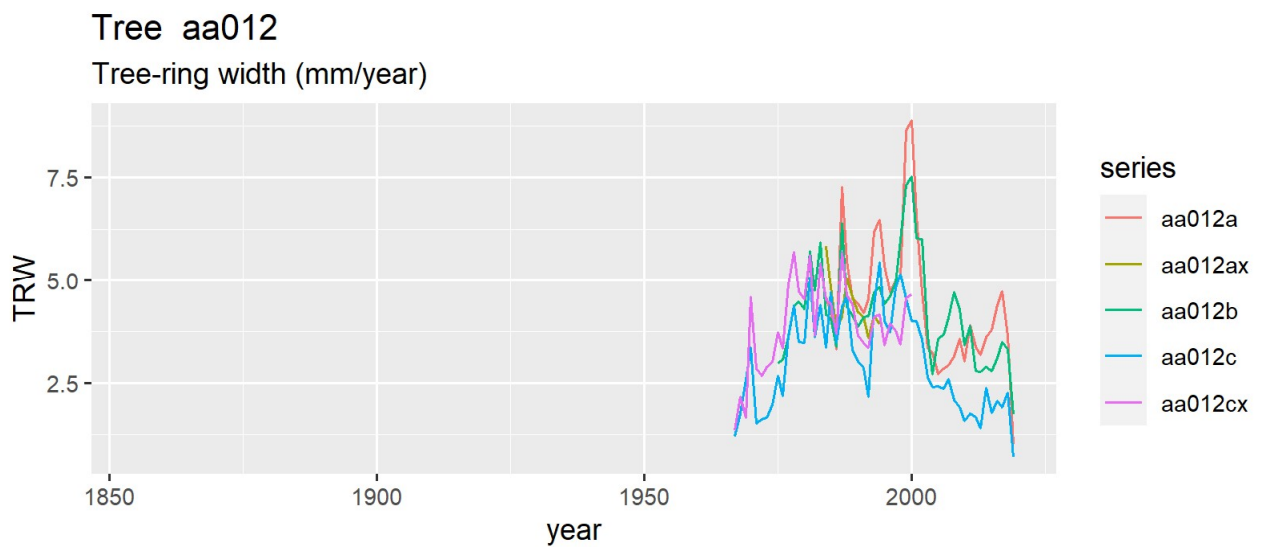
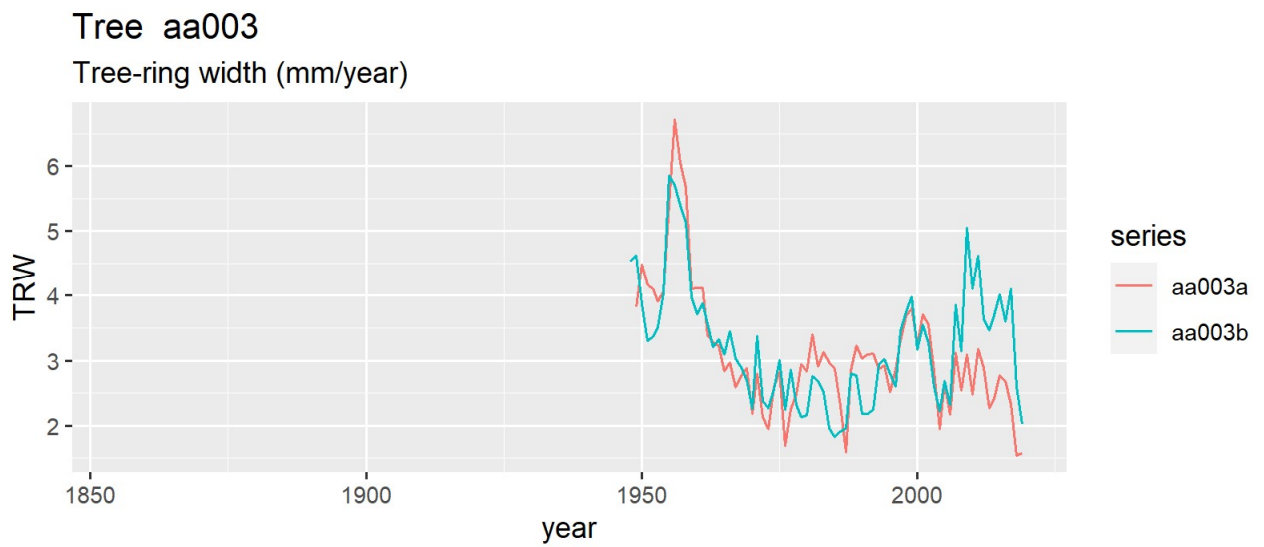
done: to obtain less but stronger event years

```
pointer.rgc(aa.rwl, nb.yrs = 4, rgc.thresh.pos = 100, rgc.thresh.neg = 100, series.thresh = 0.001)
```

```
pointer.norm(aa.rwl, window = 5, method.thresh = "Cropper", C.thresh = 1.75, series.thresh = 0.001)
```

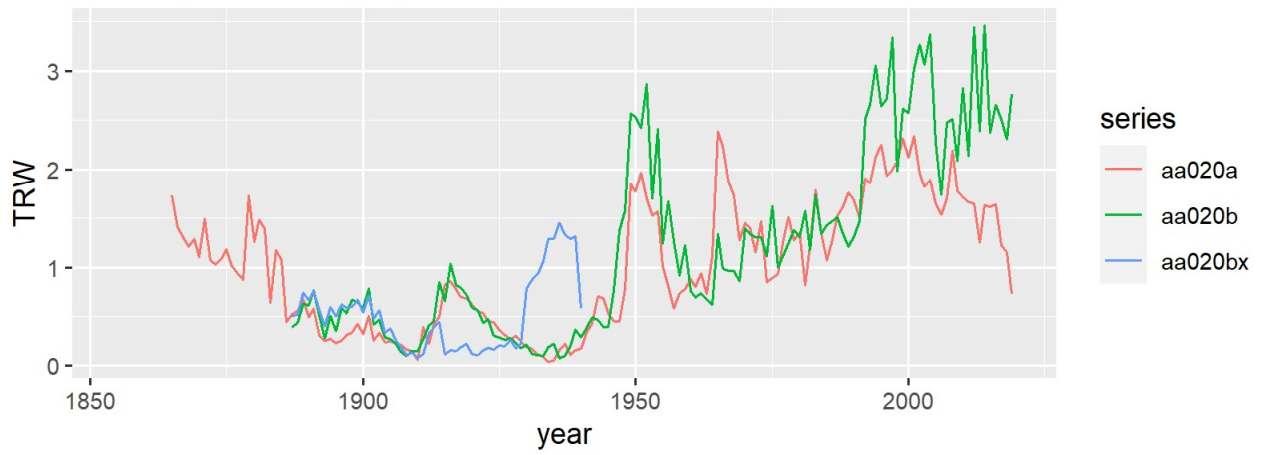
```
pointer.norm(aa.rwl, window = 5, method.thresh = "Neuwirth", N.thresh1 = 1.28, N.thresh2 = 1.645, N.thresh3 = 2.0, series.thresh = 0.001)
```

ANNEX IV: Tree-ring width diagrams



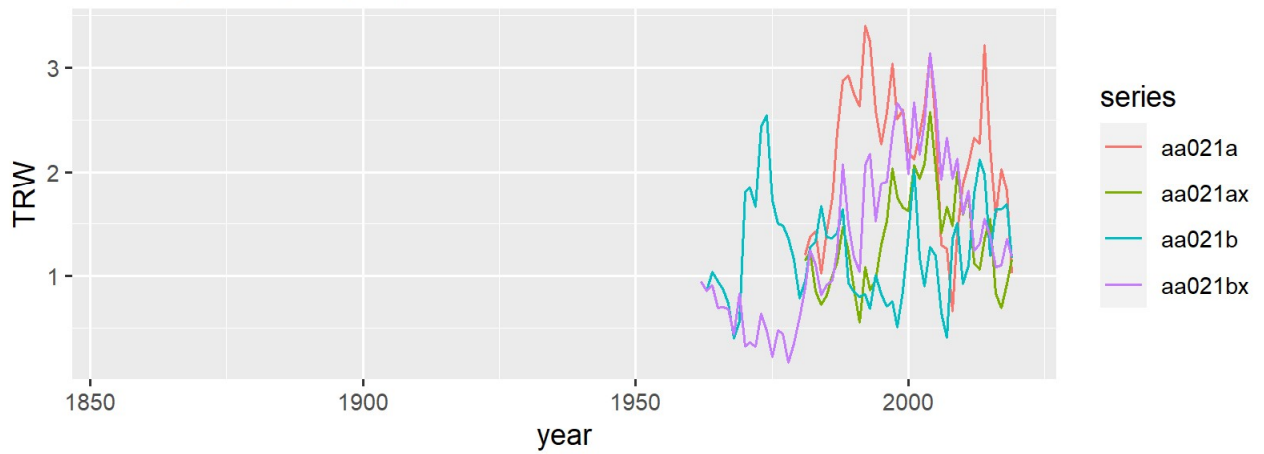
Tree aa020

Tree-ring width (mm/year)



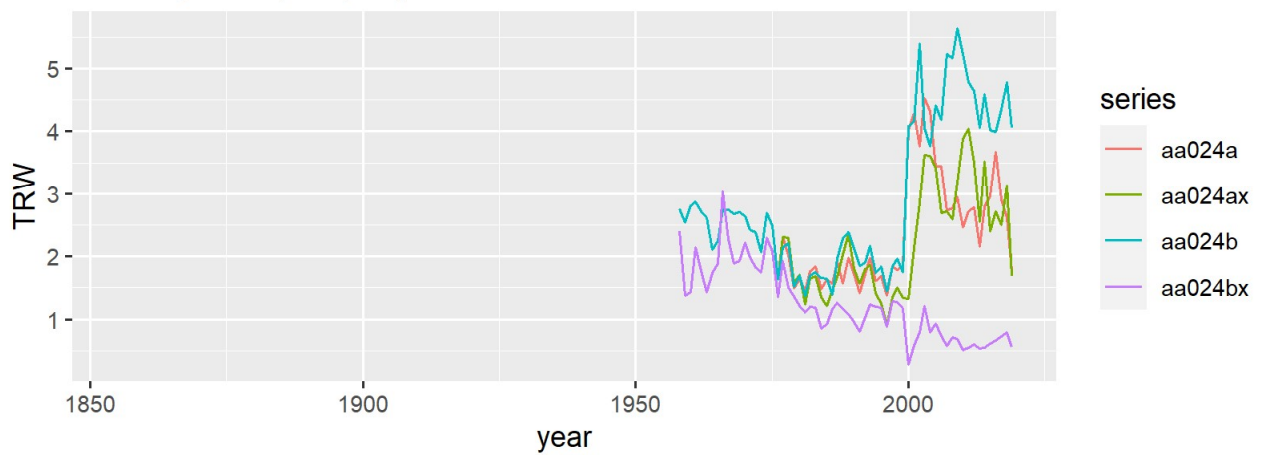
Tree aa021

Tree-ring width (mm/year)



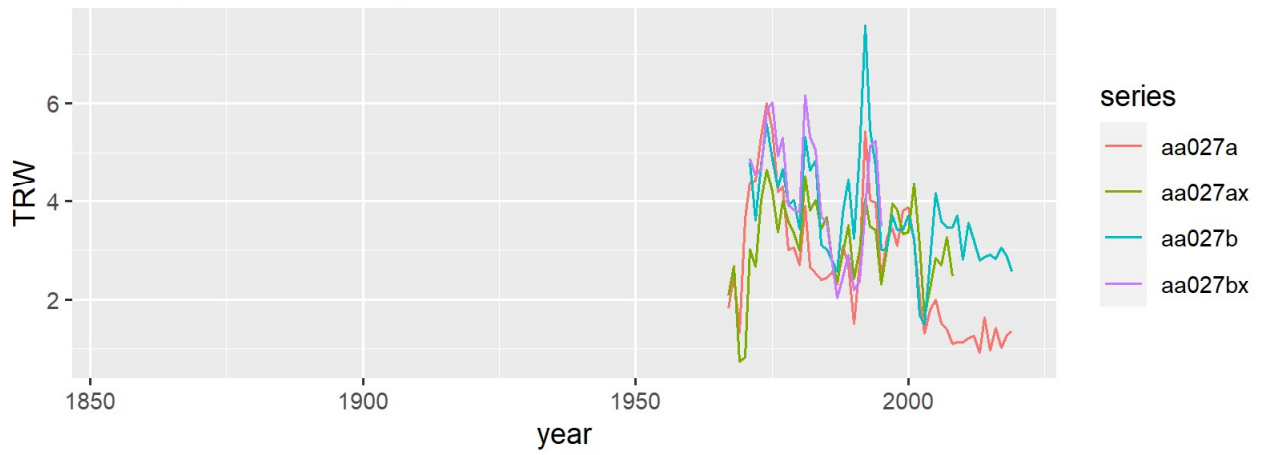
Tree aa024

Tree-ring width (mm/year)



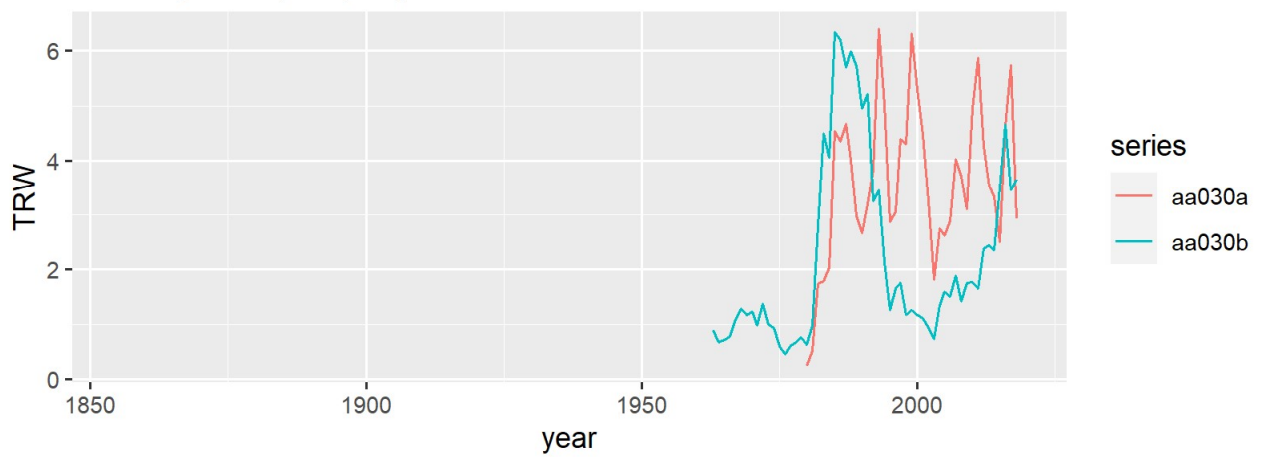
Tree aa027

Tree-ring width (mm/year)



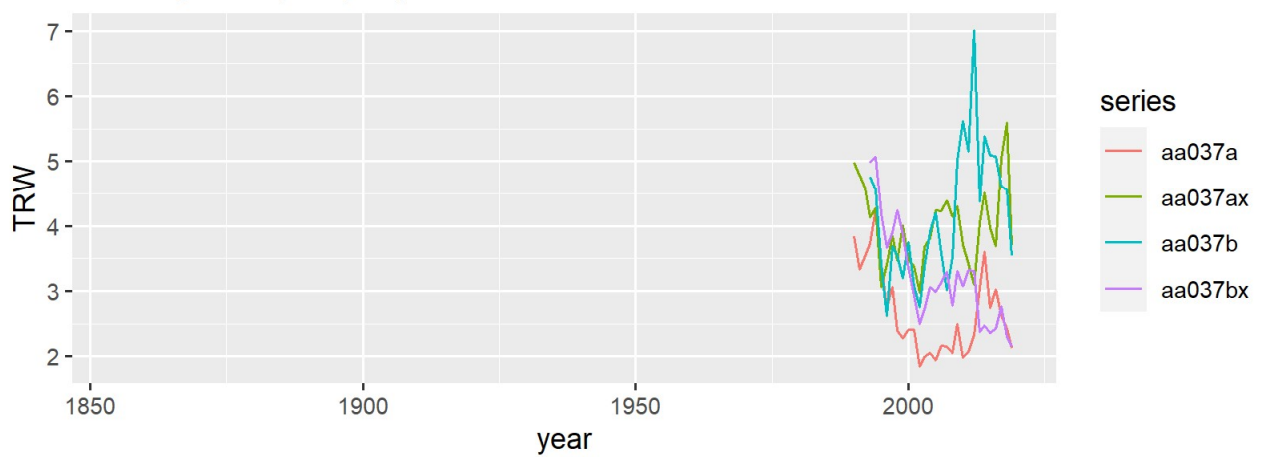
Tree aa030

Tree-ring width (mm/year)



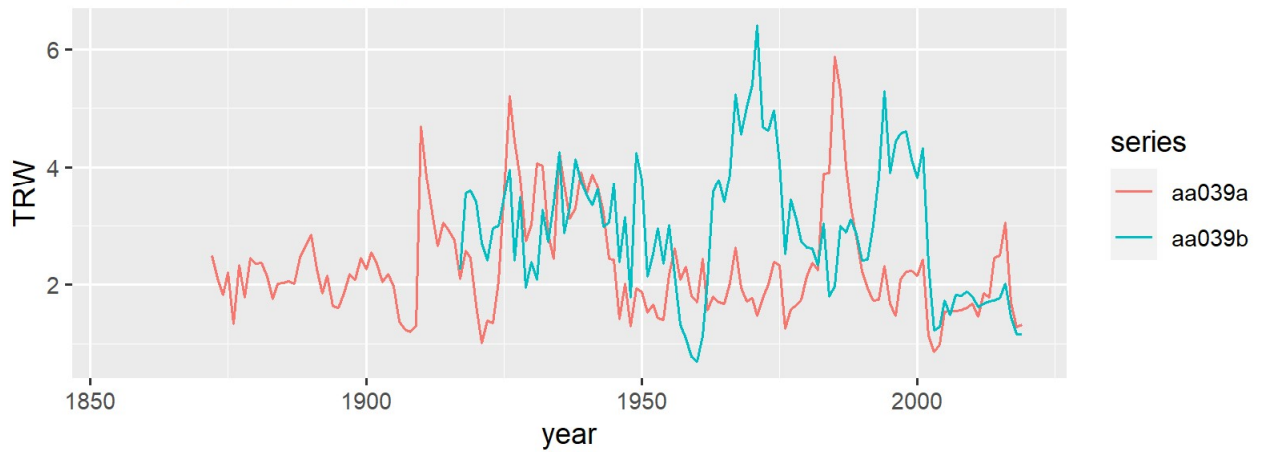
Tree aa037

Tree-ring width (mm/year)



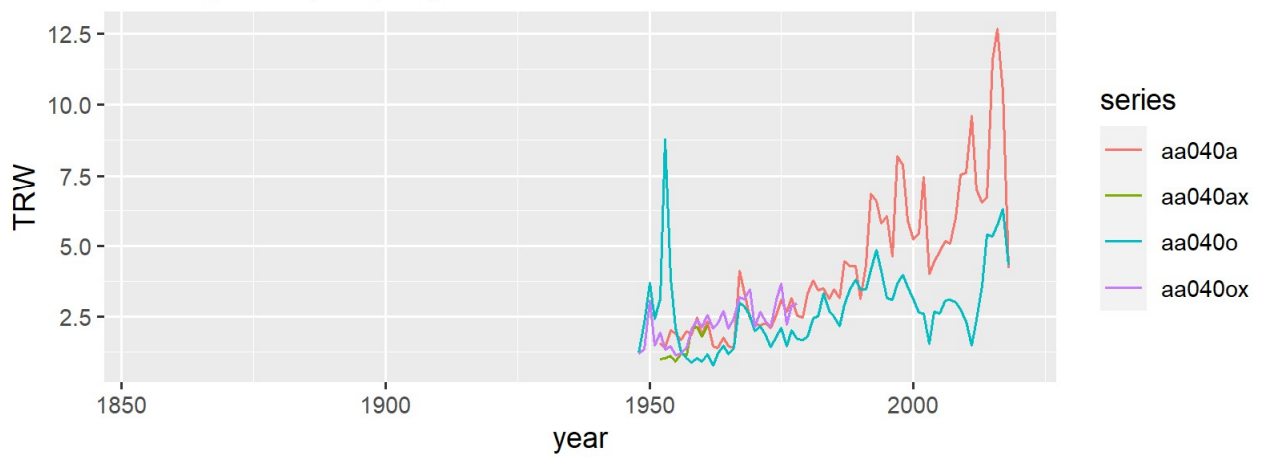
Tree aa039

Tree-ring width (mm/year)



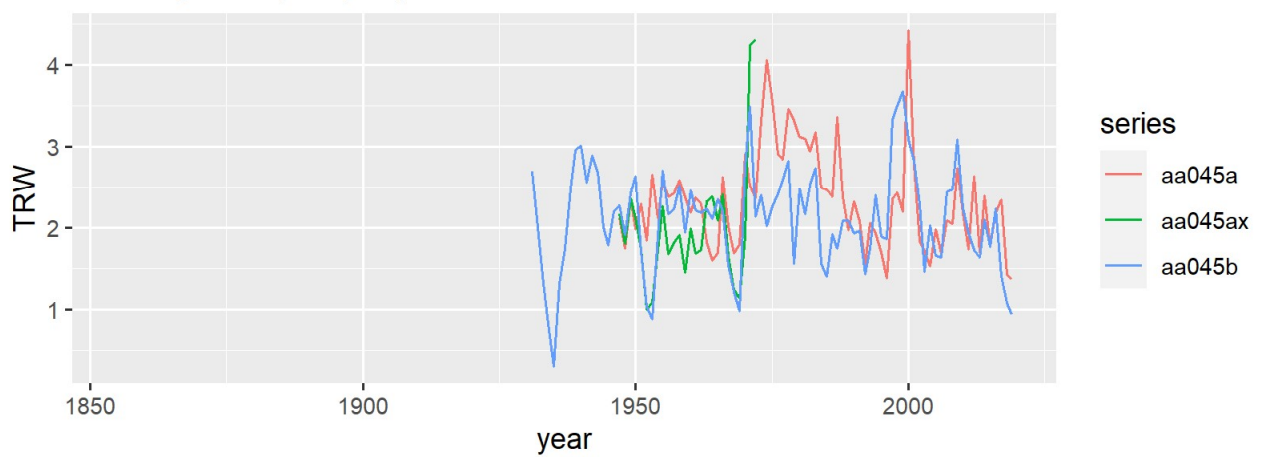
Tree aa040

Tree-ring width (mm/year)



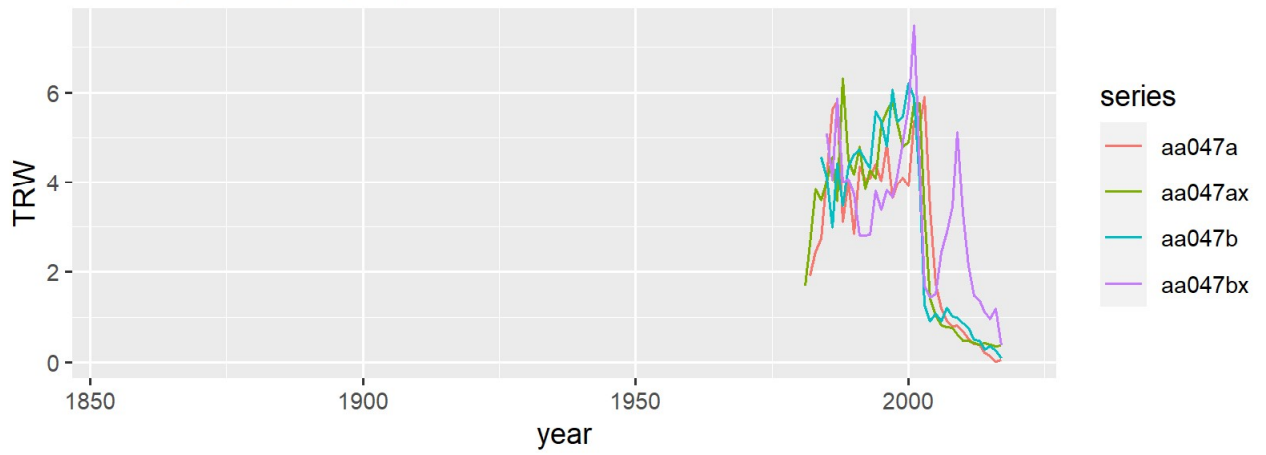
Tree aa045

Tree-ring width (mm/year)



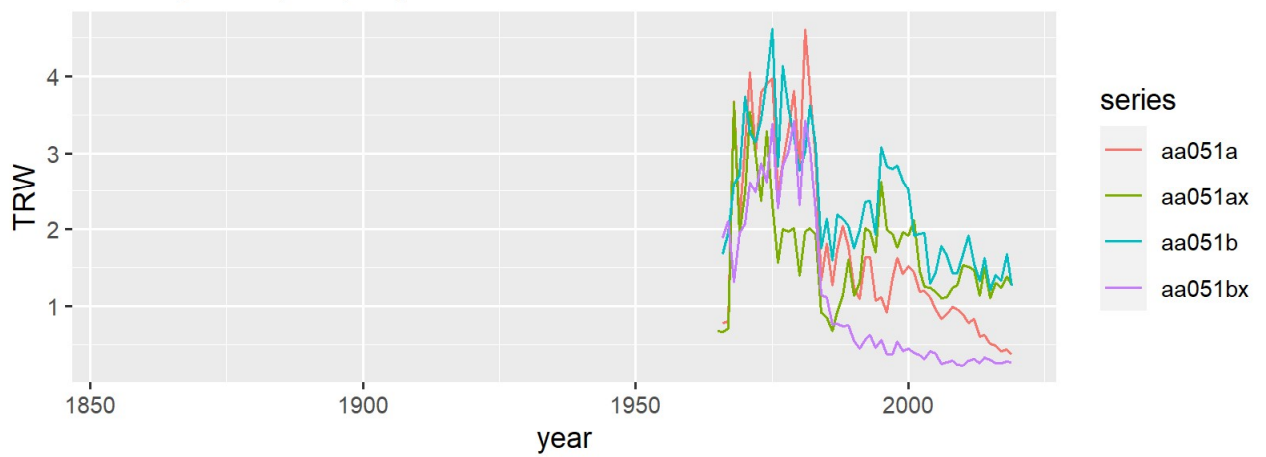
Tree aa047

Tree-ring width (mm/year)



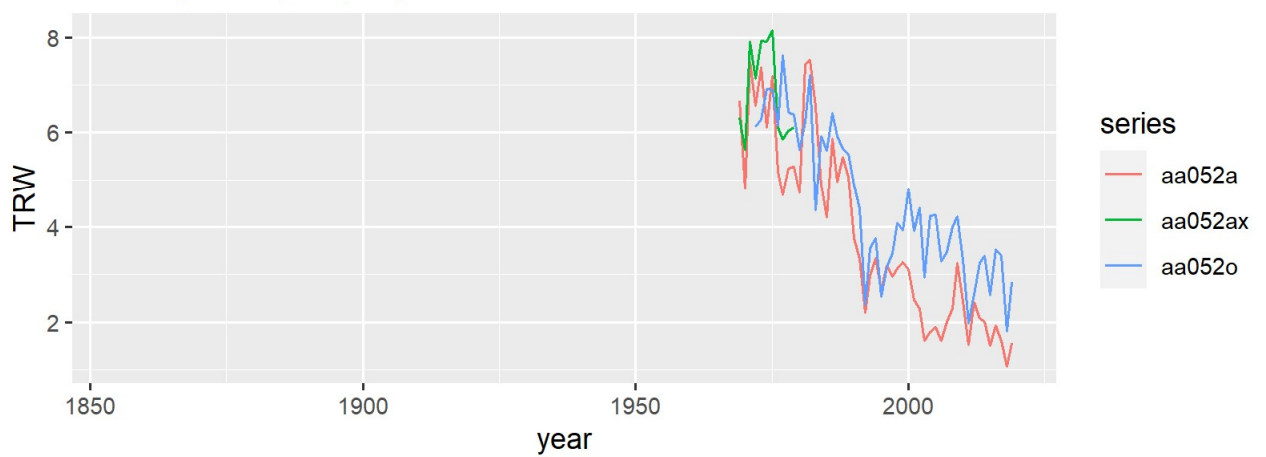
Tree aa051

Tree-ring width (mm/year)



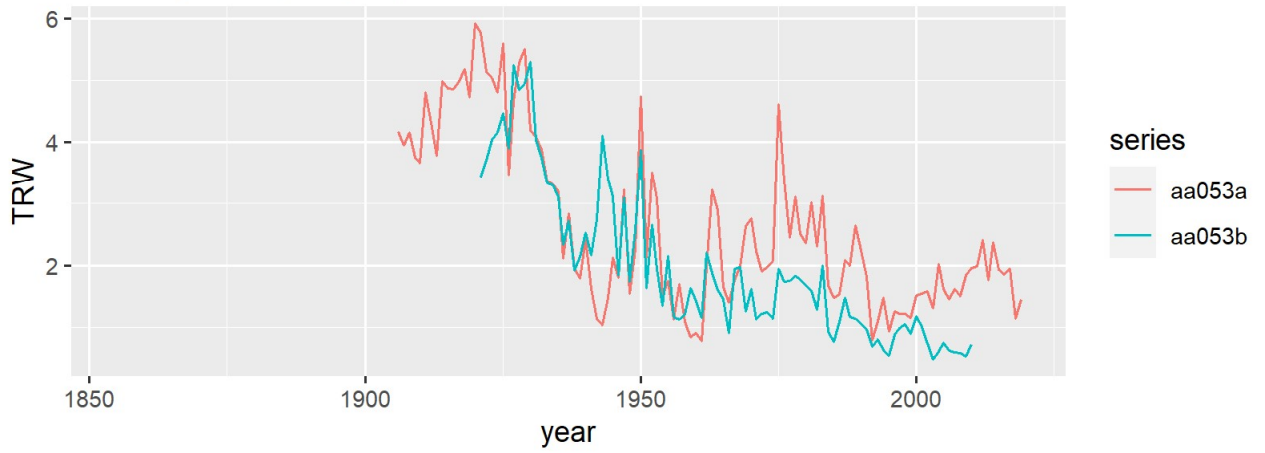
Tree aa052

Tree-ring width (mm/year)



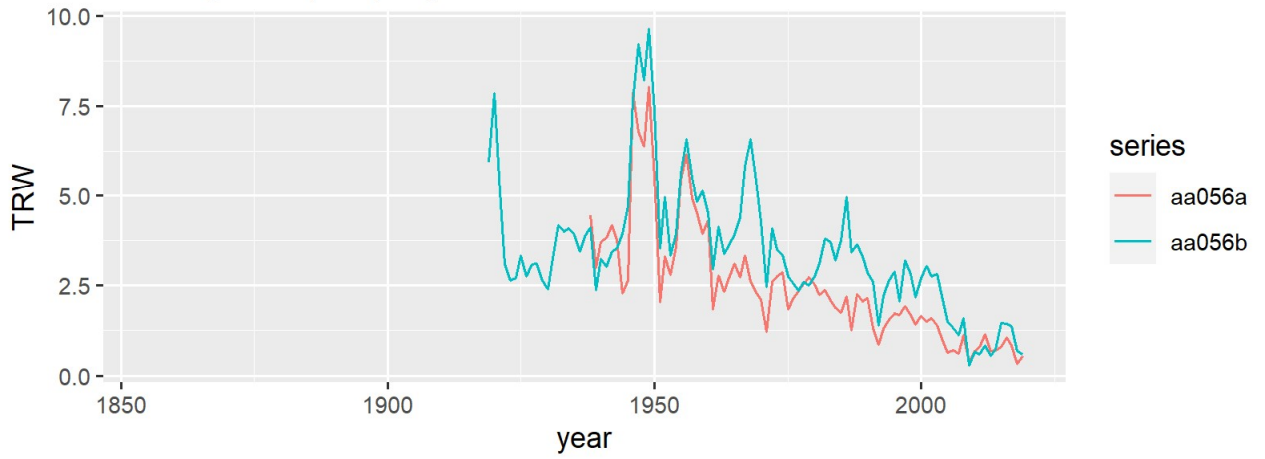
Tree aa053

Tree-ring width (mm/year)



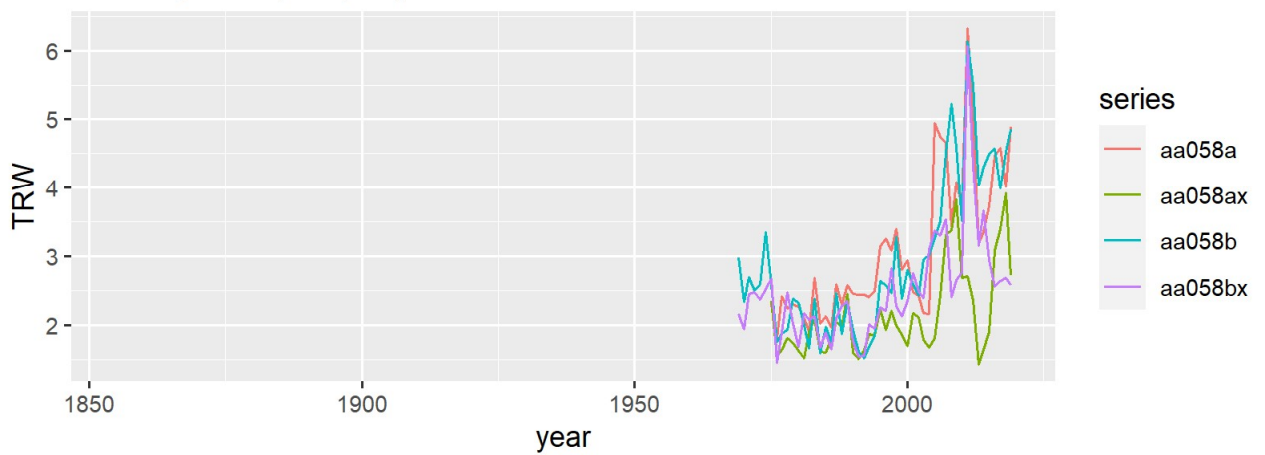
Tree aa056

Tree-ring width (mm/year)



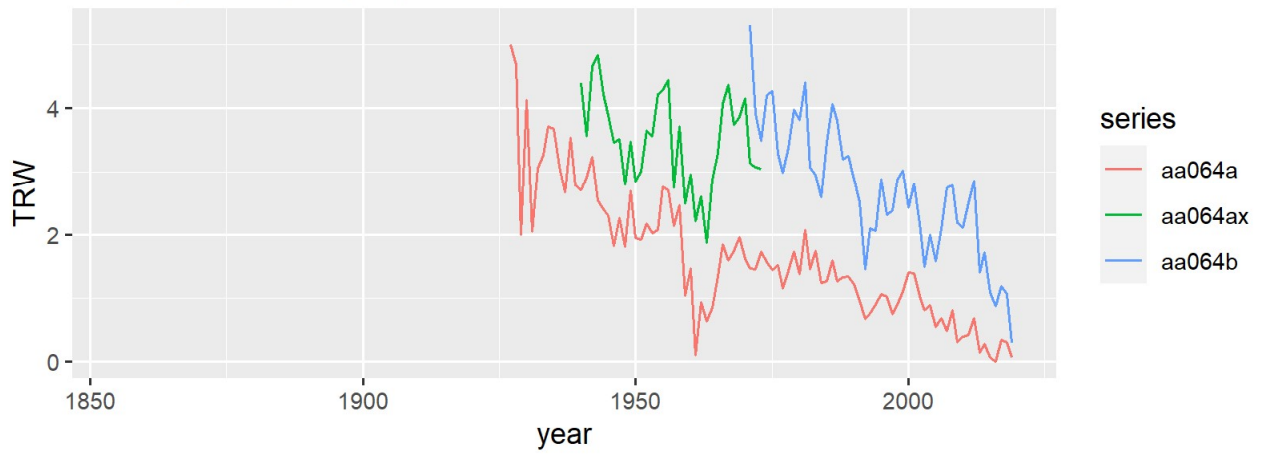
Tree aa058

Tree-ring width (mm/year)



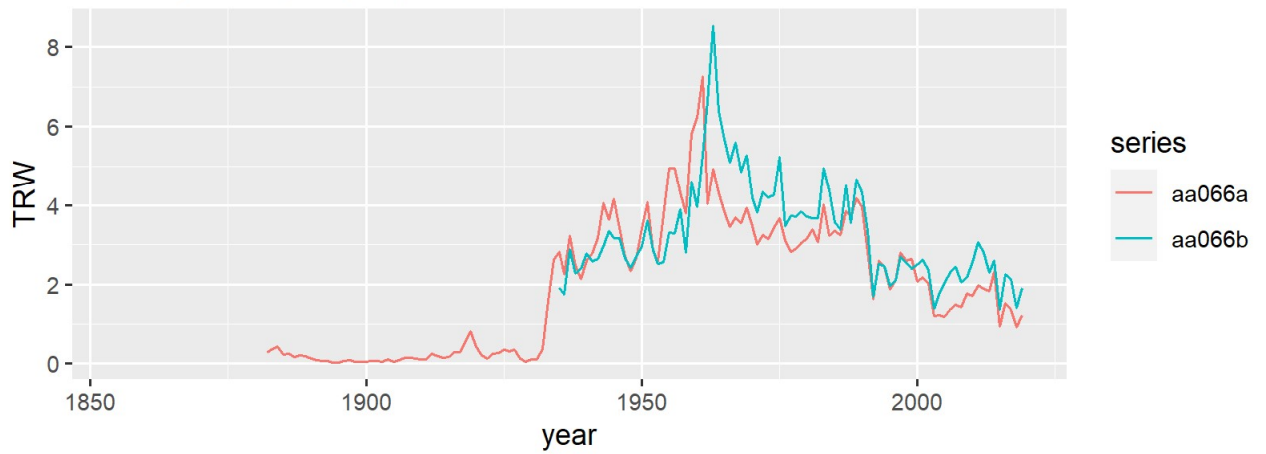
Tree aa064

Tree-ring width (mm/year)



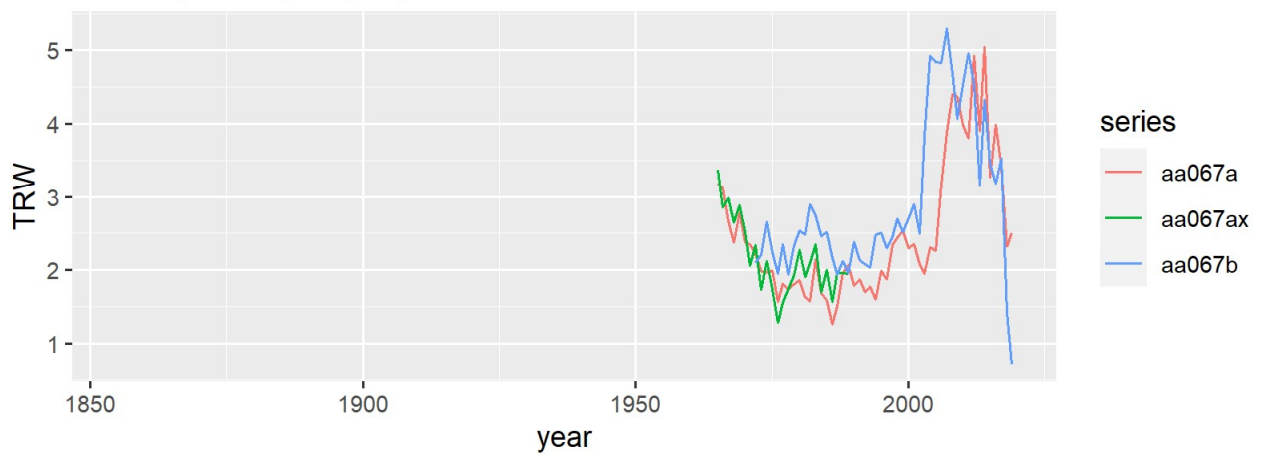
Tree aa066

Tree-ring width (mm/year)



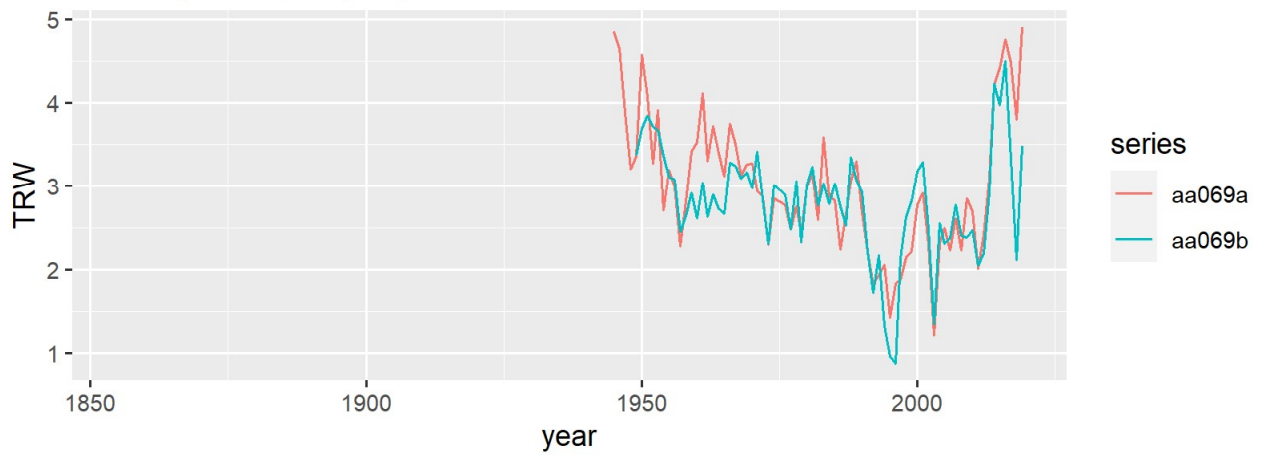
Tree aa067

Tree-ring width (mm/year)



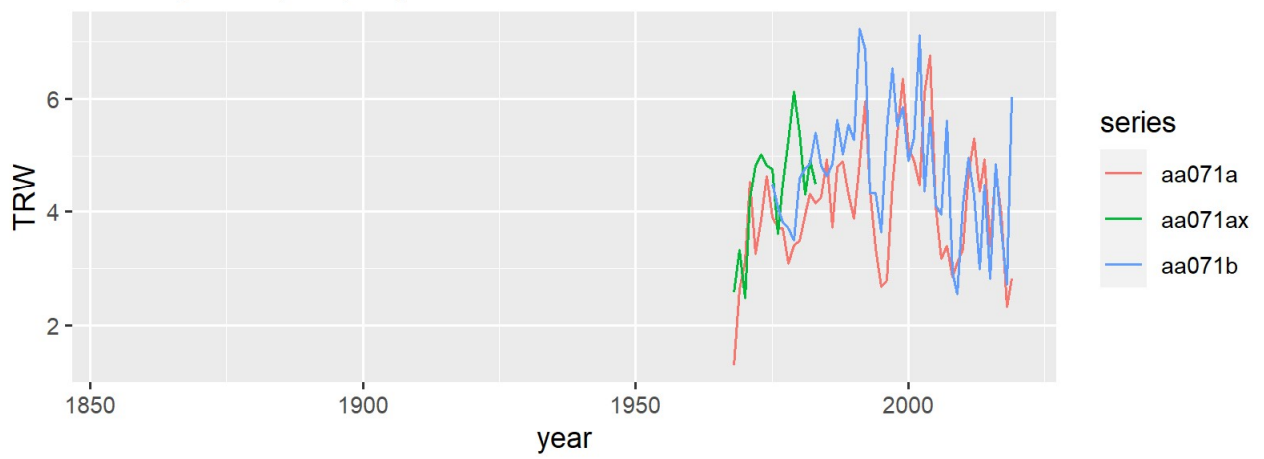
Tree aa069

Tree-ring width (mm/year)



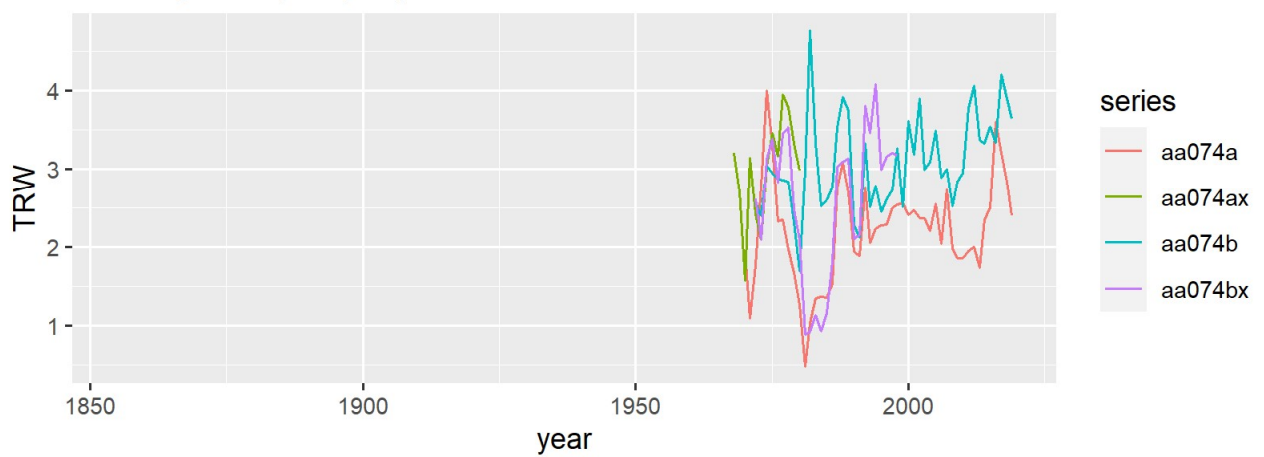
Tree aa071

Tree-ring width (mm/year)

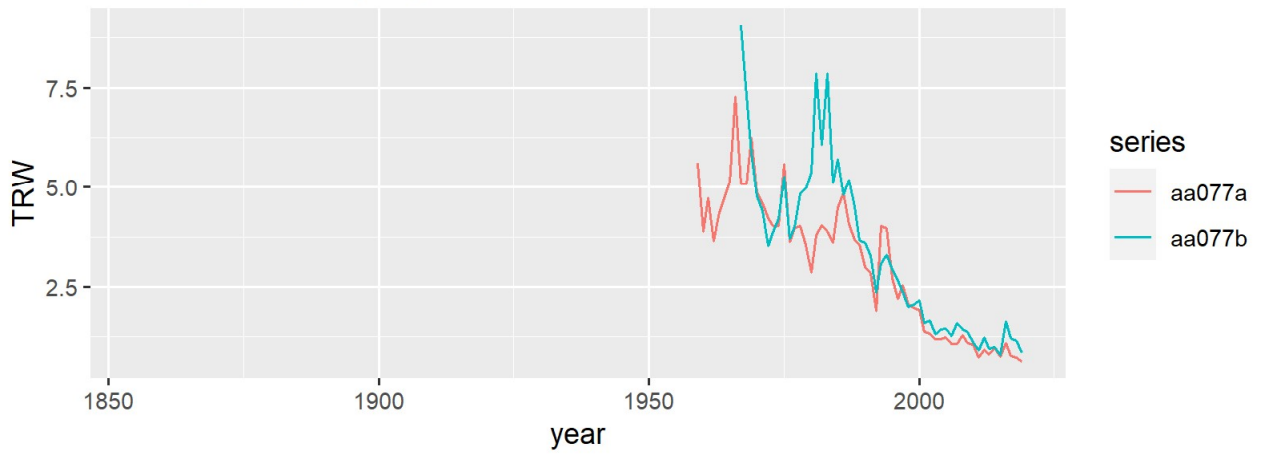


Tree aa074

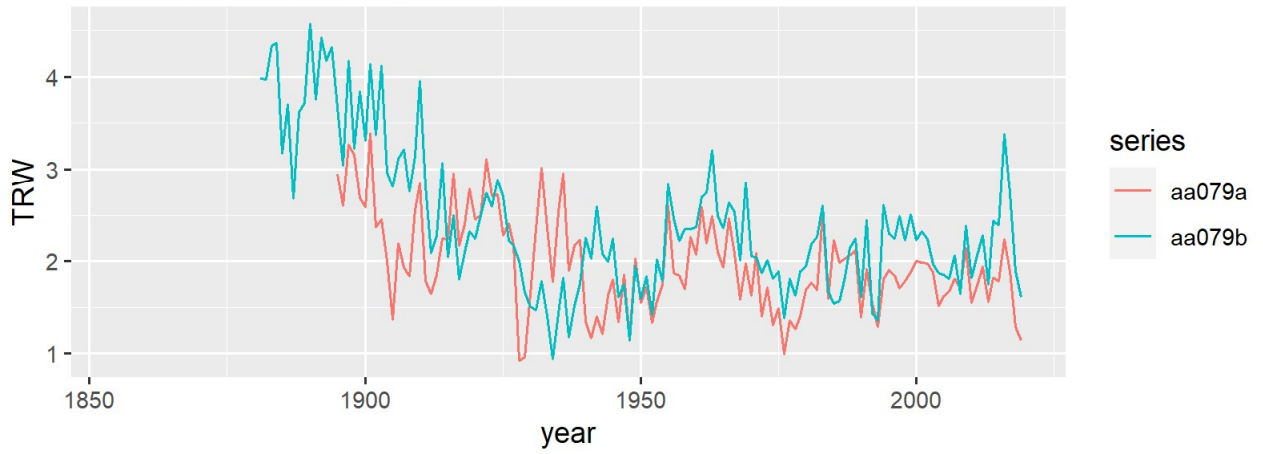
Tree-ring width (mm/year)



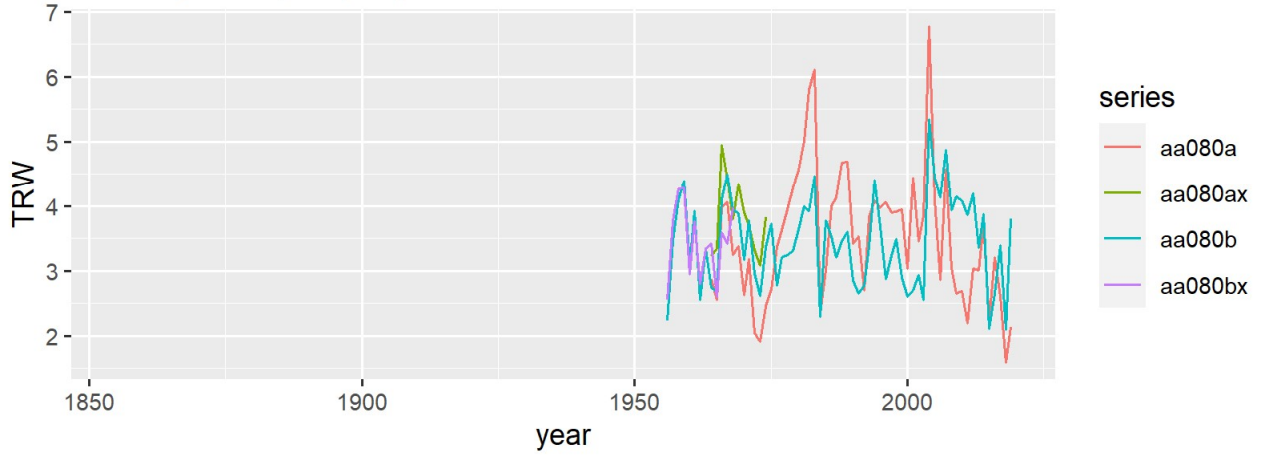
Tree aa077
Tree-ring width (mm/year)



Tree aa079
Tree-ring width (mm/year)

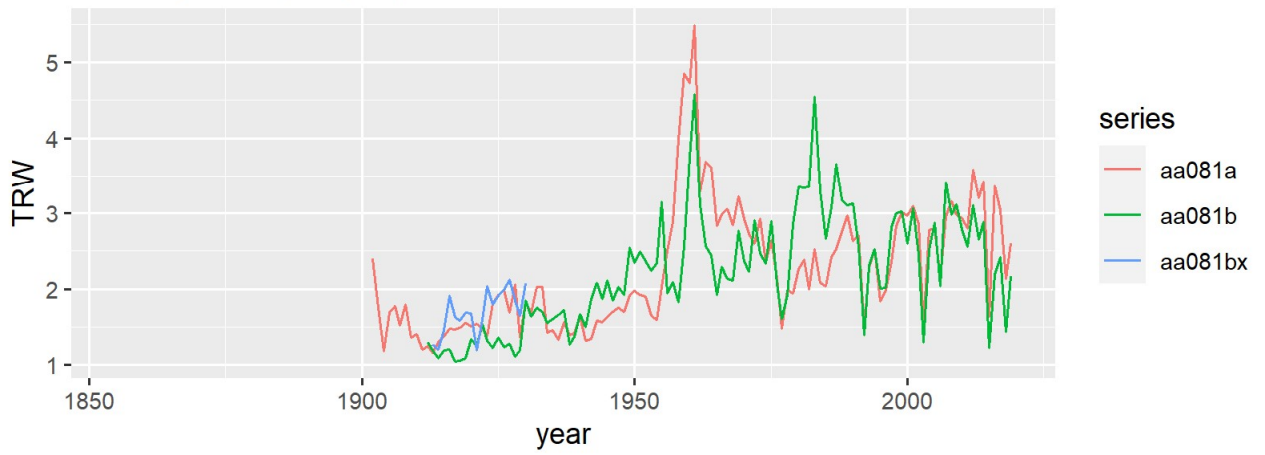


Tree aa080
Tree-ring width (mm/year)



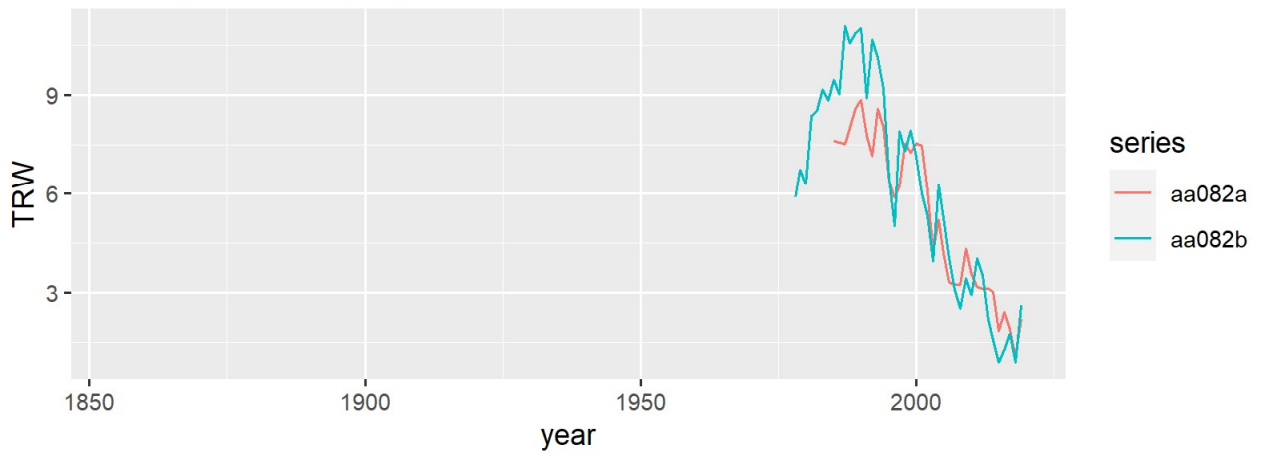
Tree aa081

Tree-ring width (mm/year)



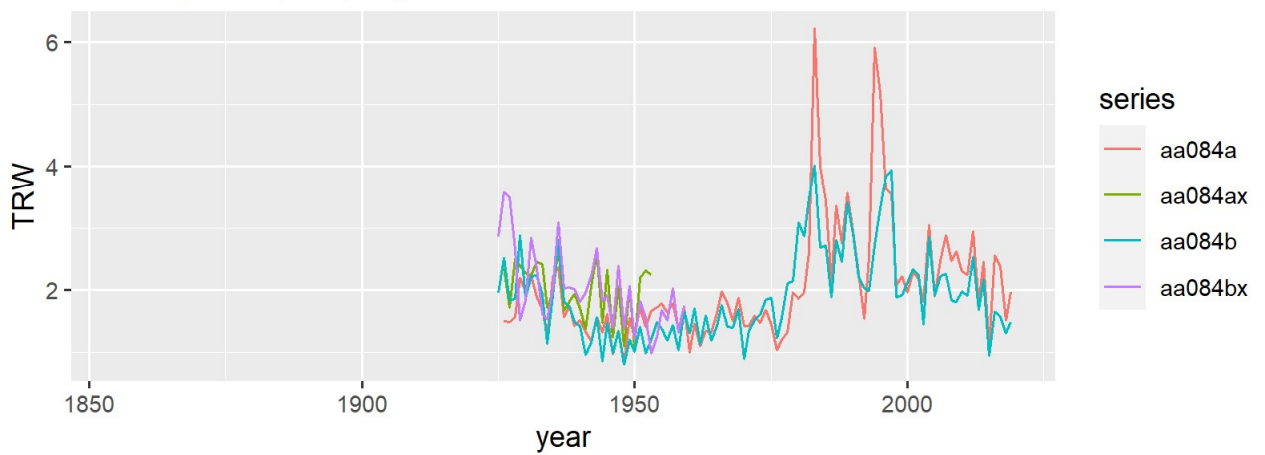
Tree aa082

Tree-ring width (mm/year)



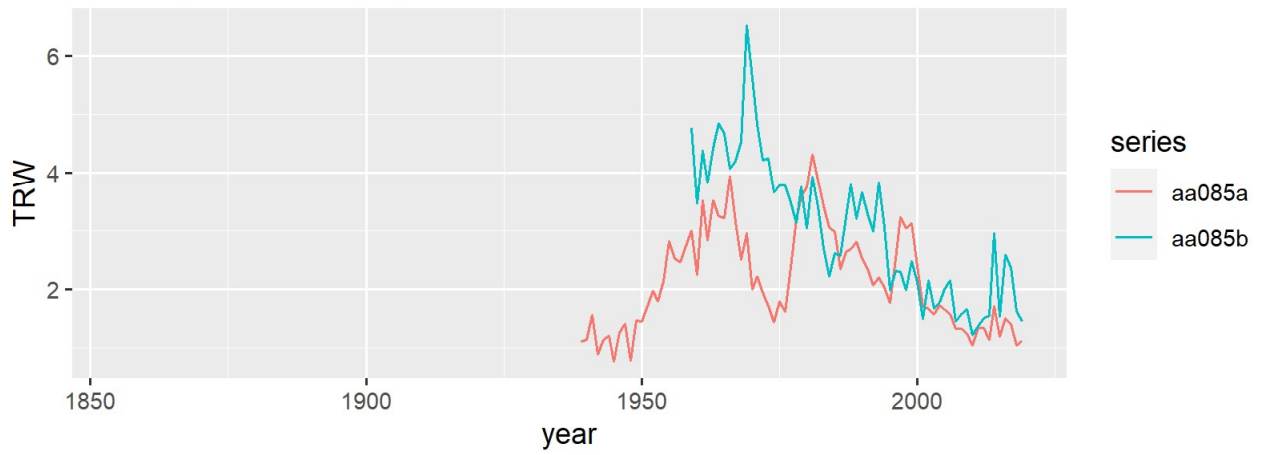
Tree aa084

Tree-ring width (mm/year)



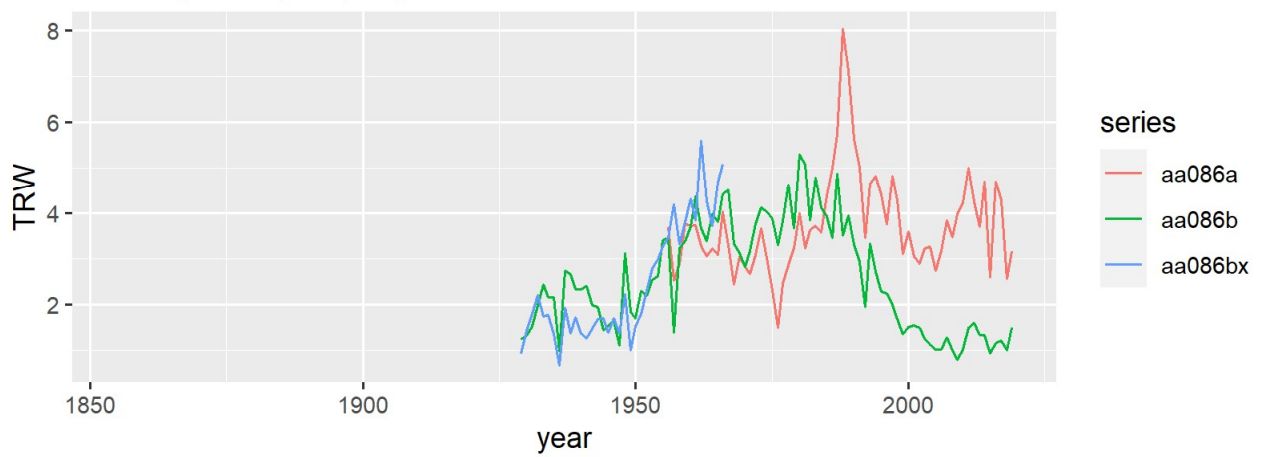
Tree aa085

Tree-ring width (mm/year)



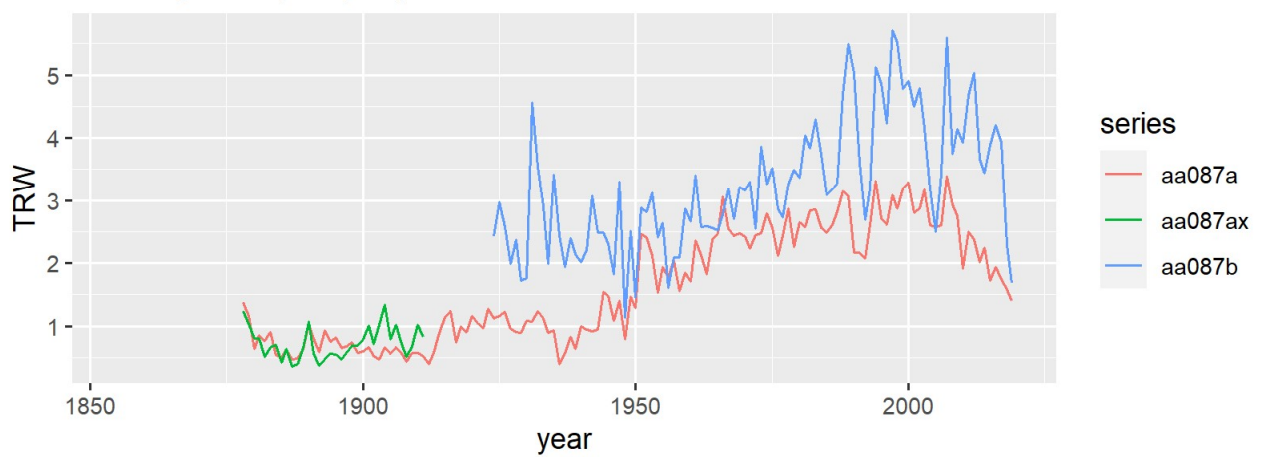
Tree aa086

Tree-ring width (mm/year)



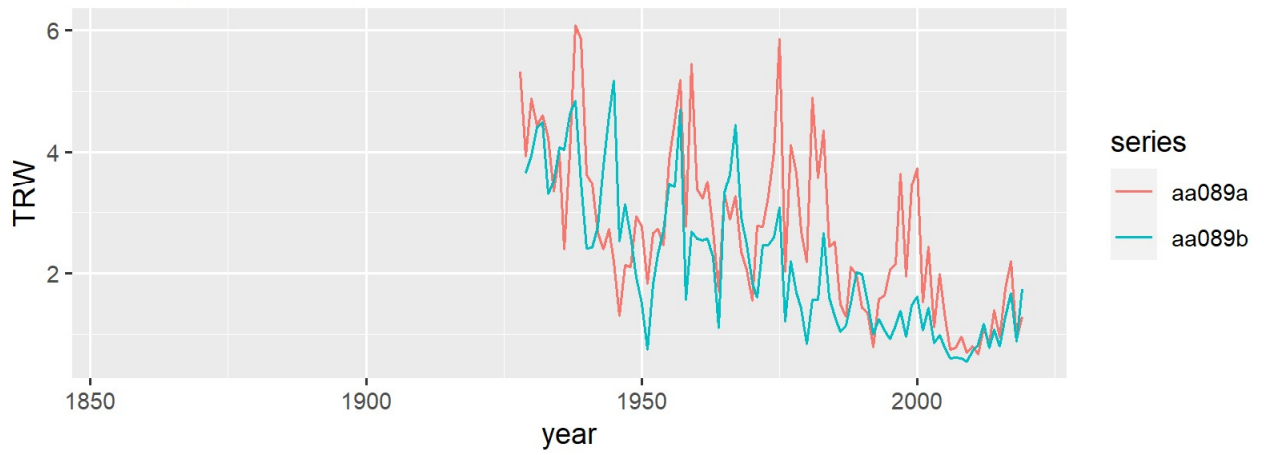
Tree aa087

Tree-ring width (mm/year)



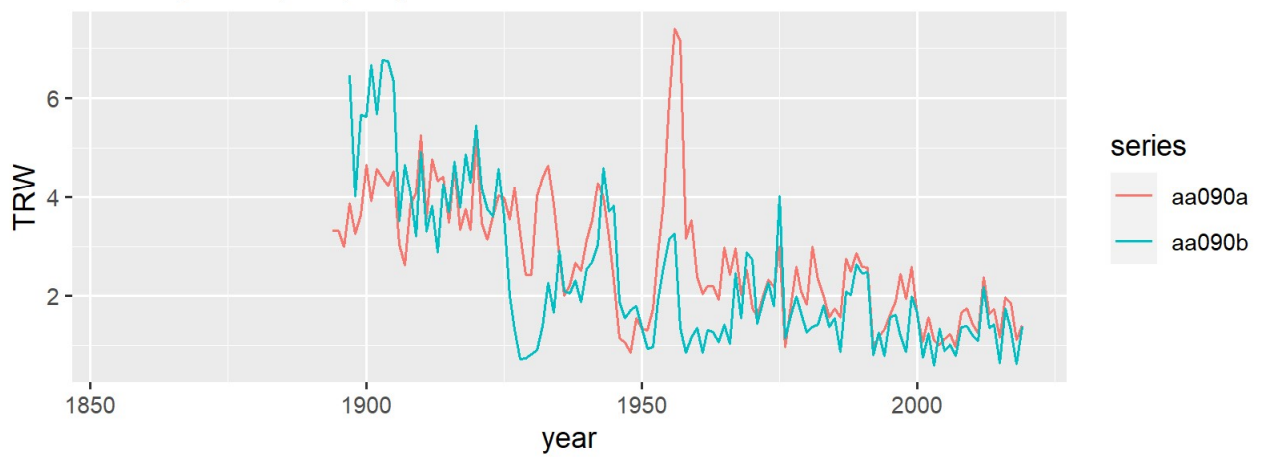
Tree aa089

Tree-ring width (mm/year)



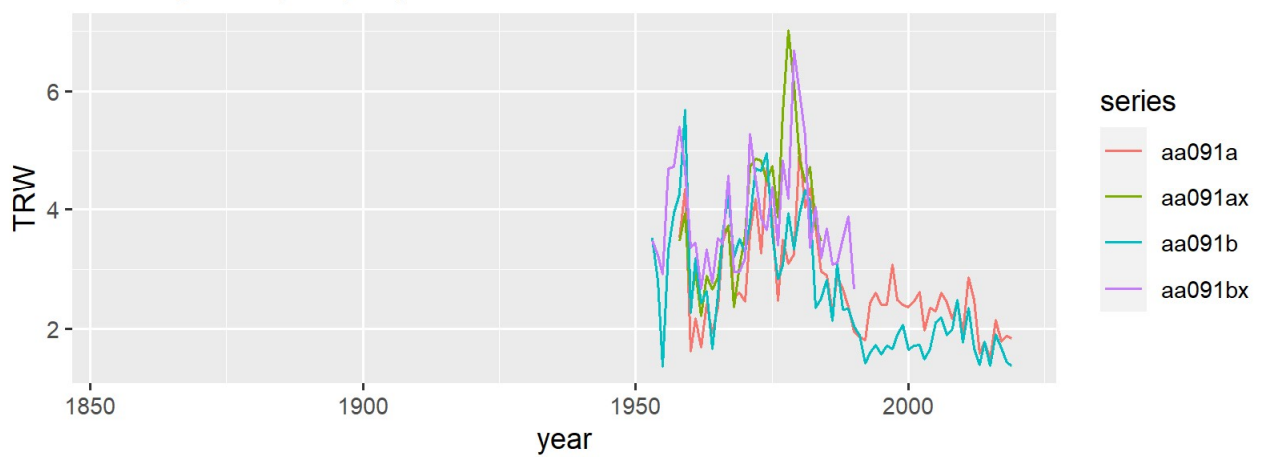
Tree aa090

Tree-ring width (mm/year)



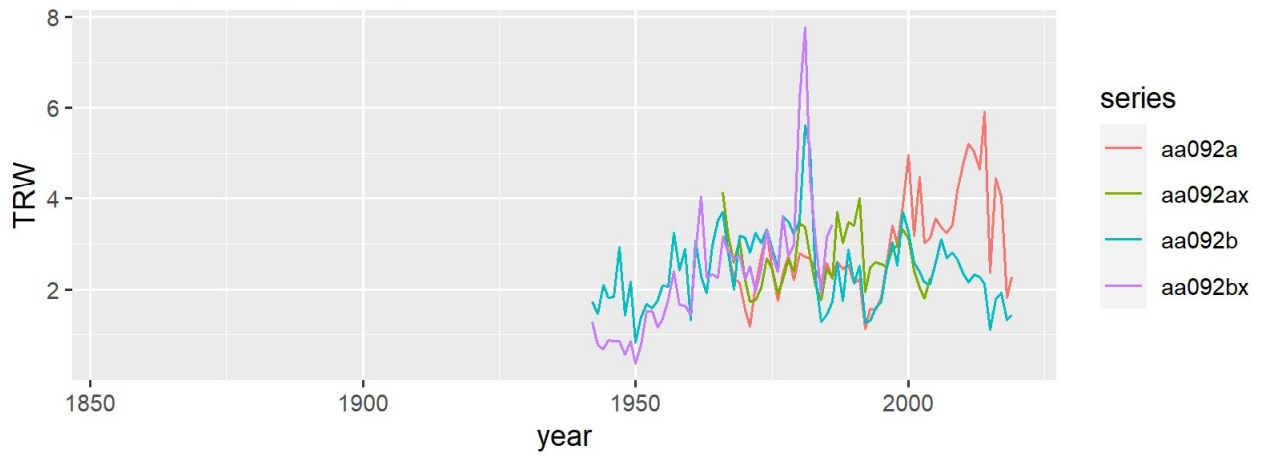
Tree aa091

Tree-ring width (mm/year)



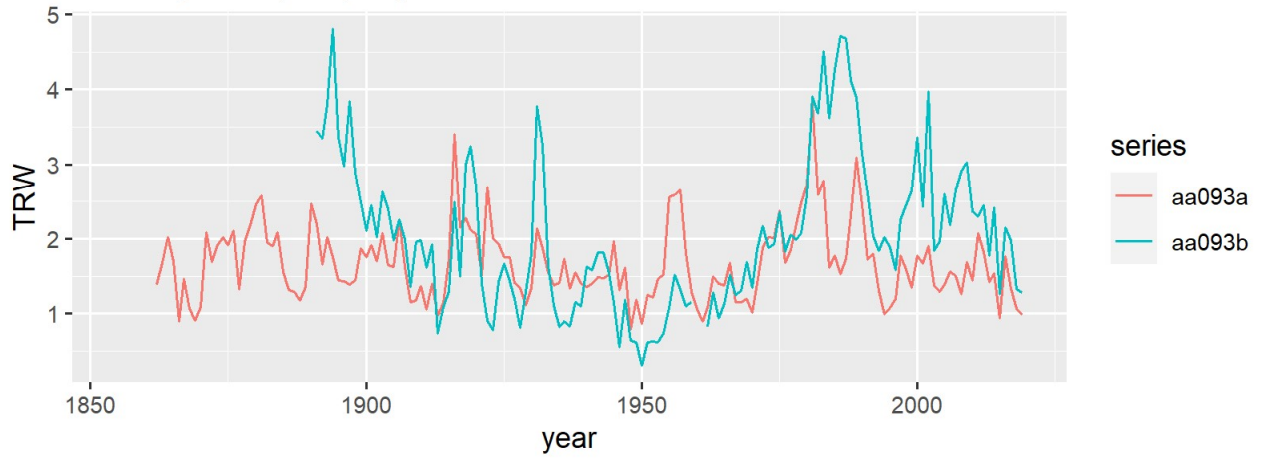
Tree aa092

Tree-ring width (mm/year)



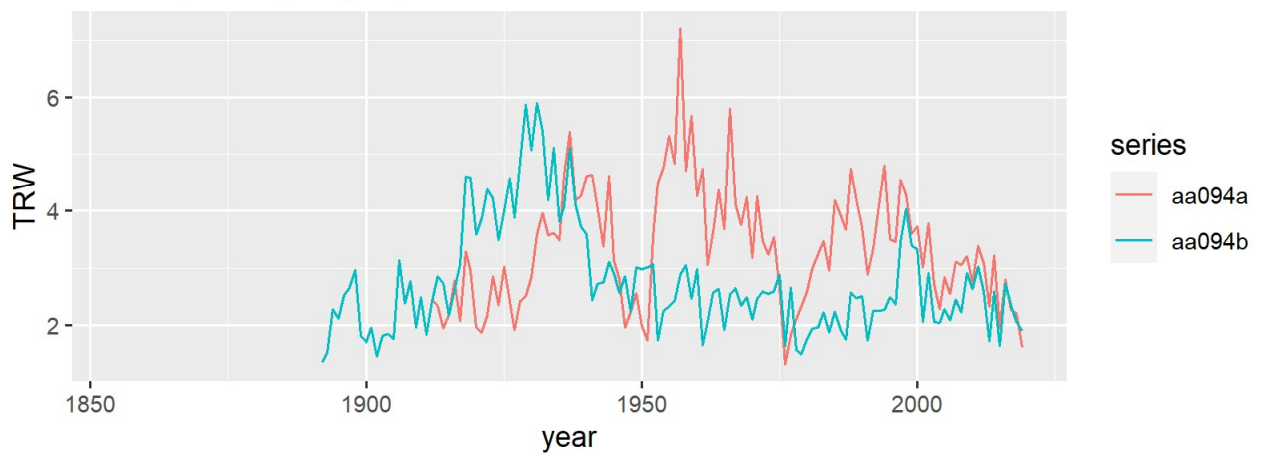
Tree aa093

Tree-ring width (mm/year)



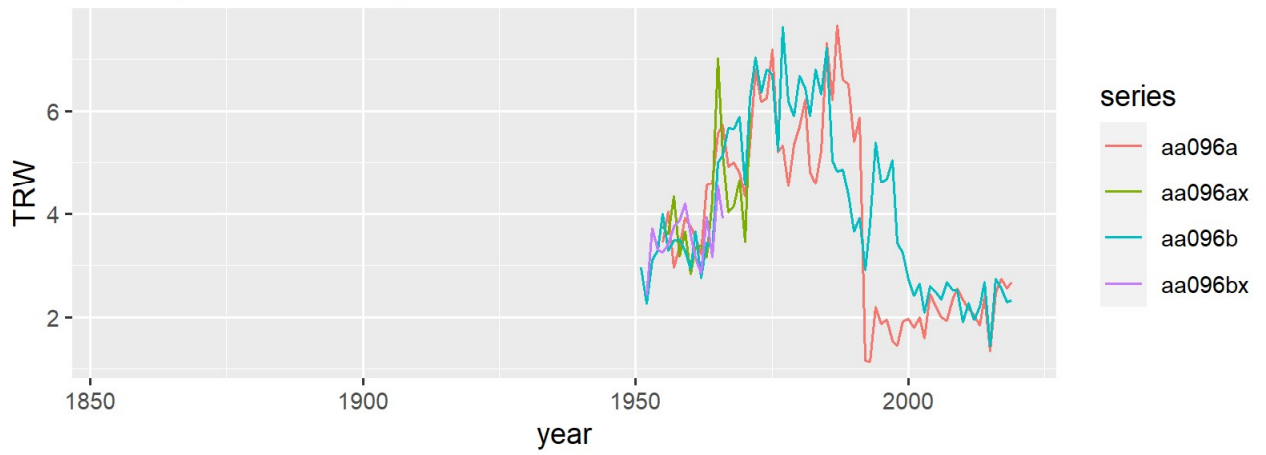
Tree aa094

Tree-ring width (mm/year)



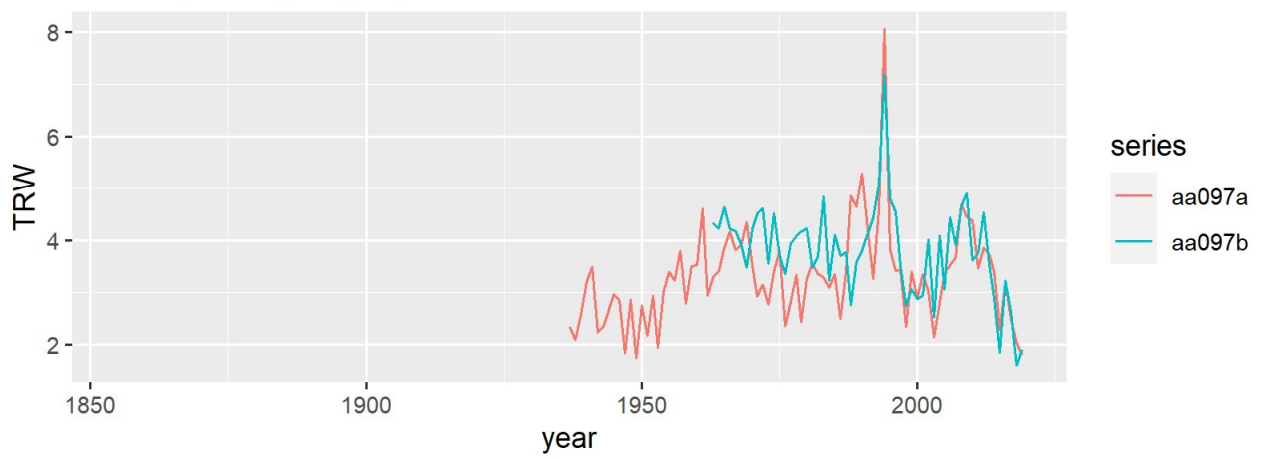
Tree aa096

Tree-ring width (mm/year)



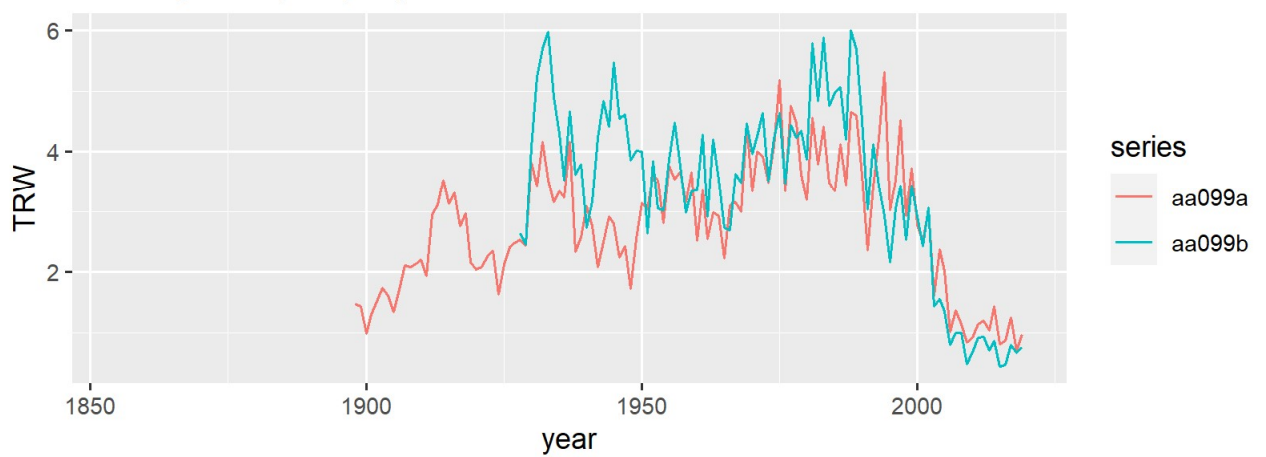
Tree aa097

Tree-ring width (mm/year)



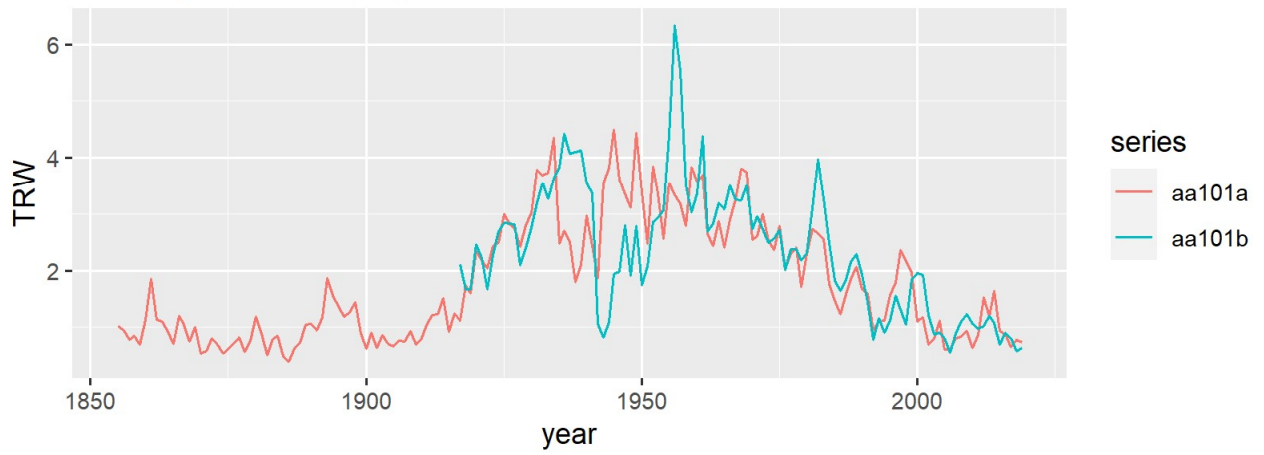
Tree aa099

Tree-ring width (mm/year)



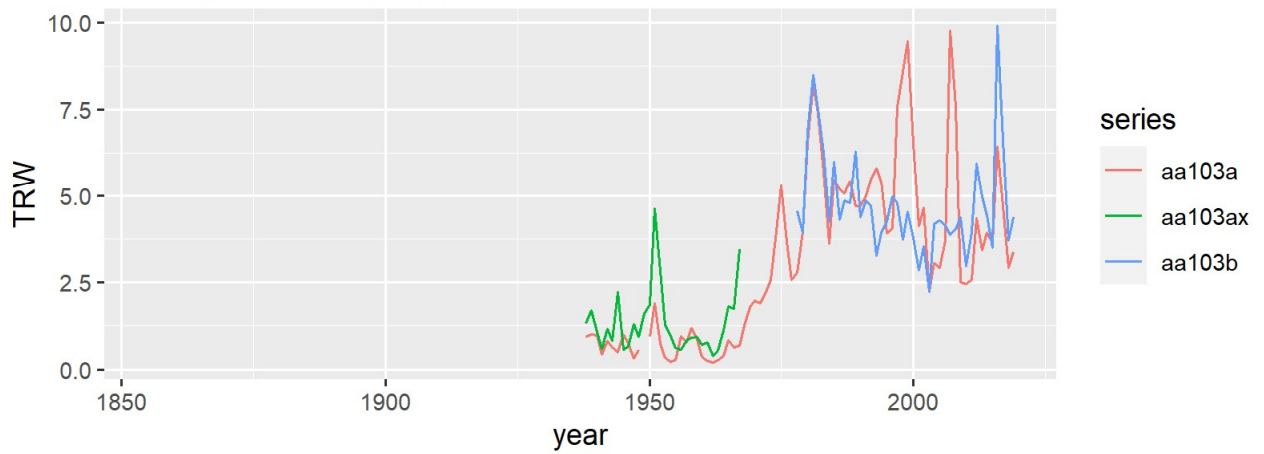
Tree aa101

Tree-ring width (mm/year)



Tree aa103

Tree-ring width (mm/year)



Tree aa104

Tree-ring width (mm/year)

